NTNU
Norwegian University of
Science and Technology

Soil Moisture Measurements and Evapotranspiration in Extensive Green Roofs

Sindre Stefferud

Civil and Environmental Engineering
Submission date: June 2016
Supervisor: Tone Merete Muthanna, IVM
Co-supervisor: Birgitte Gisvold Johannessen, IVM

Norwegian University of Science and Technology
Department of Hydraulic and Environmental Engineering

Sammendrag

Denne masteroppgaven omhandler konseptet grønne tak, for håndtering av overvann. Oppgaven tar for seg en litteraturstudie på grønne taks hydrologi og de faktorer som påvirker dets ytelse. Dette for å kartlegge eksisterende litteratur på området, samt gi bakgrunnskunnskap videre i oppgaven. Videre er det lagt ekstra vekt på temaet fordampning, eller evapotranspirasjon, som er viktig for regenerering av det grønne taks ytelse mellom nedbørshendelser. Ved å måle fuktigheten i det grønne taket vil en kunne få økt kunnskap om hvordan det gir fra seg vann gjennom fordampning. Store usikkerheter er derimot knyttet til sensorene som benyttes til dette formålet, ved bruk på grønne tak, og det er derfor utført laboratoriearbeid for å kalibrere disse.

De faktorer som påvirker grønne tak, og som drøftes i denne oppgaven, er substratkarakteristikker, takets geometri, vegetasjon og det grønne takets alder. I tillegg drøftes værforholdene mellom nedbørshendelser, nedbørshendelsenes karakteristikker og sesongmessige variasjoner. Det presenteres ulike modeller for estimering av fordampning, hvor en beregner såkalt potensiell evapotranspirasjon. Utvalgte modeller vil benyttes for å beregne dette ved det grønne taket på Risvollan i Trondheim. Sammen med korrekte data for jordfuktighet beregnes den faktiske evapotranspirasjonen. Samtidig evalueres behovet for å justere resultatene med en bestemt koeffisient.

Kalibreringen av fuktsensorene ble gjennomført under stabile forhold i et laboratorium. Sensorene registrerer såkalt dielektrisk permittivitet, og ved hjelp av en ligning som gir sammenhengen mellom volumetrisk vanninnhold og den dielektriske konduktiviteten finner man altså vanninnholdet. Først ble det gjort en såkalt standard kalibrering for de to substrattypene som benyttes ved Risvollan. Her konstateres det at de to substratene gir såpass forskjellige resultater at det bør benyttes ligninger spesifikt for jordtypene når en regner ut vanninnholdet. En kalibrering spesifikt for takets oppbygging er også evaluert. Også dette gjøres i laboratoriet, der bokser på 21x23 cm utgjør «takenes» areal. Her framkommer det avvik fra ligningene utarbeidet fra standardkalibreringen, men resultatene anses som noe usikre.

Abstract

In his master's thesis, a concept within stormwater management, the green roof, will be examined. The first part of this thesis is a literature study on the hydrology of extensive green roofs and the factors influencing the hydrological performance of the roofs. This has been done in order to map existing literature and to gain knowledge for the residual work. There is an emphasis on evapotranspiration, which is important for regeneration of the green roofs in between storm events. By measuring soil moisture for the roof, one will gain knowledge on how well the roof release water through evapotranspiration. However, there are uncertainties regarding the sensors measuring soil moisture when used on green roofs. With this in mind, a huge part of this thesis has been to calibrate these sensors, in a laboratory environment.

The factors affecting the green roofs that are being discussed are substrate characteristics, roof geometry, vegetation and the age of the green roofs, as well as the dry weather period prior to a rainfall, seasonal variations and event characteristics. Various models for estimating so-called potential evapotranspiration are presented, and a select few models will be used to calculate this for the green roof field at Risvollan, Trondheim. Along with correct data for soil moisture, the actual evapotranspiration can be calculated. The need for adjustment of the data is also evaluated.

The calibration of the sensors are carried out under stable laboratory conditions. The sensors measure the dielectric permittivity of the material, and by the use of an equation providing the relationship between this and the volumetric water content, the water content is found. At first, a standard calibration were carried out for the two types of substrates that are to be found at Risvollan. It is established that the difference between the substrates are to such a degree that there's a need for equations specifically for each substrate. A calibration specifically for the green roof build-up has also been attempted. This is done in the laboratory as well, in the scale of small boxes of 21x23 cm. It turns out there's a deviation compared to the standard calibration, when considering the roof plots with substrates. However, the results are somewhat uncertain.

Preface

This master's thesis in water and wastewater engineering is written during the spring 2016 at the Department of Hydraulic and Environmental Engineering. The work has been conducted with guidance from my supervisors, Associate professor Tone Merete Muthanna and PhD Candidate Birgitte Gisvold Johannesen.

The topic for the thesis is extensive green roofs and their hydrological functionality, as well as the importance of evapotranspiration and soil moisture conditions in relation to this. The work already started during the autumn 2015, when I wrote a project thesis in preparation for this master's thesis.

A literature study on green roofs and the factors affecting their performance and ability to regenerate through evapotranspiration has been conducted. Furthermore, soil moisture sensors to be used on a local field roof at Risvollan have been calibrated to provide accurate data from the green roof. Then potential evapotranspiration for Risvollan has been calculated and together with the soil moisture measurements, the actual evapotranspiration has been found.

I would like to thank my supervisors who has given me excellent guidance, through regular meetings and emails. And they have always been available, helpful and have answered any question at any time, and have thus been extremely valuable resources for me. For this, I am very thankful.

Table of Contents

List of Figures

List of Tables

1 Background

In green roofs, the soil moisture is a key parameter to understand the physical processes in the roof and the driving forces in water movement through the roof. Evapotranspiration is a key process for regenerating the roofs for the coming rainfall event, and in relation to this the soil moisture is a central parameter. However, the substrate of green roofs is not a homogenous soil mass, which makes soil moisture measurements more complex. This master thesis will deal with factors affecting green roof performance and regeneration, explore the measurement of soil moisture in the substrate of green roofs and estimate evapotranspiration at a local field roof.

1.1 Objectives

The overall goal of this thesis is to understand the hydrological processes of green roofs, with an emphasis on evapotranspiration and soil moisture. There is an important link between evapotranspiration and retention capacity for green roofs, and this is highlighted. Developing calibration curves to correctly measure soil moisture content in green roofs and estimating evapotranspiration based on field data is especially of interest for scientific purposes. The thesis' scope is divided into the following objectives:

- Perform a literature study on green roofs and identify factors affecting its performance.
- Discuss appropriate functions to describe evapotranspiration in Norwegian conditions.
- Calibrate a soil moisture sensor based on dielectric permittivity to work in a heterogeneous green roof substrate, and develop calibration curves for selected substrates.
- Apply calibration curves on measurements from a green roof field station and estimate soil moisture content in different green roof configurations.
- Estimate actual evapotranspiration from soil moisture measurement on field data and discuss parameters affecting it.

1.2 Methods

A literature study on the hydrology of green roofs and the factors influencing the hydrological performance was carried out. This work started already during the fall 2015, with a project thesis on the same topic (Stefferud, 2015). This has served as a background for the theoretical

part of this master thesis. The literature study has been expanded however, especially regarding evapotranspiration.

The most comprehensive part of the work in relation to this thesis has been to calibrate the soil moisture sensors. This has been carried out in a laboratory. Many experiments have been carried out, resulting in six new equations for calculating volumetric water content as a function of measured dielectric permittivity.

Potential evapotranspiration have been calculated using three different models; 1985 Hargreaves, Penman-Monteith and Thornthwaite. The two first on a daily basis, and the latter on a monthly basis.

The results from laboratory work are applied to field data from a green roof in Trondheim. Together with potential evapotranspiration calculated from three different models, the actual evapotranspiration is to be found.

1.3 Risvollan Green Roof Site

Risvollan is a district in Trondheim, approximately 5 km southeast of the city center. The climate of Trondheim is temperate and humid, and somewhat unstable due to the cold, polar climate in the north and the warm air south of Trondheim. The winters are often mild, with a January mean temperature of -3.1 ^{o}C and a lot of precipitation both in the form of snow and rain throughout the winter. The summer is usually mild, with a variation of rainy and sunny days and a mean temperature of 14.7 ^{o}C (Bratberg, 2008).

The green roof site at Risvollan was created by covering the roofing felt of an existing shed in vegetation. The roof is divided into four plots with different layers and vegetation, and runoff from each of the plots as well as precipitation is being measured. Each of the plots has a vegetation layer of sedum species, but is constructed different substrate materials. The project is established as a collaboration between manufacturers of green roofs, Risvollan housing cooperative, NVE, Trondheim Municipality, NTNU and Fremtidens byer. The aim is to compare the roofs, and assess how the vegetation is reacting and how the roofs are affecting the runoff (IVM, 2014).

FIGURE 1.1 THE GREEN ROOF SITE AT RISVOLLAN, TRONDHEIM. THE ROOF IS DIVIDED INTO FOUR PLOTS, WITH THE PLOT AT THE LEFT BEING NAMED 'PLOT 1', AND FOLLOWING FROM LEFT TO RIGHT WE HAVE 'PLOT 2', 'PLOT 3' AND 'PLOT 4' (IVM, 2014).

Precipitation is measured at a one-minute interval using a tipping bucket rain gauge, at the rooftop. The resolution is 0.1 mm per tip. The gauge is heated to avoid icing and snow accumulation. Air temperature and humidity, as well as soil temperature and humidity, are measured in 15 minutes intervals. The discharge from each of the roof plots are being collected into individual barrels for each plot, where pressure transmitters are used to monitor the water level. The water levels are logged at break points with a resolution of minimum 1 minute and maximum 1 hour. There is also a pump installed, that will automatically empty the barrels when they are full (Johannesen, 2015).

The roof plots are equally large, with a length of 7.6 meters and a width of 2 meters. This gives a surface area of 15.2 m^2. The slope of the roof is 16 %, and its orientation is towards east (Johannesen, 2015). The plots are from different manufacturers and have different configurations in terms of layers and vegetation.

2 Introduction to Stormwater Management

2.1 The Impact of Urbanization

The population worldwide is steadily becoming increasingly concentrated in urban areas. Considering Norway, numbers from SSB tells us that the population of urban areas increased by 1.6 % between 2013 and 2014, and by the 1st of January 2014 the population in these urban areas makes up around 80 % of the Norwegian population (Statistisk sentralbyrå, 2015). These numbers illustrate the mentioned worldwide trend; urban areas are increasing, in terms of both area and density. In 2050, 89 % of the Norwegian population is expected to live in urban areas. 70 % of all people in the whole world will then live in urban areas (UNICEF, 2012).

As a result of urbanization, cropland, grassland and forests are being replaced by impervious surfaces such as streets and buildings (Mentens et al., 2006). This furthermore leads to runoff during precipitation events, as the stormwater has limited areas where it can infiltrate. Additionally, increased runoff will increase stress on already existing stormwater infrastructure, and we may experience flooding from sewers. Climate changes causing more frequent rainfalls, with increased intensity, leads to further challenges for urban stormwater handling (Berndtsson, 2010, Lindholm et al., 2008), and measures has to be done.

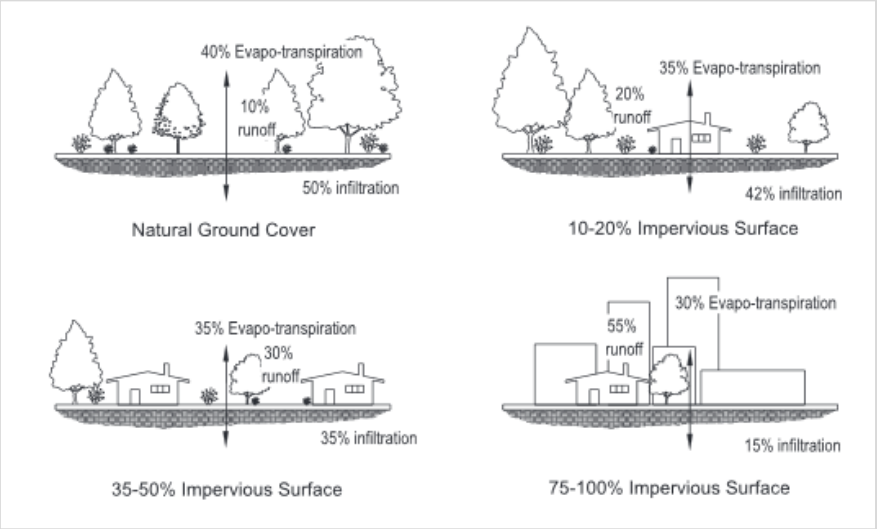

FIGURE 2.1 THE EFFECT OF URBANIZATION ON THE LANDSCAPE (COFFMAN, 1999)

Figure 2.1 is a very good illustration of the changes urbanization creates and the following consequences. Especially in dense areas, there will be a very low degree of infiltration.

$$P + G_{in} - (Q + ET + G_{out}) = \Delta S \qquad (2.1)$$

Eq. 2.1 describes the hydrological water balance, as presented in (Dingman, 2015). P is precipitation, G_{in} is the groundwater inflow, Q is surface runoff, ET is evapotranspiration, G_{out} is groundwater outflow and ΔS is the change in water storage. The equation supports the notion that a reduction in groundwater inflow through infiltration, as seen in figure 2.1, will result in an increased runoff from the surface. One should also note that the groundwater outflow won't be reduced in the same degree. Capillary forces along with gravitation provides outflow of groundwater (Brattli, 2009) that will be larger than the reduced inflow, before a new equilibrium is set. In other words a reduction of the groundwater table. This may in turn cause damage to existing infrastructure and buildings due to settlement.

To oblige these challenges, there has been a development of several concepts over the last couple of decades. We have gotten to know terms such as SUDS (Sustainable Urban Drainage Systems), LID (Low Impact Development), GI (Green Infrastructure), WSUD (Water Sensitive Urban Design) and BMPs (Best Management Practices). These terms all refers to similar concepts. The idea is to constitute a more sustainable approach to the stormwater management, by looking at more than just the quantity of runoff. It is also important to look at the factors that are water quality and amenity. Additionally, these concepts are focusing on on-site control, meaning that the rainfall is best controlled as close to the source as possible and thus should be aimed for. Yet another important factor is the combination of multiple sustainable drainage systems in a treatment train, to ensure a robust stormwater management (Stovin et al., 2013, Water Environment Federation (WEF), 2012).

3 Green Roofs

3.1 The Concept

One way of managing stormwater in urban areas that has received a growing amount of attention in recent years, is the implementation green roofs. The concept is in principle to turn the roofs green by covering them with soil and vegetation, and thus achieving numerous benefits such as reduced and attenuated stormwater runoff, thermal benefits, noise reduction, reducing air pollution and providing wildlife habitat and biodiversity enhancement (Berndtsson, 2010). As the downtown areas in many places have limited or even non-existing green space, green roofs can be a good way of providing an attractive green space.

The main layers of a green roof construction is typically vegetation, growing medium (substrate), a geotextile filter and a drainage element (Berndtsson, 2010), as illustrated figure 3.1 along with other important components such as a waterproof membrane and a root barrier.

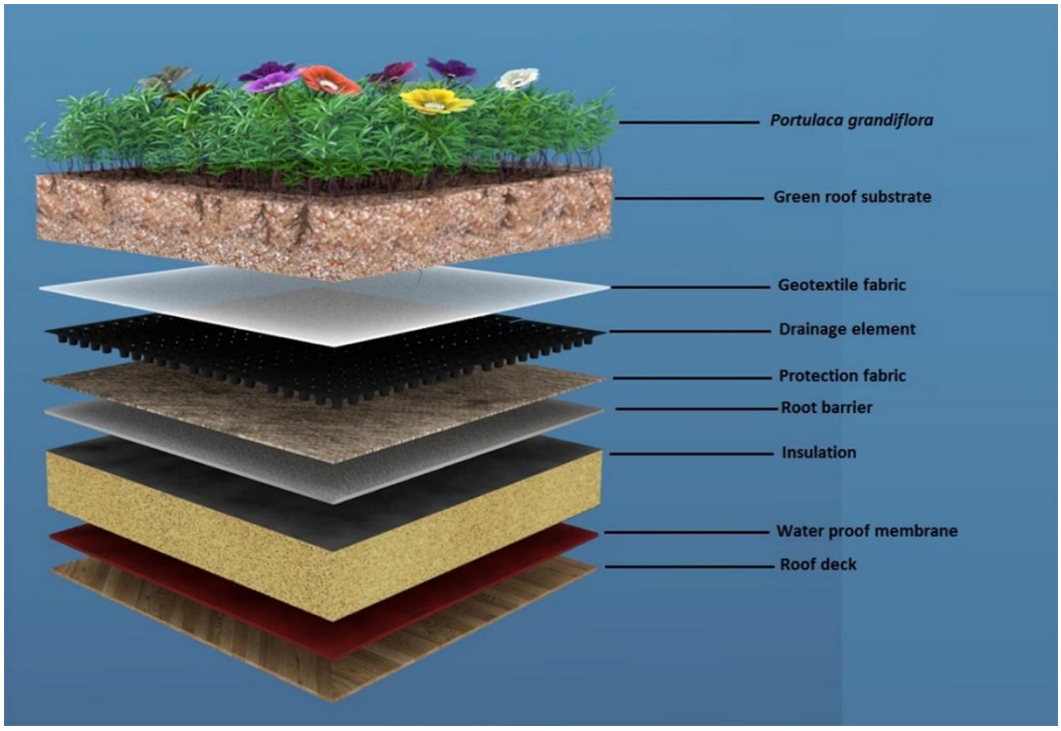

FIGURE 3.1 CONFIGURATION OF A GREEN ROOF (VIJAYARAGHAVAN AND RAJA, 2014)

3.2 Classification of Green Roofs

Green roofs are typically divided into two categories: intensive and extensive green roofs. Various types of vegetation are used for the roofs, and the choice of vegetation furthermore affects the thickness of the soil layer. There is however no clear agreement when it comes to what thickness of soil that defines the different roof types. One definition is a substrate layer of 60-200 mm for extensive green roofs and 150-400 mm for intensive green roofs (Noreng et

al., 2012). Even thinner substrates may however be used for extensive green roofs. Despite some differences between the green roof classifications, the components are in principle the same and can be seen in figure 3.1. The choice of substrate layer thickness and vegetation will depend on the objective for the green roof, as well as factors such as economy, aesthetics, hydrology, whether the building is new or standing, and location.

The fairly deep substrate layer of intensive green roofs allows them to support larger plants and bushes, which in turn may require regular maintenance such as weeding, fertilizing and watering. Extensive green roofs on the other hand have smaller plants that are expected to provide full coverage of the roof in their final stage. They are often aimed to be maintenance free, however some fertilization is often recommended for commercial products (Berndtsson, 2010). Sedum species are commonly used, and can handle both dry periods and soil with low fertility. (Noreng et al., 2012) also mention a third category that may be used, semi-intensive roofs. Typically, these roofs are covered with lawns and ground covering plants, and require some maintenance as well.

Sedum species have a typical construction height of 50-250 mm and a total dry weight of 35-40 kg/m^2, and around 50 kg/m^2 when saturated. They can be constructed as both flat and sloped roofs, and due to their low weight they may be laid directly on existing constructions (Noreng et al., 2012).

3.3 The Hydrological Processes of a Green Roof

A green roof provides two key hydrological functions, they retain water and if the retention capacity is exceeded the water is still detained. The plants evapotranspire, and thus they remove moisture from the underlying substrate. This results in a moisture deficit that provides

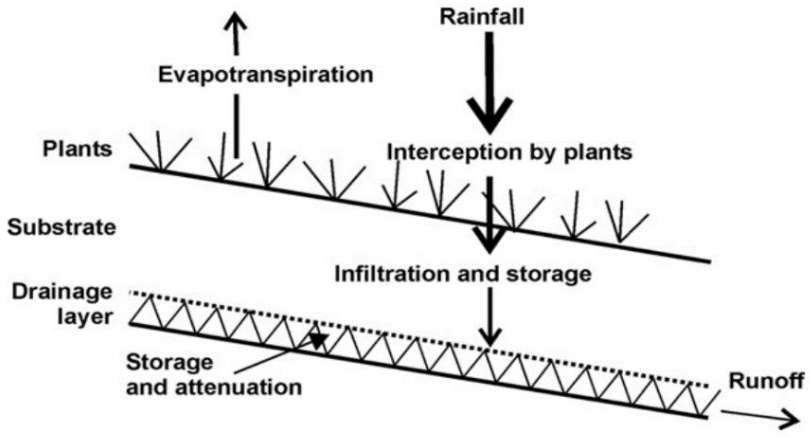

FIGURE 3.2 THE HYDROLOGICAL PROCESSES OF GREEN ROOFS (STOVIN ET AL., 2012)

the roof with capacity to retain rainfall and prevent it from ever becoming runoff (Yio et al., 2013). If the rainfall exceeds the capacity of the green roof, then the water will drain and become runoff. However, the runoff is still detained, and the peak runoff is both reduced to a certain degree and delayed. Figure 3.2 illustrates how the hydrological processes works.

As seen in figure 3.3, a conventional roof will more or less immediately generate runoff as the rainfall starts. For a green roof however, the runoff is delayed. The unit processes that a green roof provides that contributes to this volume reduction and runoff delay, are peak flow attenuation, infiltration and evapotranspiration (Water Environment Federation (WEF), 2012).

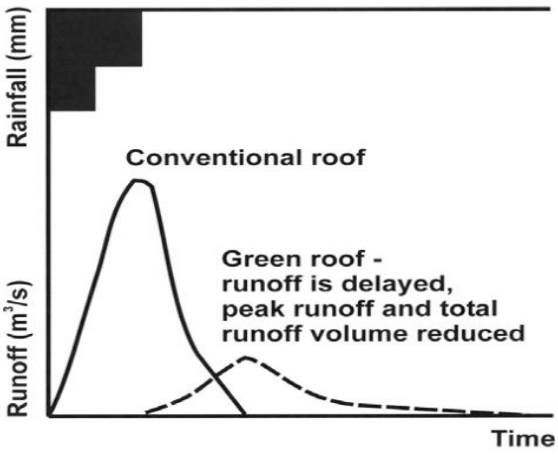

FIGURE 3.3 RAINFALL RUNOFF RESPONSE FOR A GREEN ROOF, COMPARED TO A CONVENTIONAL ROOF (STOVIN ET AL., 2012)

3.3.1 Peak Flow Attenuation

Due to lesser natural storage, shorter travel times and increased runoff volumes, peak flows are increasing. The peak flow is the highest volume of runoff for a given time unit or duration. Traditionally, peak flow attenuation has been the single focus of stormwater management, and it has typically been done by building storage facilities (Water Environment Federation (WEF), 2012). However, attenuation is more effectively achieved by also reducing the actual volume as well as extending the travel time. A green roof will primarily provide a storage attenuation, meaning the peak flow is attenuated due to water storage in the soil pores and in the vegetation.

3.3.2 Infiltration

Infiltration is a process where water enters the soil, with rates controlled by the soil water movement below the surface. The characteristics of the roof substrate will influence the movement of the soil by hydraulic conductivity and the water retention characteristics which

describes the soil's ability to store and release water (Water Environment Federation (WEF), 2012).

Field capacity is the amount of water that's held in the soil after excess water is drained by the gravity (Water Environment Federation (WEF), 2012, Dingman, 2015). Together with the soil moisture content, it determines the volume of stormwater that can be retained through infiltration. The water is stored in the empty pore space, and as long as the soil moisture is below field capacity there is very little runoff from a green roof (Bengtsson et al., 2005). When at field capacity however, runoff from the green roof will occur (Bengtsson et al., 2005).

The hydraulic conductivity of a soil is its ability to transmit water when submitted to a hydraulic gradient. It's defined by Darcy's law, and for a saturated soil it can be written as (Brattli, 2009):

$$K_{sat} = \frac{k\rho g}{\mu}, \qquad (3.1)$$

where k is the soil permeability, ρ is the fluid density and μ is the fluid dynamic viscosity. Both the density and the viscosity are functions of temperature (Brattli, 2009, Emerson and Traver, 2008), and thus the hydraulic conductivity is affected by the temperature. In turn, the infiltration rate is affected. Tests have shown that for infiltration basins, with depths of less than 100 mm, hydraulic conductivity is the most sensitive parameter (Braga et al., 2007). Green roofs generally have a high porosity, and overland flow isn't very likely when not fully saturated (Villarreal and Bengtsson, 2005). For very low temperatures however, the

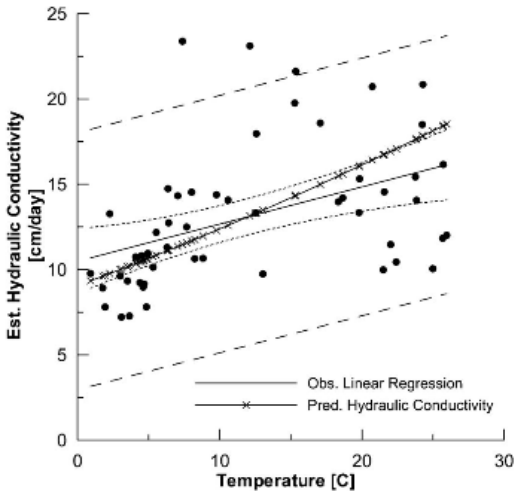

FIGURE 3.4 OBSERVED REGRESSION AND PREDICTED HYDRAULIC CONDUCTIVITY AS A FUNCTION OF TEMPERATURE (EMERSON AND TRAVER, 2008)

infiltration capacity is certainly lowered and water may run off the roof surface and more quickly into the roof drain system.

3.3.3 Evapotranspiration

Evaporation is the process where water returns to the atmosphere from soil and water surfaces, whereas transpiration occurs when plants release water vapor through their leaves (Water Environment Federation (WEF), 2012). Evapotranspiration describes the process where water returns to the atmosphere through both of these processes. It is a function of climatic factors and will thus vary as the weather changes. Statistics indicates that in humid areas, evapotranspiration accounts for around 50 % of the annual precipitation (Bengtsson et al., 2005).

The evaporation may come from interception, meaning that the some of the precipitation is intercepted by the vegetation and from there evaporates back to the atmosphere. There may also be a depression storage from a temporary pond on the roof surface, depending on the type of vegetation and the slope (Water Environment Federation (WEF), 2012). A typical value for a sloped green roofs is a ponding depth of 1 mm (Water Environment Federation (WEF), 2012). Surface evaporation may also take place, and means that water stored in the soil moves towards the surface and then evaporates. This happens when moisture in the upper layers is lost due to demand of climatic energy (Philip and De Vries, 1957).

4 Factors Influencing the Performance of Green Roofs

The annual runoff is the ratio between the runoff and the incoming rainfall for a period of one year. It can be useful for estimating discharge reductions in the sewer system (Locatelli et al., 2014). Studies conducted in different climates and with different roof configurations will show different results. Scandinavian studies have reported annual runoff reduction to be between 43 % and 68 % (Locatelli et al., 2014), 25 % (Braskerud, 2014) and 37 % (Bengtsson et al., 2005). It varies in a large degree between studies as due to a range of factors that influences the retention capacity of green roof and the runoff dynamics (Berndtsson, 2010). Studies conducted in different climates and with different roof configurations will show different results. Variations in terms of roof configurations, event characteristics and the period in between events. Evapotranspiration is known as a key factor for regeneration of retention capacity, and will depend on both roof configuration and climate.

(Berndtsson, 2010) lists the following factors related to the green roof characteristics: number of layers and type of materials, soil thickness, soil type, vegetation cover, type of vegetation, roof geometry (slope and length of roof), roof position (shadowed or faced direction) and roof age. The following weather related factors are mentioned: length of proceeding dry period, season/climate (air temperature, wind conditions and humidity) and characteristics of the rain event (intensity and duration). How these affects the performance of green roofs will now be discussed.

4.1 Substrate Characteristics

The physical properties of the substrate soil media will affect ability of the roof to retain and detain water. The time water uses to infiltrate a media is affected by its depth, as well as by the hydraulic conductivity (Li and Babcock, 2014). Furthermore, deeper substrates have greater biomass and may provide higher evapotranspiration rates (VanWoert et al., 2005). Higher rates of evapotranspiration have also been found in substrates with higher field capacity (Poe et al., 2015). A good substrate for extensive green roofs should be light weight, good anchorage for plants, provide nutrients, minimum leaching and stable, as well as having a good water holding capacity and good aeration (Nagase and Dunnett, 2011). To achieve this, it's beneficial to mix materials of different characteristics at defined ratios. It may have inorganic components such as sand, perlite, vermiculite and crushed brick, or organic matter such as coco-peat (Vijayaraghavan and Raja, 2014). Including organic matter in the substrate

helps maintaining a good soil structure, increases cation exchange capacity, supplies nutrients to the plants, and it improves water retention (Nagase and Dunnett, 2011).

A literature review analyzing 18 different studies with a total of 121 extensive and 11 intensive green roofs, presented the influence of substrate layer depth and runoff characteristics on an annual level (Mentens et al., 2006). It showed that the annual retention ranged from 75 % for intensive green roofs (average depth 210 mm), to 50 % for extensive green roofs (average depth 100 mm). The difference in maximum retention was not that big for intensive and extensive green roofs, respectively 85 and 81 %. However, the minimum retention differs greatly, being respectively 65 and 27 % for intensive and extensive green roofs. This indicates an increased sensitivity for climatic conditions for lower substrate depths.

Another study evaluated three different substrate depths, 50, 100 and 150 mm through laboratory tests (Yio et al., 2013). It shows a clear correlation between the substrate depth and the detention capacity. The detention time increases significantly as the substrate depth increases from 100 to 150 mm compared to the increase from 50 to 100 mm. The study also indicates that the content of organic matter influences the detention capacity as well. This is due to increased water-holding capacity and improved soil structure, which in turn improves the permeability of the soil.

4.2 Influence of Roof Geometry

Various studies on the slope influence on the retention capacity have been conducted in recent years, with varying results (Berndtsson, 2010). In an attempt to quantify the effect of slope on the retention capacity, (Getter et al., 2007) studied four different roof slopes over a two year period. The roof with a slope of 2 % showed the highest average retention with 85.2 %, while the 25 % roof had the least retention with 75.3 % in average.

TABLE 4.1 OVERVIEW OF THE TOTAL RAINFALL RETENTION, SHOWING THE MEAN PERCENTAGE

Slope [%]	**Light [%]**	**Medium [%]**	**Heavy [%]**	***Overall [%]***
2	93.3	92.2	71.4	*85.2*
7	94	89.5	66.4	*82.2*
15	94	88.6	58.4	*78*
25	95.5	87.8	57.1	*75.3*
Overall	*94.2*	*89.5*	*63.3*	*80.2*

Table 4.1 provides an overview of the retention of the roofs, for rain events classified as light,

medium and heavy, from the study. It indicates that slope affects the runoff retention capabilities. The retention decreases as the slope increases for medium and heavy storm events. This tendency is supported by (Villarreal and Bengtsson, 2005), where multiple controlled experiments on an extensive green roof showed that the total retention decreased as the slope increased. For a simulated 2.4 cm rain event, a green roof with a slope of 2 % retained 62 % of the precipitation. On the other hand, a green roof with a slope of 14 % retained no more than 39 % of the precipitation.

Another factor is the size of the drainage area, and how this affects the runoff. In a recent study conducted in New York (Hakimdavar et al., 2014), three different green roof sites was investigated. Having the same engineered components and age, the main difference was the drainage area. Three monitored roofs had the following drainage area: 310 (roof A), 99 (roof B) and 0.09 (Roof C) m^2. Based on the work done here, it is concluded that green roof scale and configuration are important determinants of green roof hydrological performance. More specifically, roof A and B displayed similar responses for small and medium events, with an average retention of 81 % and 46 % respectively for roof A, and 89 % and 52 % respectively for roof B. However for large rain events, roof B actually had the highest retention, with 43 % versus 25 for roof A. Roof C was lower in retention than the other roofs during small events, but it actually retained 46 % during medium events.

While there isn't a very clear relationship between roof scale and retention, the reduction in peak flow display a strong relationship to the scale of the green roofs. Especially for small and medium events, the peak flow is reduced as the green roof scale increases (Hakimdavar et al., 2014). This can be related to an increased average distance that the water must travel to the roof drain.

4.3 Vegetation

There is an agreement between many studies that what influences the retention capacity for green roofs is the substrate type and depth, rather than the vegetation (Dunnett et al., 2008, VanWoert et al., 2005, Monterusso et al., 2004). Even so, the vegetation type may impact the retention. It is found that vegetation plays a role in retaining water, especially in dry and warm periods (Dunnett et al., 2008), and having vegetation present may increase the evapotranspiration (Berghage et al., 2007). This will depend on the plant species however, and sedum in particular doesn't have very high evapotranspiration rates (Poe et al., 2015). However, it is generally observed that having multiple species instead of monocultures can

improve the retention capacity in terms of evapotranspiration, water capture and albedo (Wolf and Lundholm, 2008, Lundholm et al., 2010). The vegetation itself also affects the retention of water depending on the height of the plants, the diameter and the root and shoot biomass.

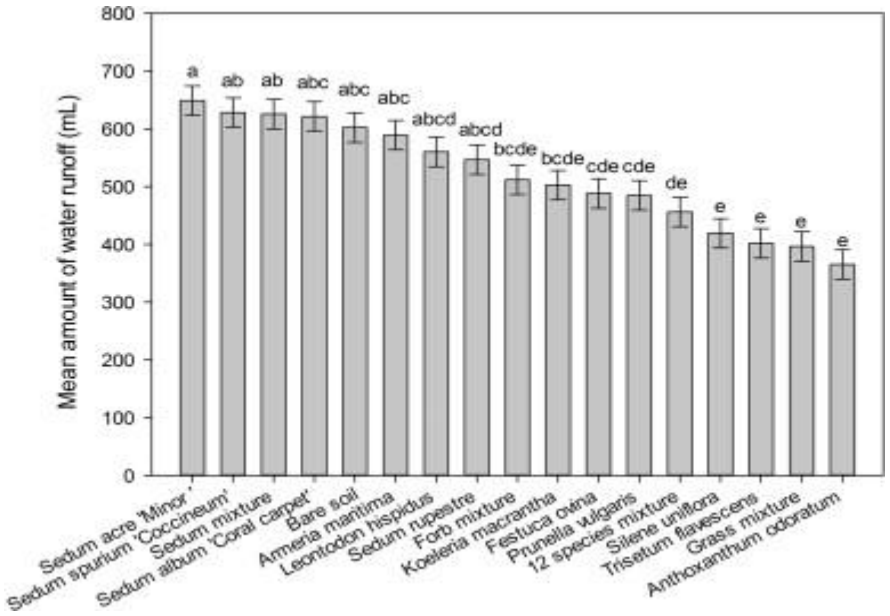

FIGURE 4.1 MEAN AMOUNT OF WATER RUNOFF FOR A SELECTION OF VEGETATION SPECIES (NAGASE ET AL., 2012)

The structural properties of the plants and the surface water holding capacity facilitates interception of rainwater (Nagase et al., 2012). The growth rate of the plants affects the amount of biomass, and slow growing species will have a low amount of this (Nagase et al., 2012).

As seen in figure 4.1, most sedum species actually provides more runoff than bare soil. There are similar findings in (Wolf and Lundholm, 2008, Butler, 2011). This could be due to the relatively low evapotranspiration rates of sedum, and also the fact that the plants covers the soil and thus may hamper the evaporation from the soil. It's also speculated that the differences in runoff among vegetation types is due to differences in substrate characteristics, rather than the vegetation itself (Monterusso et al., 2004).

4.4 Age of the Green Roof

As a green roof mature, the hydraulic conductivity of the roof may change. Over time, the pore structure and size can experience changes due to settling or changes in the organic matter content (Getter et al., 2007, Speak et al., 2013). As the roots decay or insects dig into the soil, the amount of free air space may increase. This will in turn lead to quicker initial runoff, however one study shows that while the pattern of retention may be affected, the overall quantity was not affected in a significant degree by the age of the roof (Mentens et al., 2006).

4.5 Antecedent Dry Weather Period

It is cardinal to consider the weather conditions prior to an event in addition to the event itself, when addressing the performance of green roofs. Many studies indicates the hydrological importance of the antecedent dry weather period (ADWP), among others (Stovin et al., 2012, Palla et al., 2011, Noreng et al., 2012). The saturation of the substrate at the beginning of a rain event is crucial for the retention capacity. In international literature, the typical time period used to separate rain events seems to be 6 hours, see for instance (Stovin et al., 2013, Nawaz et al., 2015, Speak et al., 2013). However, a fully saturated green roof will have a hard time drying in only 6 hours. A short dry weather period prior to the event means that the roof has less time to regenerate, and thus the soil may have a higher moisture content, so the duration of the ADWP is obviously of importance. However the weather conditions associated with this period, for instance cold or cloudy weather compared to warm and sunny weather, will greatly affect the regeneration (Stovin et al., 2012). Solar energy is the main driving factor for evapotranspiration (Marasco et al., 2015), which in turn is crucial to regenerate the water holding capacity of the roof.

A study done in a temperate climate by (Stovin et al., 2012), listed significant storm events along with various factors that were measured as part of the study. One of these factors were the ADWP. A regression plot was made for the retention against ADWP:

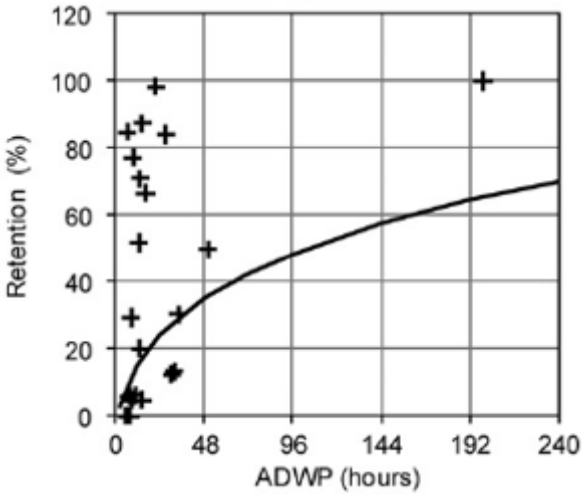

FIGURE 4.2 RETENTION % AS A FUNCTION OF ADWP (STOVIN ET AL., 2012)

The regression line indicates that the retention of water by a green roof increases as the ADWP increases. The trend isn't very evident, especially considering one single ADWP being significantly longer than the others. It is still an indication that a longer regeneration time is beneficial for the performance of green roofs. Observing the dates of the events, it is

also clear that the seasonal variations in regards of meteorological conditions also plays a part. The January events stands out as they have both very low ADWP and retention. As the climate gets warmer however, the retention is increasing. These seasonal changes will be further investigated in chapter 4.6.

4.6 Seasonal Variations

The retention capacity of green roofs depends on the meteorological conditions, and thus it will vary through different seasons (Bengtsson et al., 2005, Stovin et al., 2012, Nawaz et al., 2015). Warmer seasons provides a higher degree of evapotranspiration, through air temperature, solar radiation and relative air humidity (Poe et al., 2015, Voyde et al., 2010, Marasco et al., 2015), which provides faster regeneration of the roofs capacity. How each season is defined in the different studies varies, but generally three to four seasons are defined. In the summary of German studies (Mentens et al., 2006), a significant difference in runoff was found between the seasons 'Warm', 'Cool' and 'Cold': respectively 30 %, 51 % and 67 %.

A couple of Scandinavian studies reporting runoff reduction on a monthly basis (Bengtsson et al., 2005, Braskerud, 2014), showed that precipitation in cold weather, as rain, was not retained in any significant degree. From the Swedish study (Bengtsson et al., 2005), a retention of around 18 % was achieved. A significant difference to June, where 87.5 % of all the precipitation was retained. Measurements over the course of five years in Oslo, Norway (Braskerud, 2014), showed that the lowest reduction in runoff was in November, with no more than 3.5 % retention. The highest runoff reduction found place in May, with 55.5 % retention.

Also the rainfall characteristics varies over the year. Higher temperatures provides the air with a higher water holding capacity (Braskerud, 2014), therefore the likelihood of large storm events increases in warmer seasons. However, the higher evapotranspiration rates and a higher hydraulic conductivity means a higher retention capacity for the green roofs. In cool and cold seasons, the substrate will more likely have a higher degree of saturation due to humid conditions, low evapotranspiration and possibly, albeit not necessarily more intense ones, more frequent storm events (Poe et al., 2015, Schroll et al., 2011). In turn, this gives a reduced capacity for retaining stormwater. Figure 4.3 shows a comparison between spring and summer evapotranspiration over the course of a month, from an experimental study by (Poe et

al., 2015). It also show how the evapotranspiration rates are higher at first as the degree of saturation is higher.

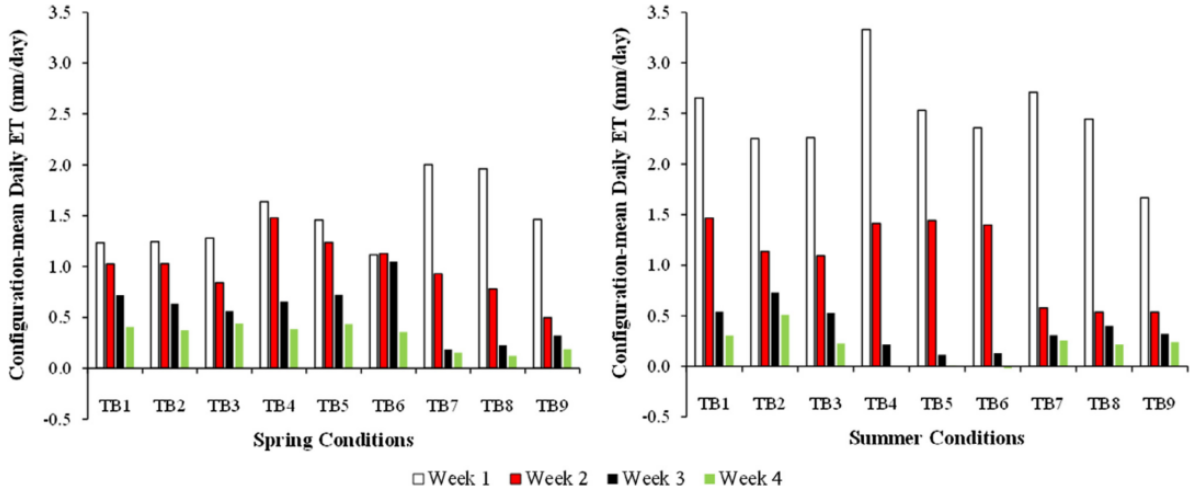

FIGURE 4.3 COMPARISON OF EVAPOTRANSPIRATION RATES FOR SPRING AND SUMMER CONDITIONS FOR NINE DIFFERENT GREEN ROOF CONFIGURATIONS (POE ET AL., 2015)

In Nordic countries especially, the influence of snow is a topic of interest. If we have precipitation in the form of snow, it will be stored at roof regardless if it's a green roof or a conventional, impervious roof. As the frozen surfaces and snow reflection will limit evapotranspiration, most the accumulated snow will eventually melt and discharge (Allen, 1998). As the snow melts however, green roofs will reduce the runoff (Braskerud, 2014).

4.7 Rainfall Characteristics and Extreme Events

The characteristics of the rain event will influence the retention capacity of a green roof to a significant degree (Berndtsson, 2010). Such rainfall characteristics include rainfall depth, intensity and duration, and results in a wide range of retention values within and between different studies (Nawaz et al., 2015, Carson et al., 2013, Palla et al., 2011, Stovin et al., 2012). It can be said to be a triangle between the rain size, intensity and duration in terms of influencing retention. A green roof is an effective control unit for stormwater quantity as long as the intensity is low and the duration of the precipitation is not very long. With higher intensity storm events however, the effectiveness is reduced (Fassman-Beck et al., 2013, Carson et al., 2013). Still it's a good tool for delaying and attenuating peak flows, which is important for avoiding combined sewer overflows. It seems that the intensity is the main driving weather factor providing runoff, but that is not always the case. Short events with intense precipitation seems to be better held back than events with longer duration, in spite of a smaller intensity (Braskerud, 2014).

In addition to the event itself, the weather characteristics prior to an event, which influences the moisture content in the substrate, is an important factor for the retention capacity in an intense event of short duration. For an event of long duration, the roof will eventually saturate after a while (Noreng et al., 2012). Still, for any given length, for a lower intensity in precipitation the retention capacity of a green roof will increase, and even more so if the roof has a low degree of saturation by at start of the event (Villarreal and Bengtsson, 2005). This is an important part of urban stormwater management, because even if a rainfall is small, retaining it can still help prevent CSOs which in turn reduces the risk of pollutants entering water recipients (Getter et al., 2007, Fassman-Beck et al., 2013).

A study conducted in Sheffield, UK, found a median retention 30.2 %, and thus a reduction in runoff intensity of 69.8 %. These numbers was found by considering 21 storm events with return periods above one year, and with a median mean intensity of 1.83 mm per hour. There was a median of 18 minute delay in peak runoff, with a total reduction close to 60 % (Stovin et al., 2012). For the most significant event, with a return period of 16 years, no more than 13.2 % of the precipitation was retained.

According to (Noreng et al., 2012), SINTEF has conducted two studies on green roofs, where a constant precipitation of 1 mm/minute was applied to a sedum roof for 60 minutes, in a controlled experiment. For the sedum roof, it took 75 minutes before the runoff was equal to that of a conventional roof when the green roof had a saturation of 11 % to begin with. With an initial saturation 60 %, it took 35 minutes for the runoff to equal that of a conventional roof.

NVE released a report on extreme precipitation measured on a green roof site in Oslo (Braskerud, 2014). The site consists of two green roof plots with sedum vegetation and a 30 mm substrate, in addition to a conventional reference roof. One plot (GT1) had a drainage layer and one plot (GT2) had a felt mat. Considering the most intense events for each month over the course of a year, the following retention was achieved:

TABLE 4.2 MONTHLY RETENTION OF THE MOST INTENSE 5 MINUTES PRECIPITATION (MAX) AND RETENTION OF THE AVERAGE PRECIPITATION (AVERAGE) FOR TWO GREEN ROOF BEDS, AND A REFERENCE ROOF

	GT1		GT2		Reference	
Month	**Max**	**Average**	**Max**	**Average**	**Max**	**Average**
January	74	71	78	73	46	67
February	66	20	75	19	63	-6
March	48	-47	49	-53	36	-66
April	43	-55	52	-27	-1	-87
May	70	55	75	54	2	6
June	57	40	62	43	22	5
July	58	40	69	41	9	11
August	49	28	56	29	3	7
September	55	24	65	25	6	4
October	49	18	65	20	14	0
November	52	3	59	4	4	-3
December	75	24	67	20	39	2

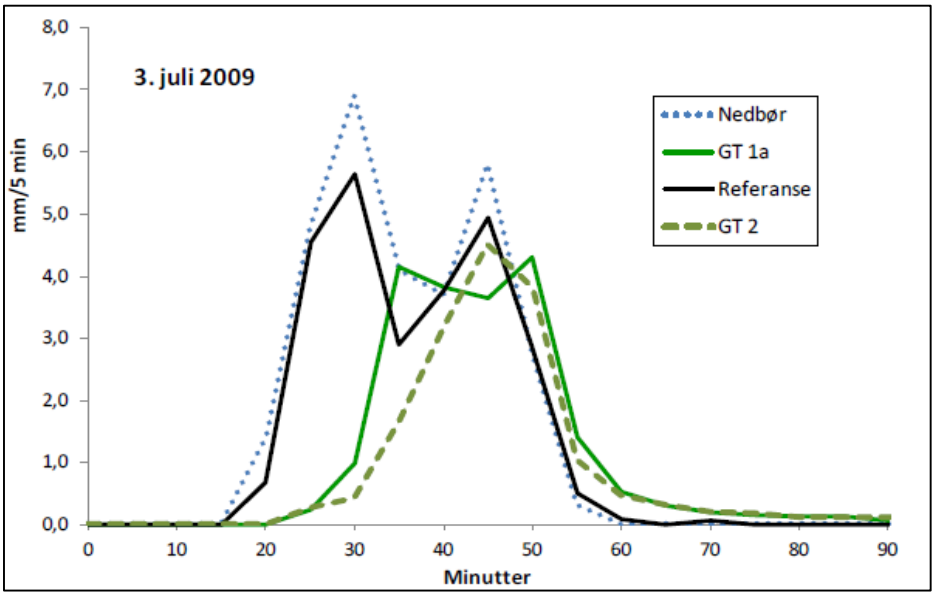

FIGURE 4.4 GREEN ROOF RESPONSE EON A STORM EVENT IN OSLO, WITH A RETURN PERIOD OF 40 YEARS (BRASKERUD, 2014)

Due to accumulation of snow, the retention numbers during winter may be high. Likewise, when the snow melts, the values are negative due to runoff from the snow storage in addition to the precipitation. Through the months April – November, the retention were generally good for the most intense events. In the same report, an event with an intensity of 29.4 mm in 30

minutes, or 163 l/(s*ha), was presented in detail. It is of special interest as the substrate was considered to be completely dry at the beginning of the event.

Roof GT1 generally retains less water than roof GT2, and for this event it has a quicker runoff response. 5 minutes after the peak rainfall intensity, roof GT 1a reaches its first peak with 27 % attenuation. Interestingly the rainfall has two peaks and so does GT 1a, and is delayed by 5 minutes and attenuated by 13 % as the roof is already saturated. Around 15 minutes after the first rainfall peak, roof GT 2 reaches its peak with an attenuation of 35 %.

TABLE 4.3 A COMPILATION OF THE RUNOFF FROM THE TWO GREEN ROOFS FOR DIFFERENT RAINFALL INTENSITIES

Duration [min]	Rainfall intensity [l/(s*ha)]	GT 1a runoff [%]	GT 2 runoff [%]
5	230	38	35
10	195	32	29
20	171	22	36
30	156	35	48
60	83	33	46

Another study (Hakimdavar et al., 2014) reports runoff as a function of different rainfall characteristics. Considering the event duration, the retention was 85 % for events with a duration less than 10 hours, 67 % for events lasting 10-20 hours, and only 55 % for events lasting longer than 20 hours. Considering the total rainfall depth, events less than 20 mm resulted in retention of 85 %, whereas it was 48 % for 20-40 mm storm events. For rainfall as heavy as above 40 mm, the retention was no more than 32 %. The peak reduction was respectively 89, 62 and 51 %. A similar trend is also found in (Carter and Rasmussen, 2006, Carson et al., 2013, Getter et al., 2007) among other studies.

A model of green roof single event and long term hydrological performance, calibrated and validated using measurements from a green roof site in Denmark, is described in (Locatelli et al., 2014). Simulations of both 10 minutes peak reduction per event and volume reduction as a function of different return periods, illustrates the effect of green roofs in different storm event sizes:

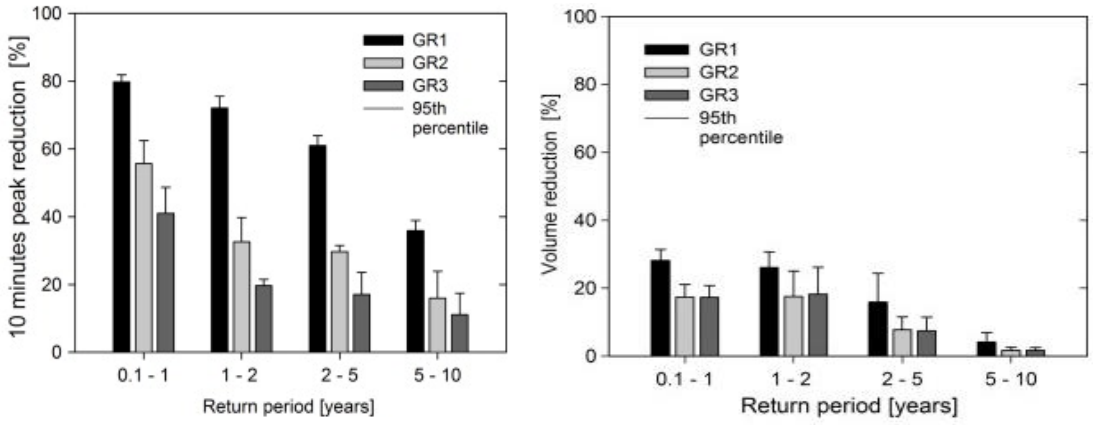

FIGURE 4.5 SIMULATED PEAK REDUCTION AND VOLUME REDUCTION FOR THREE DIFFERENT GREEN ROOFS (LOCATELLI ET AL., 2014)

The roof's characteristics are given in table 5.3. The roofs are quite effective in attenuating peak flows, however the volume reduction is minimal especially for larger return periods. It is clear that roof GR1 performs best, despite a smaller area and steeper slope. It has the highest overall thickness and a significantly higher water holding capacity.

	GR1	GR2	GR3	Reference roof
Location	Odense	Copenhagen	Copenhagen	Copenhagen
Area (m^2)	9	20	20	20
Slope (°)	10	4.3	4.3	4.3
Overall thickness (mm)	80	70	60	–
Vegetation type	Sedum and herbs	Sedum and herbs	Sedum and herbs	–
Saturated weight (kg/m^2)	130	55	45	–
Drainage (mm)	40	40	[a]	–
Drainage material	Mineral wool	Exapanded foam	Holes in plastic trays	–
Substrate depth (mm)	40	30	60	–
Substrate material	Soil	Crushed clay, medium-fine peat, compost	Crushed clay, medium-fine peat, compost	–
Water holding capacity (l/m^2)	53	31	No data	–

FIGURE 4.6 CHARACTERISTICS OF THE THREE GREEN ROOFS WHOSE PERFORMANCE IS GIVEN IN FIGURE 4.2 (LOCATELLI ET AL., 2014).

GR3 has no data on the water holding capacity, but a lower saturated weight indicates a lower water holding capacity than the other roofs. The drainage material used in GR1 and GR2 will hold some water whilst GR3 has drainage holes placed 1 cm above the bottom, and the only water holding material is the substrate.

5 Modelling Evapotranspiration

5.1 Background Theory

As defined in chapter 3.3.3, evapotranspiration is the process where water returns to the atmosphere through both evaporation and transpiration. It depends on the access to water, energy influx, positive gradient in saturation and surface type (Dingman, 2015). It is therefore affected by the vegetation, substrate characteristics and the climate conditions following a storm event. Due to it's direct relationship to the soil moisture, the evapotranspiration is vital for restoration of the retention capacity of a green roof. Hence, gaining knowledge of the behavior of green roofs regarding soil moisture and evapotranspiration is of great importance. By looking at the water balance equation, the relationship between soil moisture and evapotranspiration is given (Berretta et al., 2014).

$$\frac{\Delta\theta}{\Delta t} = P - R - ET, \qquad (5.1)$$

where Δθ is the change in moisture content, over a period Δt, P is precipitation, R is runoff and ET is the evapotranspiration. However, in dry weather periods, P and R are assumed to be zero. This means that theoretically, soil moisture loss is due to evapotranspiration solely and should be equal. For a sloped roof however, this may not be entirely correct as water will slowly discharge towards lower parts of the roof. Also, regardless of the slope, some water will infiltrate through the substrate and into the drainage layer.

It is important to separate potential evapotranspiration (PET) and actual evapotranspiration (AET). PET gives the maximum possible evapotranspiration, when there is no limitation by plant or soil moisture content. AET on the other hand accounts for water limited substrate moisture content and differences in surface conditions, plant physiology, plant health and weather (Hendriks, 2010, Marasco et al., 2015).

A precise estimation of actual evapotranspiration is useful in many aspects. Not only stormwater management, but also the study of climate change, crop water requirement management, drought forecasting, and development and utilization of water resources, among other things (Zhao et al., 2013). Evaporation estimation methods used in hydrological models may be classified into two groups. One estimates water surface evaporation, soil evaporation and vegetable transpiration separately, and then integrates them. The other group of methods estimates the potential evapotranspiration, before converting it into actual evapotranspiration by applying the soil moisture extraction function (SMEF), as given below (Zhao et al., 2013).

$$AET = PET(\frac{SMT}{SMC}), \quad (5.2)$$

where SMT is actual soil moisture, and SMC is field moisture capacity. SMC is the amount of water that's held in the soil after excess water is drained by the gravity, as defined in chapter 3.3.2. This is a basic function, and describes AET at a generic time t. There are however various variants of the SMEF and examples of these can be found in (Zhao et al., 2013). One may also introduce a factor K to account for the specificity of green roof substrates, and differences between the sedum vegetation of interest and the reference grass crop used in the PET model (Berretta et al., 2014). This factor is often referred to as the crop coefficient.

5.2 Evapotranspiration Models Studied on Green Roofs

An overview of various models that may provide a good estimate for PET in Norwegian conditions can be seen in table 5.1 below.

TABLE 5.1 MODELS FOR ESTIMATING POTENTIAL EVAPOTRANSPIRATION

Name	Function	Reference	Eq.
1975 Hargreaves	$ET_0 = 0.00135R_s(TC + 17.8)$	(Hargreaves and Allen, 2003)	*5.3*
1985 Hargreaves	$PET_H = 0.0023R_a(T_{mean} + 17.8)(T_{max} - T_{min})^{0.5}$	(Hargreaves and Allen, 2003)	*5.4*
Priestley-Taylor	$PET_{PT} = 0.408 \propto \frac{\Delta}{\Delta + \gamma(R_n - G)}$	(Priestley and Taylor, 1972)	*5.5*
Penman	$PET_P = 0.408\frac{\Delta}{\Delta + \gamma(R_n - G)} + \frac{\gamma}{\gamma + \Delta}E_A$	(Penman, 1948)	*5.6*
Penman-Monteith ASCE standardized reference ET	$RET = \frac{0.408\Delta(R_n - G) + \gamma(\frac{C_n}{T + 273})u_2(e_s - e_a)}{\Delta + \gamma(1 + C_d u_2)}$	(Marasco et al., 2014)	*5.7*
FAO-56 Penman-Monteith	$ET_0 = \frac{0.408\Delta(R_n - G) + \gamma\frac{900}{T + 273}u_2(e_s - e_a)}{\Delta + \gamma(1 + 0.34u_2)}$	(Allen, 1998)	*5.8*
Thornthwaite	$PET_{TH} = PE_x\frac{DT}{360}$	(Wilson, 1990)	*5.9*
Blanley- Cridle	$ET_{BC} = p(0.46 * T_{mean} + 8)$	(Brouwer and Heibloem, 1986)	*5.10*

While quantification of evapotranspiration and soil moisture haven't been given a lot of attention historically, various studies have measured evapotranspiration in green roofs, often by the use of a lysimeter (Marasco et al., 2015, Wadzuk et al., 2013, DiGiovanni et al., 2013). A lysimeter measures evapotranspiration by isolating a volume and measuring incoming precipitation, along with runoff and change in soil moisture content. The following water balance can be set up, when using a weighing lysimeter (Wadzuk et al., 2013):

$$ET = P - R - \Delta\theta z_s, \qquad (5.11)$$

where $\Delta\theta$ is the average moisture content change of the soil, z_s is the depth of the soil, P is the precipitation and R is the surface runoff. It is however of interest to also be able to model evapotranspiration. Historically this has been for predicting water needs for agricultural irrigation (Wadzuk et al., 2013), but various green roof studies in recent years have also evaluated different PET models.

Generally PET models will overestimate evapotranspiration during draught and underestimate it during periods with heavy precipitation (Marasco et al., 2015). At substrate field capacity, AET will be equal to PET. This is especially the case for the different variants of Penman, as seen in (DiGiovanni et al., 2013, Wadzuk et al., 2013, Marasco et al., 2015). This has to do with an assumption that moisture is in abundant supply and that ET won't be constrained by the soil moisture deficit (Wilson, 1990, Poe et al., 2015). However, there will only be short periods where the green roof is completely saturated. When less than saturated, the soil moisture deficit will constrain the AET. This means that PET models will often overestimate.

In Sheffield, UK, (Stovin et al., 2013) modelled long term volumetric and storm event runoff retention performance for extensive green roofs. For this a hydrological flux model was developed, and included a SMEF which enabled evapotranspiration to be predicted from a PET function. They used the Thornthwaite temperature-based formula. The results were somewhat imprecise, and they found that further work is required to better reflect the evapotranspiration within specific green roof configurations. Another study prior to this suggested using a modified Thornthwaite by multiplying by a constant of 0.75, as the model generally correlated well with observed data but tended to overestimate (Kasmin et al., 2010).

Yet another study from Sheffield modelled PET by using the FAO64 Penman-Monteith and 1985 Hargreaves (Berretta et al., 2014). Fairly similar results were achieved by the two models, but they recommend using a model based on Hargreaves due to the lesser data

requirements. The study supports the importance of using a crop coefficient when calculating AET, together with a SMEF function.

Various models were examined by (Wadzuk et al., 2013). Experiments were performed at temperatures above 10 ^{o}C and the monthly evapotranspiration varied between 50-200 mm. They found that the 1985 Hargreaves overestimated substantially and was considered a bad indicator for daily evapotranspiration, however for longer periods it works better. Priestley-Taylor underpredicted slightly. Both Blaney-Criddle and Penman ASCE both over- and underestimated but performed quite well overall, and were closest to the observed evapotranspiration.

5.3 Models to be Used on Local Field Data

In this thesis, evapotranspiration from the green roof at Risvollan will be modelled. In order to estimate the PET, three different models will be used and the results will be compared. These are the 1985 Hargreaves, Penman-Monteith and Thornthwaite. A SMEF will then be implemented to calculate AET. Following is a more detailed description of the models of interest.

The models are chosen as they have been used in various green roof studies, and further due to their diversity. It is of interest to compare the well-known but rather complex Penman-Monteith to models that require less data. 1985 Hargreaves only requires temperature and an estimation of the extraterrestrial radiation, while Thornthwaite only needs temperature data. The latter model also calculates PET on a monthly basis.

5.3.1 1985 Hargreaves

The 1985 Hargreaves is developed from the 1975 Hargreaves model, but do not require data for global solar radiation (R_s) (Hargreaves and Allen, 2003). Its simplicity in terms of input data makes it popular for hydrological modelling, and it should provide good estimations for longer time periods. In this thesis, the PET is calculated with moving average of daily values from 5 day periods. As given in table 5.1 (Eq. 5.4):

$$PET_H = ET_0 = 0.0023 * R_a * (T_{mean} + 17.8) * (T_{max} - T_{min})^{0.5}, \quad (5.4)$$

where T_{max} and T_{min} is the mean daily maximum and minimum temperatures for the 5 day period, in Celsius, and T_{mean} is the mean value of T_{max} and T_{min} ((T_{max}+T_{min})/2). R_a is the average extraterrestrial radiation over five days, in mm/day (Hargreaves, 1994, Hargreaves and Allen, 2003). R_a is calculated using the latitude for the location of interest, which in this

case is Risvollan with a latitude of 63.43° (eKlima, 2016). It can be calculated for each day of the year, where 1st of January is day number 1, and 31st of December is day number 365. The following stepwise calculation is carried out using Microsoft Excel as a calculation tool (Alfredsen and Killingtvet, 1999, Iqbal, 2012):

1. Convert the latitude (lat.deg) from degrees to radians (lat.rad).

$$Lat.rad = lat.deg * \frac{\pi}{180}, \quad (5.4a)$$

2. Calculate magnetic declination in radians (decl.rad).

$$decl.rad = 23.45 * \sin\left(\pi * \frac{360}{365*180} * (daynumber * 284)\right) * \frac{\pi}{180}, \quad (5.4b)$$

3. Calculate the eccentricity (Eccs).

$$E_{ccs} = 1 + 0.033 * \cos\left(\frac{2\pi}{365} * Decl.rad\frac{180}{\pi}\right), \quad (5.4c)$$

4. Calculate the sun angle (sun.ang) in radians.

$$sun.ang = -1 * \tan(lat.rad) * \tan(decl.rad) \quad (5.4d)$$

If the absolute value of sun.ang is larger than 0.99, then the angle is 180°, and $R_a = 0$. If not then the angle is as calculated in Eq. 5.4.4, and R_a is as calculated in the next step.

5. You can now calculate the daily extraterrestrial radiation, R_a:

$$R_a = \frac{lat.deg}{\pi} * E_{ccs}^2 * (sun.ang * \sin(lat.rad) * \sin(decl.rad) * \cos(lat.rad) * \cos(decl.rad) * \sin(sun.ang) * 689) \left[W/_{m^2}\right], \quad (5.4e)$$

6. Lastly, R_a has to be converted into mm/day before it's implemented into the PET model. 1 Watt equals 1 Joule per second, while MJ/(m^2day) equals 0.408 mm/day. The latter relationship is based on an assumption of a temperature of 20 °C, but for temperatures within 30 and 10 °C the variance is less than 1 % (Allen, 1998, Hargreaves, 1994).

$$R_a \left[\frac{W}{m^2}\right] * 86400 \left[\frac{seconds}{day}\right] * 10^{-6} * 0.408 = R_a \left[\frac{mm}{day}\right], \quad (5.4f)$$

5.3.2 FAO-65 Penman-Monteith

The FAO-56 Penman-Monteith version of the Penman formula is used for estimating reference crop evapotranspiration, ET_0, on a daily or monthly basis, and is as given in table 5.1 (Eq. 5.8):

$$ET_0 = \frac{0.408\Delta(R_n - G) + \gamma\frac{900}{T+273}u_2(e_s - e_a)}{\Delta + \gamma(1 + 0.34u_2)}, \quad (5.8)$$

This standardized scheme is considered to be the standard method in hydrological and irrigation applications at well-watered meteorological stations with varying conditions and locations (Valiantzas, 2013). The following accurate approximate will be used, as proposed by (Valiantzas, 2013):

$$ET_0^{(P-M)} \approx 0.051(1-\alpha)R_S\sqrt{T+9.5} - 0.188(T+13)\left(\frac{R_S}{R_a} - 0.194\right)\left(1 - 0.00015(T+45)^2\sqrt{\frac{RH}{100}}\right) - 0.0165R_S u^{0.7} + 0.0585(T+17)u^{0.75} * \frac{\left((1+0.00043*TR^2)^2 - RH/100\right)}{1+0.00043*TR^2} + 0.0001Z, \quad (5.12)$$

where α is a constant of 0.23, R_a is the extraterrestrial radiation in MJ/m^2 per day estimated as described in chapter 5.3.1, R_S is the global solar radiation in MJ/m^2, T is the mean temperature, TR is the difference between the maximum and minimum temperature. All temperature input is in Celsius. RH is relative air humidity, u is wind speed in m/s and Z is the elevation of the site, in meters. The field roof lies approximately 110 meters above sea level (Johannesen, 2016). The wind speed and global solar radiation is measured at Risvollan Urban Hydrological station. Wind speed has been measured at green roof field at Risvollan since February 2016. Due to the short time period it hasn't been applied for calculating evapotranspiration, but a relationship for the wind speed measured at the green roof and the Urban Hydrologican station has been developed (Johannesen, 2016).

$$u_{GR} = 2.664 * u_{RUH} - 0.484, \quad (5.13)$$

where u_{GR} is the approximate wind speed at green roof site, and u_{RUH} is the wind speed at Risvollan Urban Hydrological station. R_s is assumed to be equal for the two sites.

5.3.3 Thornthwaite

One of the simplest formulas for estimating evapotranspiration is the Thornthwaite model, which only requires the monthly mean temperature as input. It is an empirical formula based on measurements for potential evapotranspiration from USA, with vegetation being short and close-set, and with adequate water supply (Kasmin et al., 2010). As given in table 5.1 (Eq. 5.9):

$$PET_{TH} = PE_x\frac{D*T}{360}, \quad (5.9)$$

where PE_x is the potential evapotranspiration for any month, D is the number of days in the month, and T is the average number of hours between sunrise and sunset in the month. PE_x is given as

$$PE_x = 16(\frac{10t}{J})^a, \quad (5.9a)$$

where the yearly heat index J is given as

$$J = \sum_1^{12} j \ (for\ the\ 12\ months), \quad (5.9b)$$

where j is the monthly 'heat index', and a summation of these over the course of a year gives the yearly heat index. It's calculated from the following formula:

$$j = (\frac{t_n}{5})^{1.514}, \quad (5.9c)$$

where t_n is the average monthly temperature of the consecutive months of the year in degrees Celsius. The parameter a is calculated as follows:

$$a = (675 * 10^{-9})J^3 - (771 * 10^{-7})J^2 + (179 * 10^{-4})J + 0.492 \quad (5.9d)$$

In order to calculate T, the daylight for each day in a year is calculated based on the latitude of the area of interest. The monthly average will then give the average hours between sunrise and sunset for each month. In (Forsythe et al., 1995) this model is evaluated to provide a very precise estimate for daylight:

$$T = 24 - \frac{24}{\pi} * \arccos\left(\frac{\sin(0.8333 * {}^{\pi}/_{180}) + \sin(lat.deg * {}^{\pi}/_{180}) * \sin(P)}{\cos(lat.deg * {}^{\pi}/_{180}) * \cos(P)}\right), \quad (5.9e)$$

where lat.deg is latitude entered in degrees and P is calculated by the formula

$$P = \arcsin(0.39795 * \cos(0.2163108 + 2 * \arctan(0.9671396 * \tan(0.0086 * (Yd - 186))))), \quad (5.9f)$$

where Yd is the day of the year.

6 Calibration Methodology

6.1 Description of the Sensor

In order to measure the humidity in the green roof plots, a Decagon 5TM VWC & Temperature sensor has been installed. The sensor measures the dielectric permittivity (ε_a, unitless) of the soil, or eventually any other media, by using capacitance/frequency domain technology. It additionally measures temperature. The difference in the dielectric permittivity in air and water is large. Air should give ε_a =1 and water should give ε_a =80, and thus the water content in a porous material can be seen as a function of dielectric permittivity. Signal filtering minimizes salinity and textural effects. Factory calibrations are included for mineral soils, rockwool and perlite. The influence volume of the sensor is 715 ml and is illustrated in figure 6.1.

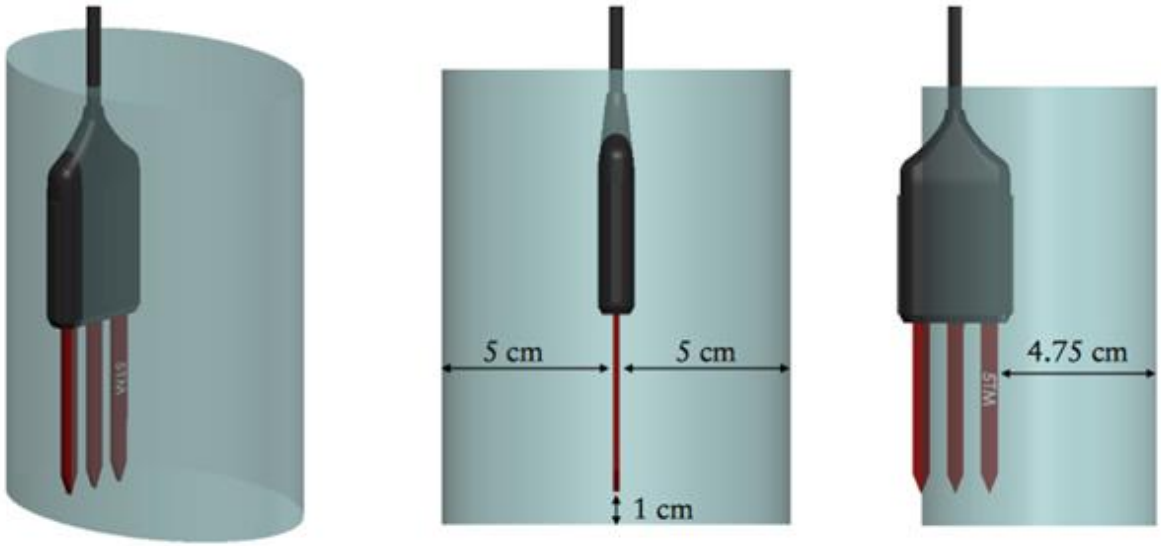

FIGURE 6.1 IDEALIZED MEASUREMENT VOLUME OF DECAGON 5TM SENSOR (DECAGON DEVICES INC, 2015)

From the manufacturer the sensor is calibrated for use in normal mineral soil with saturation extract electrical conductivity <10 dS/m, giving an accuracy of $\pm$ 3 % VWC (Inc, 2016). The following equation is presented in the manual (Topp equation) and used for automatic calibration of the field instrument (Topp et al., 1980, Inc, 2016):

$$VWC = 4.3 * 10^{-6}\varepsilon_a^3 - 5.5 * 10^{-4}\varepsilon_a^2 + 2.92 * 10^{-2}\varepsilon_a - 5.3 * 10^{-2} \qquad (6.1)$$

For soilless growth substrates, such as potting soil, rockwool and cocus, an accuracy of $\pm$ 5% is expected. For more accurate readings, or if the soil has a very high electrical conductivity or non-normal mineralogy one should conduct a soil specific calibration. Calibration

equations for non-soil media exist from the manufacturer for potting soil, rockwool and perlite.

6.2 Equipment and Materials

The following equipment were needed for the calibrations:

- 3 x Beaker glass 2 l, diameter 130 mm, height 185 mm
- 3 x Glass boxes, depth 150 mm, area 210*230 mm
- Soil core sampler for determining field bulk density
- Data logger and three sensors
- Plastic containers/boxes for soil storage
- Tablespoon
- Scale, resolution 3 g
- Drying oven at 80 ^{o}C
- Erlenmeyer flask, 50 ml and 100 ml
- Distilled water
- Table to keep sedum mats on, width 1.5 m, length 1.35 m
- Plant lights, 58 W
- Climate room/freezer for temperature calibration

The following materials were ordered prior to the laboratory work:

- ‘Roofgarden substrate extensive’ substrate from Sempergreen B.V. (Substrate S1)
- ‘Sedum Jord SH’ substrate from Grønn Vekst Sør (Substrate S2)
- ‘Substrate plates S50’ Grodan (rockwool) mat from Seempergreen, 50 mm thickness
- VT filt from VegTech AB, 10 mm thickness
- Filt mat SSM45 from Zinco Norge AS, 5 mm thick
- Floradrain FD 25-E drainage mat from ZinCo Norge AS
- Xv Green 20 Drainage mat from Oldroyd AS
- ‘SF systemfilter’ from Zinco Norge AS, 0.6 mm thickness
- Roof membrane
- ‘Bergknapp sedummix’ sedum mats from Bergknapp AS

6.3 Soil Specific Calibration

In order to measure the correct humidity of materials used in green roofs and to investigate the need for calibration specifically for each substrate, a standard calibration is first carried

out. A standard calibration, or a soil specific calibration, means measuring in a sample that in size is bigger than the influence volume of the sensor. After such a calibration is completed, a field specific calibration will be carried out. For this case it means a calibration with the actual configuration of the green roofs, in order to find measuring errors due to materials being thinner than the actual influence volume. This is described further in chapter 6.4.

A calibration routine is given in (Cobos, 2010). In this procedure, the water content is controlled by taking a sample of the material, and then weighing and drying this. An alternative calibration routine is to take a known sample volume and add a known amount of water. Then the water content can be calculated, instead of taking samples. It is decided to use a procedure based on the latter procedure in this laboratory work, and it will be described in detail in the following.

6.3.1 Calibration Procedure

Two types of substrates will be used for calibration. The substrate will be mixed well and about 2 l of sample is taken out. It is then at first air dried with the soil spread out in a thin layer, before it's dried in an oven at 80^{o}C.

Each experiment is run in 3 parallels with the same material. For the calibration specific to the two substrate types, the procedure has been as follows:

1. Measure the weight of the beaker.
2. Pack 1.5 litres of dry substrate in calibration container and find the density.
3. Insert the sensor vertically. The sensor should be surrounded by soil for a radius of 5 cm as in the description of ideal mounting.
4. Wait for å stable reading and collect raw data.
5. Measure 50 ml of distilled water in an Erlenmeyer flask, control by weight.
6. Pour the sample into a plastic box, sprinkle the water over the sample and mix before the sample is put back into the beaker glass. Sensor is inserted.
7. Cover the sample with a plastic foil and leave until reading is stable; 10 minutes after water addition to the last parallel.
8. Collect raw data, which due to minor variations are the mean value of the last five registered values.
9. Repeat from step 5-8 until the sample is saturated.

6.4 Field Specific Calibration

In order to investigate eventual errors caused by the specific field setup, a field specific calibration is conducted. The mounting of the sensors and the influence volume deviates from the standard setup, so this is important to investigate. The calibration experiments has basis in the four roof plots at Risvollan and will imitate these through four calibrations. With the same components in the different layers, small box scale samples of the roof plots are built up. The equipment is as described for the standard calibration, and the specific setup for each calibration is described below in chapter 6.3.1.

6.4.1 Sample Preparation

A glass box with an area of 21x23 cm is filled with dry materials to copy field conditions at Risvollan. This is done in three equal parallels.

TABLE 6.1 AN OVERVIEW OF THE BOX SCALE SAMPLES FOR FIELD SPECIFIC CALIBRATION, ALONG WITH THE GREEN ROOF CONSTRUCTIONS AT THE RISVOLLAN FIELD ROOF

Roof plots	**Laboratory box scale samples**
Plot 1: Roof membrane in bottom Felt mat from VegTech AB Sedum mat on top	Plot 1: Roof membrane in bottom Felt mat from VegTech AB Sedum mat on top
Plot 2: Roof membrane in bottom Grodan mat from Seempergreen B.V. Sedum mat on top	Plot 2: Roof membrane in bottom Grodan mat from Seempergreen B.V. Sedum mat on top
Plot 3: Roof membrane in bottom SSM45 felt from Zinco Flodrain FD25-E from Zinco SF systemfilter from Zinco 5 cm substrate, S2 Grønn Vekst Sør Sedum mat on top	Plot 3: 5 cm substrate, S2 Grønn Vekst Sør Sedum mat on top

Plot 4: Roof membrane in bottom Drainage element from Olderoy 5 cm substrate, S1 Sempergreen B.V. Sedum mat on top	Plot 4: 5 cm substrate, S1 Sempergreen B.V. Sedum mat on top

6.4.2 Calibration Procedure

Each experiment is run in 3 parallels with the same material. All experiments are done in room temperature.

1. Measure the weight of the glass tray.
2. Fill and place sensor according to one of the alternatives described above.
3. Measure weight and volume of sample
4. Wait for å stable reading and collect raw data.
5. Remove the sedum mat.
6. Measure distilled water in an Erlendmeyer flask. Amounts are given in chapter 6.4.
7. Sprinkle the water over the sample.
8. Put the sedum mat back.
9. Cover the sample with plastic foil or aluminium foil and leave until reading is stable.
10. Collect raw data.
11. Repeat from number 5 until sample is saturated/field capacity is reached.

6.5 Specific Description of the Experiments

In this chapter, each experiment will be described in detail in order to exemplify the general procedure and to provide a deeper understanding of the conditions underlying the calibrations. Please note that through this laboratory work, a lot of time and effort were spent in order to work out a procedure. Various experiments were unsuccessful or considered trials, and these are not accounted for. Seven counting experiments were conducted and will be described in the following.

6.5.1 Soil Specific Calibration for S1

Roofgarden substrate extensive, produced by Sempergreen B.V. and delivered by Natur & Utemiljø AS, is named substrate S1 in this project. It is an extensive substrate consisting of lava, bims and compost, and is a suitable material for extensive green roofs. Its field capacity is approximately 30 % VWC.

Three beaker glasses of 2 litres was filled with well mixed soil. Slightly more than 1.5 litres was added and then compressed. For each parallel, the bulk density at 1.5 litres is 1.17 kg/l and the weight is 1750 g. The room temperature as the experiment begun was 20.4 ^{o}C, as the average value given by the sensors. The water addition was conducted by taking the soil out of the beaker glass and into a plastic tray, and then distributing the water evenly before mixing and returning the soil to the beaker glass. This ensured a more even distribution of water. 50 ml of distilled water was added every 10 minutes after addition to the last parallel, when the data was stabilized. Due to minor variations in the registered dielectric permittivity, the value collected is the average value of the last five minutes before another 50 ml of distilled water is added. This will give a representative value. This exact procedure was also followed for the remaining soil specific calibration.

In this case, 50 ml of distilled water was added 12 times in total to each parallel. However, field capacity was reached by the 9th addition. This gives a representative amount of 450 ml of distilled water at saturation. The results will be discussed in chapter 7.

6.5.2 Soil Specific Calibration for S2

The S2 substrate is a product by Grønn Vekst Sør and was delivered by ZinCo Norge AS, and is named Sedum Jord SH. It's a soil mixture consisting of fractioned brick, peat, leca and up to 15 vol-% composted garden waste. Its field capacity is approximately 40 % VWC.

Similarly to the soil specific calibration of S1, three beaker glasses of 2 litres was filled with well mixed soil. Slightly more than 1.5 litres was added and then compressed. For each parallel, the bulk density at 1.5 litres is 0.87 kg/l and the weight is 1303 g. The room temperature was 20.5 ^{o}C. Following the procedure as described in previous chapters, distilled water was added until saturation. To reach field capacity it took 13 additions of 50 ml water. In other words, 650 ml of distilled water was added until the substrate reached its field capacity.

FIGURE 6.2 SOIL SPECIFIC CALIBRATION. 1.5 LITER OF SOIL INSIDE A BEAKER GLASS OF 2 LITER

6.5.3 Soil Specific Calibration for S2 at 5 ^{o}C

It is of interest to see how the measurements are affected by temperature. The soil and water was kept in a cooler overnight and thus had a temperature of 5 ^{o}C at the beginning of the experiment. The material was then kept in the cooler throughout the whole procedure. Aside from this, the procedure was equal to the one at room temperature.

6.5.4 Field Specific Calibration with Felt

Roof plot 1 at Risvollan consists of only a felt mat from VegTech underneath the sedum. The mat had a thickness of 10 mm and a total volume of 483 cm^2. The density is 1280 g/m^2 and the water holding capacity is 8 l/m^2 according to VegTech (VegTech, 2013). Room temperature was 20.9 ^{o}C. A layer with roof membrane covered the bottom of the tray, and then the felt mat was put on top of that. At Risvollan, the sedum mat is sheared and the sensor is simply put inside and laid between the felt and the sedum mat. This was imitated in the laboratory as seen below. The water amount added each step was 35 ml, in order to get at least 10 steps before water holding capacity was reached. For each addition of water, the sedum mat was removed.

FIGURE 6.3 AN ILLUSTRATION OF HOW THE SENSOR WERE MOUNTED DURING THE EXPERIMENT WITH FELT

There is an issue of lack of contact between the sensor and the material, both in field and especially for the laboratory setup. The sedum mat at the field roof is considered to contribute with some weight, and during the experiment various measures were attempted in order to create a better contact area for the sensor. However, no decisive differences were observed.

6.5.5 Field Specific Calibration with Grodan

Roof plot 2 has a Grodan mat from Sempergreen. It has a dry weight of 4 kg/m^2 and a water absorbing capacity of 30 l/m^2. Room temperature was 19.5 ^{o}C. The thickness of the grodan mat both at Risvollan and in the laboratory was 50 mm.

FIGURE 6.4 FROM THE CALIBRATION OF GRODAN

Many trials were needed before the counting experiment were conducted, due to huge variations in the data collected by the three sensors. Due to the fact that the water were gathering towards the bottom, the sensors were eventually mounted near the bottom. For the calibration the underside of the sensors were 1 cm above the bottom of the grodan, and centered horizontally.

6.5.6 Field Specific Calibration with S2

Roof plot 3 at Risvollan has a substrate layer of 5 cm S2 material. The roof build-up was imitated at first, including all layers of the field roof. However, due to leakage from the substrate onto the drainage element, the underlying layers were removed. The sample in the final and counting calibration included 5 cm substrate and sedum mat only. This was equal for all three parallels, and achieved by carefully weighing the material, with 2060 g for all three parallels. It was then added to the glass trays at a fixed volume of 21x23x5 cm. This gave a density of 0.87 kg/l as for the standard calibration, although with minor variances between the parallels due to variations in the material. Room temperature by the start of the experiment was 23 ^{o}C. For roof specific calibration, the substrate is not put in a separate container when water is added. Instead, only the sedum mat is removed and distilled water is then sprinkled directly on to the substrate. It took between 20 and 30 minutes for the data to stabilize. Due to this as well as an increased volume, 100 ml were added with each step.

FIGURE 6.5 FROM THE FIRST ATTEMPT AT FIELD SPECIFIC CALIBRATION WITH SUBSTRATE S2, DRAINAGE ELEMENT IS INCLUDE

6.5.7 Field Specific Calibration with S1

Roof plot 4 at Risvollan has a substrate layer of 5 cm S1 material. Similarly to the other roof specific calibrations, an imitation of the roof plot were attempted. 5 cm of substrate with a weight of 2640 g were added to each parallel. This gave a density of 1.1 kg/l. The room temperature were 22.9 ^{o}C. For this experiment, 100 ml of distilled water were sprinkled on to the substrate after removal of the sedum mat. The procedure is equal to calibration 6, but with only two parallels due to the material being nearly empty.

FIGURE 6.6 FIELD SPECIFIC CALIBRATION OF S1, ONLY 5 CM OF SUBSTRATE WITH A SEDUM MAT ON TOP OF IT

6.6 Gathering Calibration Equations

The data from the sensors are collected through the software LoggerNet every minute of the experiments. The sensors measure the dielectric permittivity, as well as the temperature. The volumetric water content is automatically calculated using Topps equation. Data for these three parameters are collected in a table and saved as a DAT-file, and then generated in Microsoft Excel. Figure 6.7 below shows an extract of the data, with columns for permittivity and temperature. The raw permeability is given directly as dielectric permittivity.

TOA5	CR1000	CPU:Backup-14	65508	Min			
TIMESTAMP	RECORD	Raw_perm_1	Raw_perm_2	Raw_perm_3	Jordtemp_1	Jordtemp_2	Jordtemp_3
TS	RN				deg C	deg C	deg C
		Smp	Smp	Smp	Smp	Smp	Smp
29.02.2016 12:55	16021	8.16	8.93	7.36	20.5	20.4	20.4
29.02.2016 12:56	16022	8.16	8.93	7.36	20.5	20.4	20.5
29.02.2016 12:57	16023	8.16	8.94	7.36	20.5	20.4	20.5
29.02.2016 12:58	16024	8.15	8.94	7.36	20.5	20.5	20.5
29.02.2016 12:59	16025	8.16	8.92	7.37	20.5	20.4	20.5
29.02.2016 13:00	16026	8.15	8.9	7.36	20.5	20.5	20.5
29.02.2016 13:01	16027	8.16	8.91	7.35	20.5	20.5	20.5
29.02.2016 13:02	16028	8.16	8.92	7.35	20.5	20.5	20.5
29.02.2016 13:03	16029	8.15	8.91	7.36	20.5	20.5	20.5
29.02.2016 13:04	16030	8.16	8.91	7.36	20.5	20.5	20.5
29.02.2016 13:05	16031	8.15	8.9	7.36	20.5	20.4	20.5
29.02.2016 13:06	16032	8.16	8.91	7.35	20.5	20.5	20.6
29.02.2016 13:07	16033	8.15	8.93	7.35	20.5	20.5	20.6
29.02.2016 13:08	16034	8.12	8.94	7.35	20.5	20.5	20.6
29.02.2016 13:09	16035	8.13	8.92	7.35	20.5	20.5	20.6
29.02.2016 13:10	16036	8.15	8.9	7.33	20.5	20.6	20.6
29.02.2016 13:11	16037	8.14	8.9	7.35	20.6	20.5	20.6

FIGURE 6.7 EXTRACT OF A TABLE WITH RAW DATA, IMPORTED FROM LOGGERNET TO MICROSOFT EXCEL

The data is now workable. The dielectric permittivity is collected when the data is stable after each addition of water. For all calibrations this is done after at least 10 minutes. Due to minor variations even then, the value collected is an average of the last five values. Each collected value for dielectric permittivity from start to finish is tabulated along with the actual volumetric water content, which is calculated from the added sample volume. This is done equally for all three parallels and these are then plotted together before a curve is fitted. The equation for this curve gives the equation for the volumetric water content as a function of dielectric permittivity. Below is an example of how the final results may look like. See appendix for a full overview. Volumetric water content is given as θ.

Sensor 1	Sensor 2	Sensor 3	Sample 1	Sample 2	Sample 3	Sensor 1	Sensor 2	Sensor 3	Sample 1	Sample 2	Sample 3
ε_a	ε_a	ε_a	θ_sample	θ_sample	θ_sample	θ_measured	θ_measured	θ_measured	V_w	V_w	V_w
2.566	2.37	2.666	0.0 %	0.0 %	0.0 %	2 %	1 %	2 %	0	0	0
3.624	3.342	3.64	3.3 %	3.3 %	3.3 %	5 %	4 %	5 %	0.05	0.05	0.05
4.228	4.28	4.368	6.7 %	6.7 %	6.7 %	6 %	6 %	6 %	0.1	0.1	0.1
5.294	4.94	5.13	10.0 %	10.1 %	10.0 %	9 %	8 %	8 %	0.15	0.152	0.15
5.85	5.496	5.422	13.3 %	13.5 %	13.5 %	10 %	9 %	9 %	0.2	0.202	0.202
6.562	6.192	6.196	16.7 %	16.8 %	16.8 %	12 %	11 %	11 %	0.25	0.252	0.252
8.088	8.93	7.326	20.0 %	20.1 %	20.1 %	15 %	17 %	13 %	0.3	0.302	0.302
6.274	7.618	7.544	23.3 %	23.5 %	23.5 %	11 %	14 %	14 %	0.35	0.352	0.352
9.262	8.39	11.938	26.7 %	26.8 %	26.8 %	17 %	16 %	22 %	0.401	0.402	0.402
16.274	18.684	16.666	30.2 %	30.1 %	30.1 %	30 %	33 %	30 %	0.453	0.452	0.452
17.02	19.31	17.854	33.5 %	33.5 %	33.5 %	31 %	34 %	32 %	0.503	0.502	0.502

FIGURE 6.8 AN EXAMPLE OF TABLES WITH BOTH MEASURED DATA AND ADDED WATER CONTENTS

7 Results and Discussion

7.1 Results From Calibration

In this chapter, the results from the laboratory measurements described in chapter 6 will be presented and consecutively discussed. With the objective of calibrating a soil moisture sensor based on dielectric permittivity to work in a heterogeneous green roof substrate, calibration curves has been developed to give a precise indication of the saturation of green roofs.

A weakness of the original Topps equation (Eq. 6.1) is the lack of decimals. The equation for a regression plot shows two decimals as standard, which is also the case for Topps equation. However, the actual equation may actually have way more decimals, and the chosen number of decimals may have a huge impact on the outcome. By assessment of this, it is found that using a number of seven decimals provides a reasonable estimation.

7.1.1 Soil Specific Calibrations

First a soil specific calibration was conducted for the substrates S1 and S2, as described in chapter 6. The curves and equations are compiled from measurements from 0 Vol-% water up to field capacity, which is respectively 30 Vol-% and 40 Vol-% for S1 and S2. The values for field capacity are observed during the experiments, and are also supported by field data, see chapter 7.2.1. Table 7.1 provides a summary of the characteristics for each calibration.

TABLE 7.1 CHARACTERISTICS FOR THE SOIL SPECIFIC CALIBRATION EXPERIMENTS

Calibration number	1	2	3
Substrate material	**S1**	**S2**	**S2**
Volume of substrate	1.5 l	1.5 l	1.5 l
Mass of substrate	1750 g	1303 g	1300 g
Dry bulk density	1.17 kg/l	0.87 kg/l	0.87 kg/l
Stepwise addition of water	50 ml	50 ml	50 ml
Room temperature	20.4 ºC	20.5 ºC	5 ºC

Data from all three parallels are plotted together and from that a new equation for the volumetric water content is made, by curve fitting.

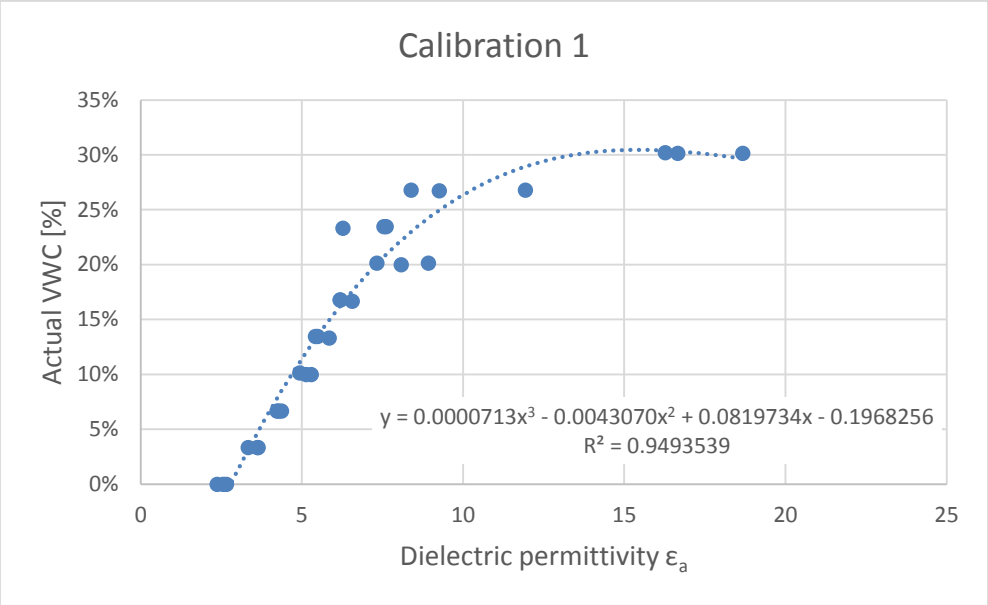

FIGURE 7.1 SOIL SPECIFIC CALIBRATION FOR SUBSTRATE S1

From this curve a new equation for the volumetric water content is found:

$$VWC = 7.13 * 10^{-5}\varepsilon_a^3 - 4.307 * 10^{-3}\varepsilon_a^2 + 8.519734 * 10^{-2}\varepsilon_a - 1.968256 * 10^{-1} \quad (7.1)$$

The data from the three parallels does correlate for the most part, however deviations occurs. This is especially present as the water content increases. Despite following a general procedure, there will be small variations each time water is added. The substrate is taken out of the beaker glass and into a separate plastic container, water is added and then the soil is put back in the beaker glass. Small losses of substrate as well as water did occur during this process, especially after the water content exceeded 20 Vol-%. The error is considered to be minimal though, and is not accounted for. Another small source of error finds place when adding water to the sample. The amount is controlled both by volume and by weight, however 1 ml of water to or fro may occur.

Each water addition of water also requires the sensors to be pulled out and then re-mounted. This is a considerable source of error, potentially. Each parallel will have a slight variation in the how the substrate is packed to begin with, and for every mounting of the sensor further variances are created. Through repeated testing, it was found that the dielectric permittivity could be up to five values off when not mounted properly.

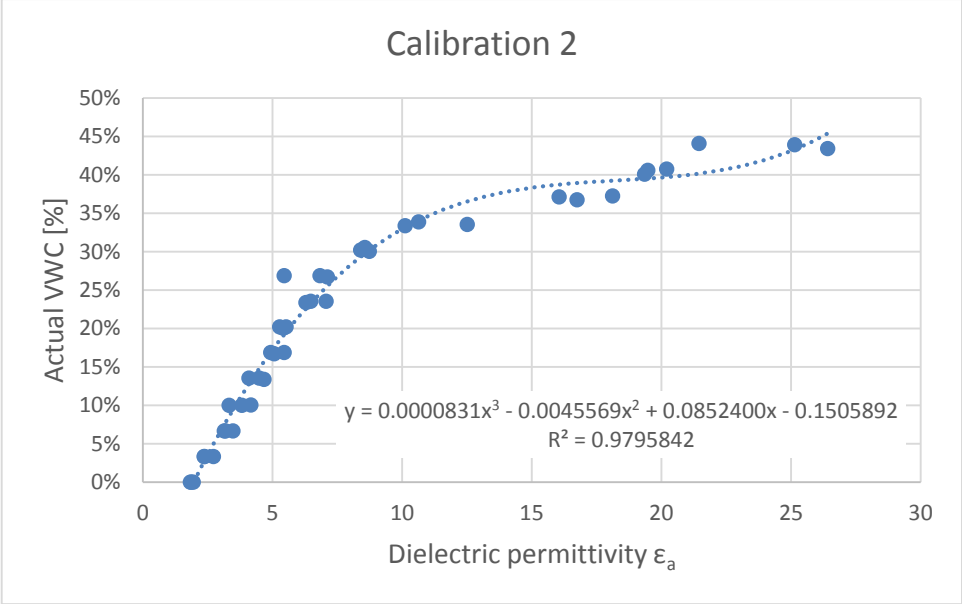

FIGURE 7.2 SOIL SPECIFIC CALIBRATION FOR SUBSTRATE S2

The following equation was obtained for S2:

$$VWC = 8.31 * 10^{-5}\varepsilon_a^3 - 4.5569 * 10^{-3}\varepsilon_a^2 + 8.524 * 10^{-2}\varepsilon_a - 1.505892 * 10^{-1} \qquad (7.2)$$

There is a slight difference when comparing eq. 7.1 (S1) and 7.2 (S2). This is to be expected when taking the different characteristics of the substrates into consideration. Both equations might to provide a good estimation of the volumetric water content in general, however for precise values the VWC should be calculated with substrate specific equations.

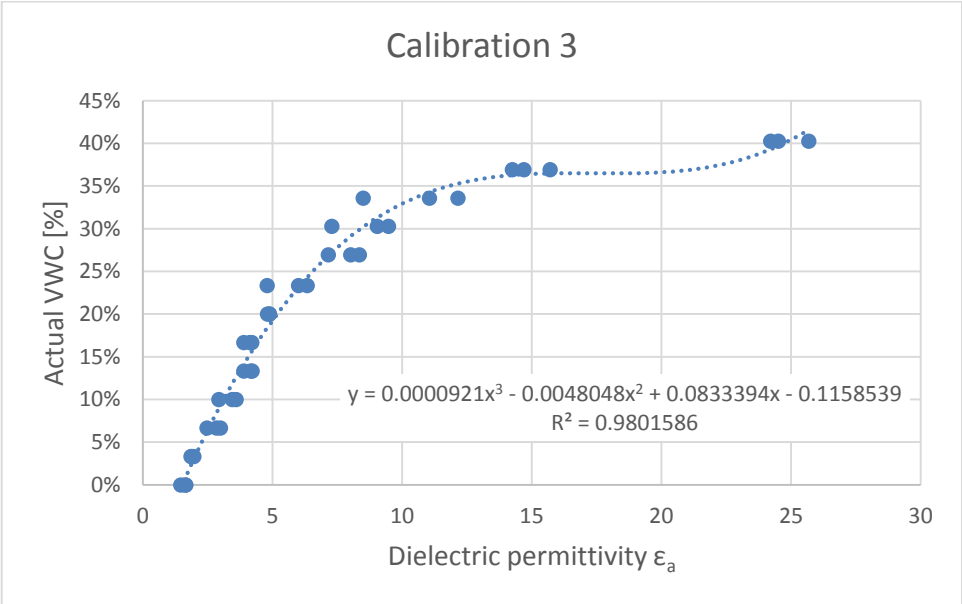

FIGURE 7.3 SOIL SPECIFIC CALIBRATION FOR SUBSTRATE S2, AT ONLY 5 °C

$$VWC = 9.21 * 10^{-5}\varepsilon_a^3 - 4.8048 * 10^{-3}\varepsilon_a^2 + 8.33394 * 10^{-2}\varepsilon_a - 0.1158539 \qquad (7.3)$$

For the S2 substrate, a calibration at a temperature of 5 ^{o}C was also carried out. It shows a good correlation to the calibration at room temperature, and thus it indicates that the sensors are able to make a reasonable adjustment to the temperature changes that occurs within a season. While there is a slight variation, it's still considered acceptable. By studying the sensors while measuring dielectric permittivity in air and in water, under varying temperature conditions, it further validates that the values the sensors provide does not need to be corrected for varying temperatures.

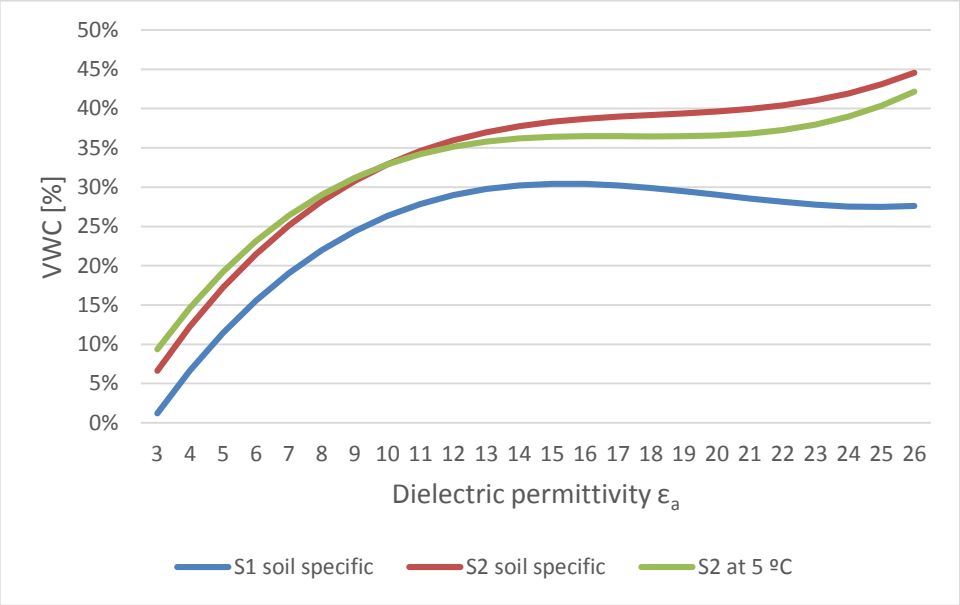

FIGURE 7.4 A COMPARISON OF THE SOIL SPECIFIC CALIBRATIONS

It is concluded that the sensors can adjust data according to the temperature. For different substrates however, it is recommended that different equations are being implemented to calculate the volumetric water content based on the dielectric permittivity. For these two substrates, S2 is a more lightweight substrate with higher porosity, higher organic content and a finer gradation than S2. A higher field capacity is thus to be expected, and so is a variation in the calibration curves.

7.1.2 Field Specific Calibrations

Field specific calibration trials were conducted by copying the build-up of the field roof at Risvollan, for four roof plots. Three equations have been developed, however with some uncertainties that could not be eliminated due to lack of time and materials. The results will be presented and discussed, but further work on the methodology of these calibrations is recommended.

TABLE 7.2 CHARACTERISTICS OF CALIBRATIONS FOR FIELD ROOFS WITHOUT SOIL SUBSTRATES

Calibration number	4	5
Material	**Felt**	**Grodan**
Volume	0.48 l	2.4 l
Mass of substrate	-	-
Dry bulk density	-	-
Stepwise addition of water	35 ml	100 ml
Room temperature	20.9 ºC	19.5 ºC

Roof plot 1 and 2 at Risvollan consists of respectively a felt mat and a grodan mat, as described in chapter 6.4.1. Having carried out multiple experiments with grodan and specific calibration for both roof plot 1 and 2, it is evident that the sensors may provide inadequate data. This is the case for plot 1 especially, having only a felt mat beneath the sedum.

The lack of full contact between the sensor and the felt mat is considered a fundamental error source, and the humidity values are too low. The diagram in figure 7.5 illustrates how the volumetric water content varies through the experiment.

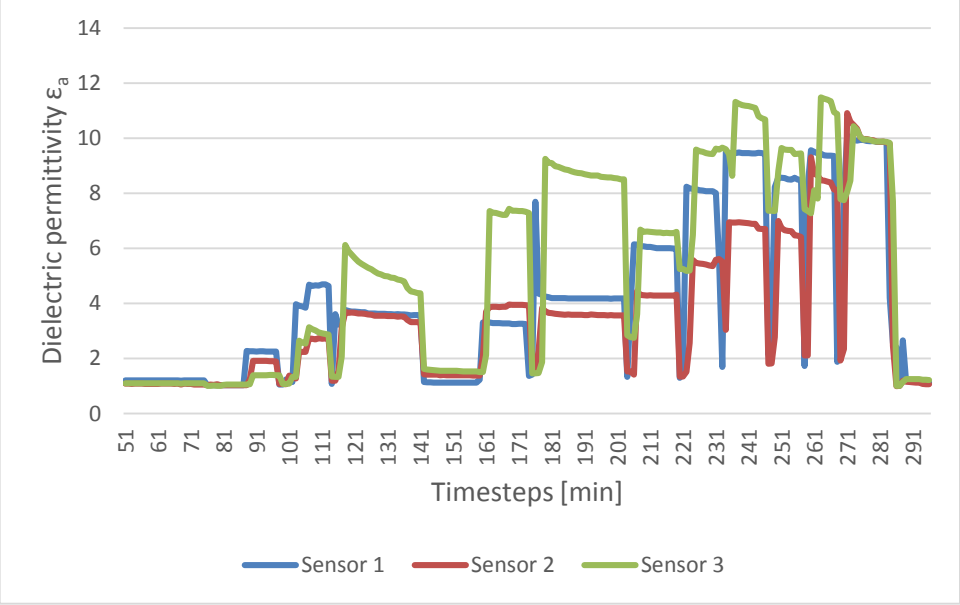

FIGURE 7.5 SENSOR DEVELOPMENT THROUGH THE TRIAL CALIBRATION WITH FELT

What's observed here is that the peaks, which occur when the sensors are mounted under the sedum mat, barely gets any larger. Apparently the sensors are unable to register the actual dielectric permittivity due to lack of contact. In an attempt account for this, more weight was added on top of the sedum mats but without success. Furthermore, there are three completely

different results for each of the sensors. Many attempts to adjust the sensors and account for this were done during the experiment, however it proved to be difficult. Minor adjustments to the mounting would affect the results, which can be considered random. The conclusion is that for this laboratory setup, it is not possible to provide a useful equation for converting the dielectric permittivity to volumetric water content.

In order to investigate whether or not it is of any use to monitor moisture at a field roof with felt mat, data from Risvollan has been investigated. One sensor is mounted in the center of the roof plot ("upper") and one is mounted near the bottom ("under"). For a rain event that occurred in August 2014, the sensors provided the following data:

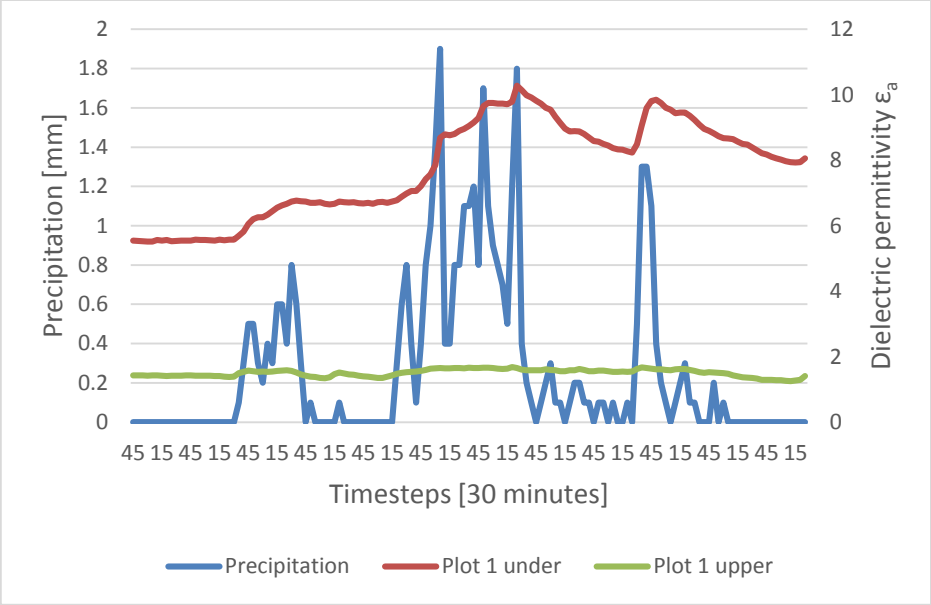

FIGURE 7.6 FIELD MEASUREMENTS FROM ROOF PLOT 1

As the green roof at Risvollan is sloped, water will drain towards the bottom. There is a tendency of slightly higher water content near the bottom of the roof plots, although this may vary. However for plot 1, with only the felt mat underneath the sedum, the upper sensor is barely able to register any water at all, and it does not react to the precipitation. The bottom sensor however shows a distinct variation in water content, and the curve correlates fairly well with the other roof plots, although it's slightly lower. Because of the low depth of the felt mat, a higher Vol-% of water is to be expected. This, along with the lack of responsiveness for the upper sensor indicates a need for a certain water amount for the sensors to be able to register anything. It may also indicate a mounting sensitivity, as the upper sensor probably has a low degree of contact with the sedum mat and roof membrane.Regarding grodan, the sensors may not be able to register the actual water content. Especially for low amounts of water. Small

variations in how the sensor is mounted also affects this. The influence volume of the sensors seems to be smaller for this material, and considering how the water is gathering towards the bottom, the sensors were mounted with the lower edge being 1 cm above the bottom of the grodan mat. The following data was obtained:

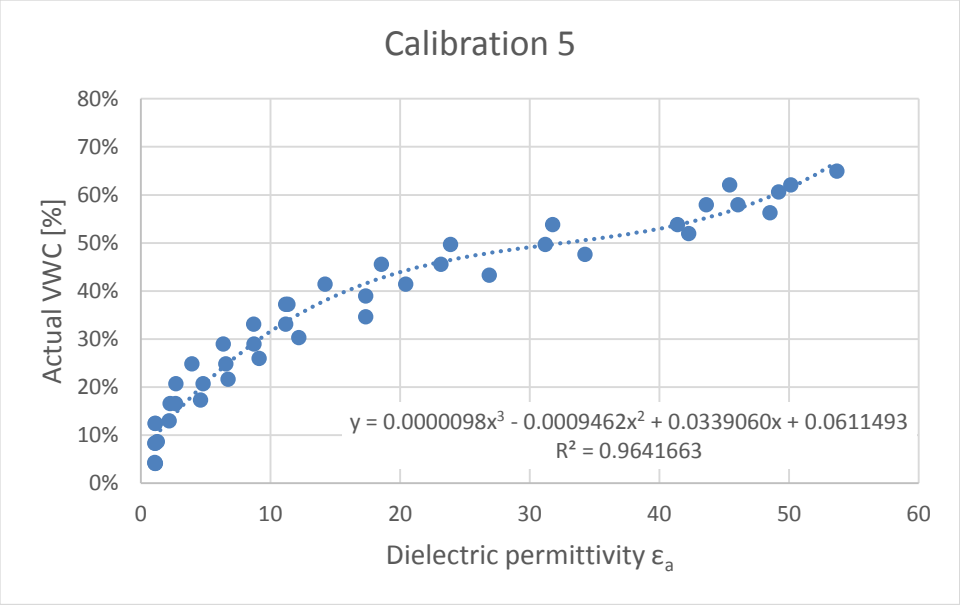

FIGURE 7.7 CALIBRATION CURVE FOR PLOT 2 WITH GRODAN

From the curve an equation for grodan is found:

$$VWC = 9.8 * 10^{-6}\varepsilon_a^3 - 0.0009462\varepsilon_a^2 + 0.033906\varepsilon_a + 0.0611493 \qquad (7.4)$$

For low amounts of water, beneath 10 Vol-%, the sensors may not be able to register the water content. However for longer durations and more water, experiments indicates a gradually increasing accuracy. By implementing the new equation for volumetric water content, specific for grodan, a good indication of water content is provided.

The mounting of the sensors on a green roof differs from what is described as ideal mounting. The thin substrate may also influence results in terms of influence volume, horizontal insertion of sensor and other possible error sources. So for the soil substrates, it is considered important to at least investigate a specific roof build up despite having conducted soil specific calibration. Calibration 1, 2 and 3 established that for converting dielectric permittivity into volumetric water content, equations obtained from calibrating for the specific substrates should be used. The next step has then been to attempt a field specific calibration.

TABLE 7.3 SPECIFICATIONS FOR THE ROOF SPECIFIC CALIBRATION FOR PLOT 3 AND 4

Calibration number	6	7
Material	S2 (plot 3)	S1 (plot 4)
Volume of substrate	2.4 l	2.4 l
Mass of substrate	2060 g	2640 g
Dry bulk density	0.86 kg/l	1.1 kg/l
Stepwise addition of water	100 ml	100 ml
Room temperature	23 °C	22.9 °C

As briefly mentioned in chapter 6.5, the specific roof samples does not contain underlying layers that the field roof has. This was attempted for both of the substrates, but the results were affected by leakage. However, through the experiment and further testing, it was observed from the raw data that having a certain water content in the layers below the substrate does not affect the registered dielectric permittivity of the soil. This is crucial for being able to precisely monitor humidity conditions in green roofs. It also provided background for the new approach to the field specific calibration, with no layers underneath the substrate. For roof plot 3, the following results were achieved:

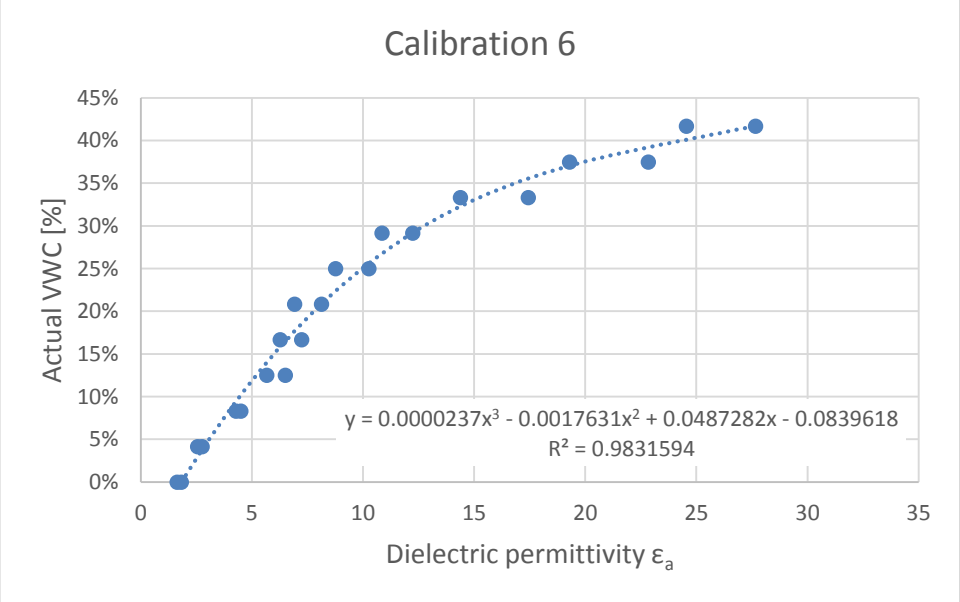

FIGURE 7.8 FIELD SPECIFIC CALIBRATION FOR ROOF PLOT 3, WITH SUBSTRATE S2

This gave the following equation:

$$VWC = 2.37 * 10^{-5}\varepsilon_a^3 - 1.7631 * 10^{-3}\varepsilon_a^2 + 0.0487282\varepsilon - 0.0839618 \quad (7.5)$$

One of the parallels had to be removed. Two of the parallels however, responded very well and within expectations when water was added. There is a minor deviance throughout the experiment, increasingly as the water content. This is probably caused by slight variances in the mountings. While there has been an effort to achieve an ideal mounting in the center of the substrate sample, it may not be 100 % ideal in this case. As already discussed for the soil specific calibration, small differences in the mounting affects the measurements. Small differences in the grain size distribution in the two samples may also have affected the measurements. Figure 7.9 is a comparison of the soil and roof specific calibration.

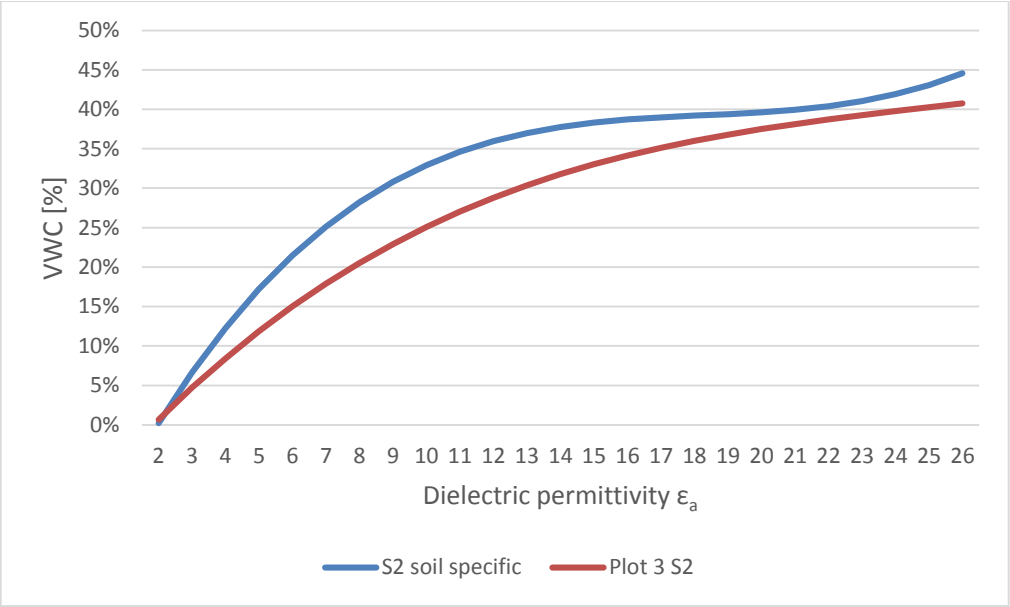

FIGURE 7.9 SOIL SPECIFIC AND FIELD SPECIFIC CALIBRATIONS FOR SUBSTRATE S2 PLOTTED TOGETHER

For Calibration 7, only two sensors were put to use because it was only enough substrate for two parallels. The two sensors had a similar development, however with one sensor providing slightly higher values than the other one.

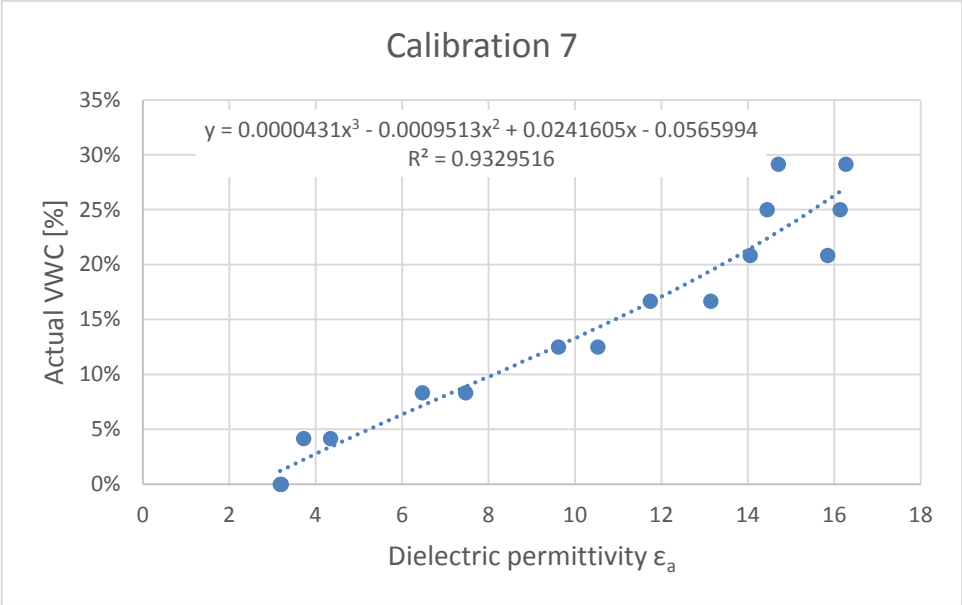

FIGURE 7.10 CALIBRATION CURVE FOR ROOF PLOT 4, WITH SUBSTRATE S1

$$VWC = 4.31 * 10^{-5}\varepsilon_a^3 - 0.0009513\varepsilon_a^2 + 0.0241605\varepsilon_a - 0.0565994 \quad (7.6)$$

There is a remarkable difference in how the curve develops compared to the soil specific calibration. The curve for field specific calibration develops rather slowly at first, due to dielectric conductivity corresponding well to the added water. Both sensors were carefully mounted in the center of the sample and mounting error is not likely. The sample volume was equal and the surface was well leveled. The measurements were therefore considered to be reliable. However, one has to question whether it is a representative curve.

For volumetric water contents above 20 %, the dielectric permittivity barely changes at all. This could indicate that field capacity is close, even though it has been found to be close to 30 Vol-%. By taking samples from the field when it's been relatively wet, then weighing and drying it, a VWC between 20-25 % have been found. When studying field measurements, it's observed a maximum dielectric permittivity of around 15. At the same time, it's rarely above 10. When calculating the water content using equation 7.6, it varies between 10 and 15 Vol-% for the biggest storm events. Using the soil specific calibration gives values between 25 and 30 Vol-%.

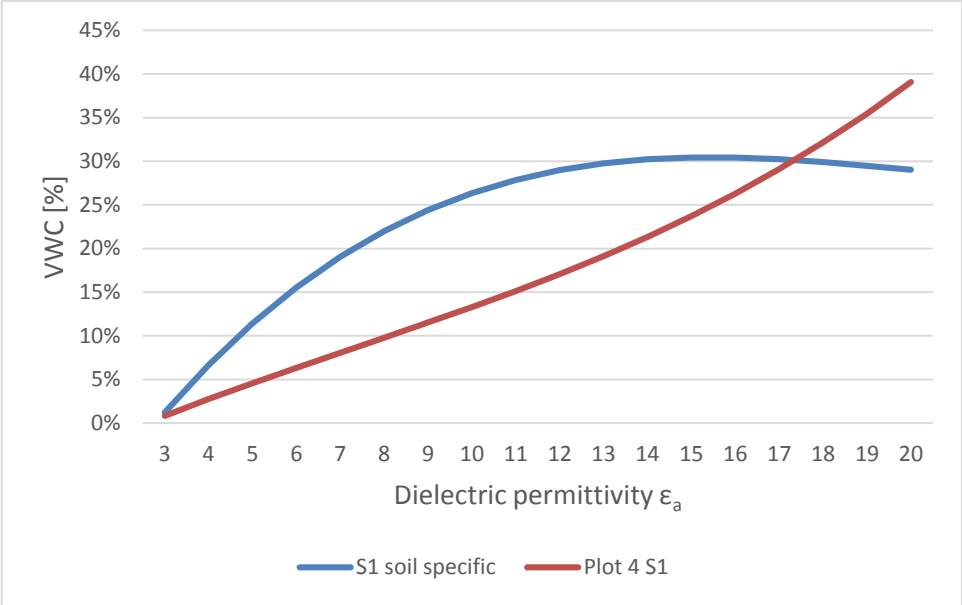

FIGURE 7.11 SOIL SPECIFIC AND FIELD SPECIFIC CALIBRATIONS FOR SUBSTRATE S1 PLOTTED TOGETHER

The difference between these two curves is rather interesting, as if they are from two different materials. When comparing figure 7.9 and 7.11, it is present that for both substrate types the curve from field specific calibration is lower than for the soil specific. The substrates are only 5 cm and this may affect the results. Furthermore, for the soil specific calibrations the soil has been taken into a separate container and mixed each time water has been added. This has not been the case for the field specific calibrations. Mixing the wet soil may help utilize the capillary suction and increase water holding capacity. This in turn provides a relatively seen larger pore volume and a higher volumetric water content for lower values of dielectric permittivity.

Still, the S1 soil is more affected by this than the S2 soil. Possibly, due to horizontal insertion of the sensors, there is a "water shadow" underneath that causes a drier area. At the same time, a bigger portion of the added water will stay above the sensor and possibly affect the readings. Perhaps the will be droplets of water touching the sensor as it lays horizontally causes too high dielectric permittivity. Differences in porosity may have caused S1 to be more affected by this than S2. Regardless, the results must be considered uncertain.

Due to uncertainties for the field specific calibrations for soil substrates, the soil specific calibration will be used. For S1 this seems necessary in order to gain a realistic estimation of the volumetric water content. It has been decided to do the same for S2, even if the curve seems reasonable. Further work needs to be done for the field specific calibration. Even more important is it to study the actual field VWC. By taking samples from the field roof, close to

the sensors, and comparing the actual VWC to the measured, one will eventually validate the correct equation for VWC. For now, equation 7.1 and 7.2 is considered to provide good estimations.

7.2 Soil Moisture at the Risvollan Field Roof

Data from Risvollan, from August 2014 up until April 2016, has been collected and processed using the software Microsoft Excel. Daily precipitation measurements throughout the periods gives the following distribution:

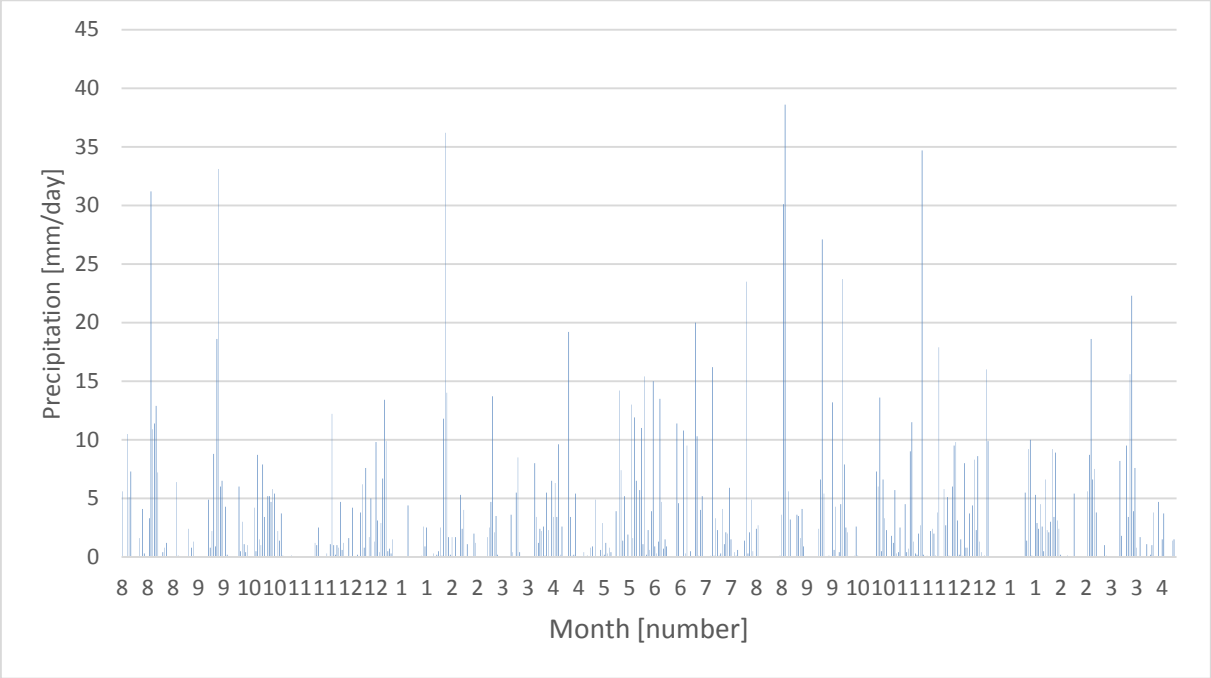

FIGURE 7.12 PRECIPITATION DISTRIBUTION FROM AUGUST 2014 UNTIL APRIL 2016

An objective for this thesis is to estimate the moisture content in different green roof configurations, so the equations for volumetric water content will be applied to the data from Risvollan. A selection of storm events will be investigated, and it is of interest to consider some of the heavier events. Furthermore, evapotranspiration will be estimated. With this in mind, the chosen events are from periods with temperate climate in order to have a reasonable amount of evapotranspiration. A distribution of soil moisture throughout the whole period as seen in figure 7.13 illustrates how water content of the roof plots vary over time. Measurements from sensors mounted at the lower part of the roof plots ("under") are chosen. There are sensors mounted around the middle of the roof as well, and it was not a matter of course what to use. Averaged measurements were considered used, however strange measurements occasionally occurs from the upper sensors. For the most part the slope of the moisture content development is equal, but it's not always the case. For roof plot 3, the upper

sensor mostly provides lower values than the sensors mounted in the lower part. For roof plot 4, it varies more what sensor provides the highest value. Roof plot 2 should be carefully considered, as one of the sensors occasionally shows close to zero change in moisture content, despite either rain or drought.

Roof plot 1 is not part of the comparison due to the uncertainties in the measurements.

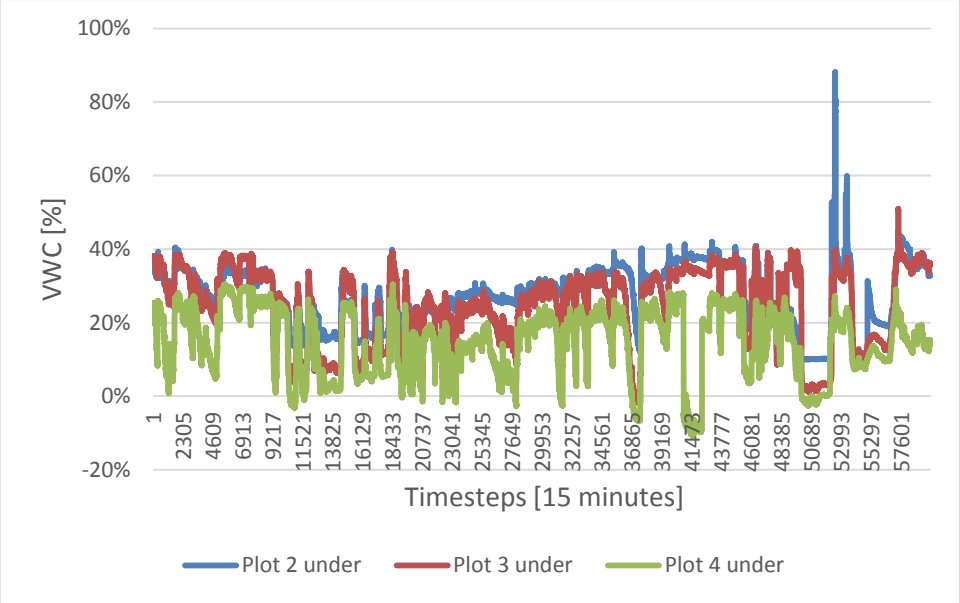

FIGURE 7.13 VOLUMETRIC WATER CONTENT MEASURED AT FIELD ROOF AT RISVOLLAN

Before actual evapotranspiration is calculated, the field capacity of the substrates must be decided. It has not been within the capacity of this thesis to do a proper test for this, but based on field measurements illustrated in figure 7.13 as well as laboratory observations, the substrates has the following field capacities:

TABLE 7.4 FIELD CAPACITIES FOR GRODAN AND SUBSTRATE S1 AND S2

Substrate	Field capacity [Vol-%]
Grodan (plot 2)	40
S2 (plot 3)	40
S1 (plot 4)	30

7.2.1 Substrate Moisture Behavior During Storm Events

Three events have been chosen in order to examine the soil moisture behavior at the green roof at Risvollan, by applying equations for VWC to the field measurements of dielectric permittivity.

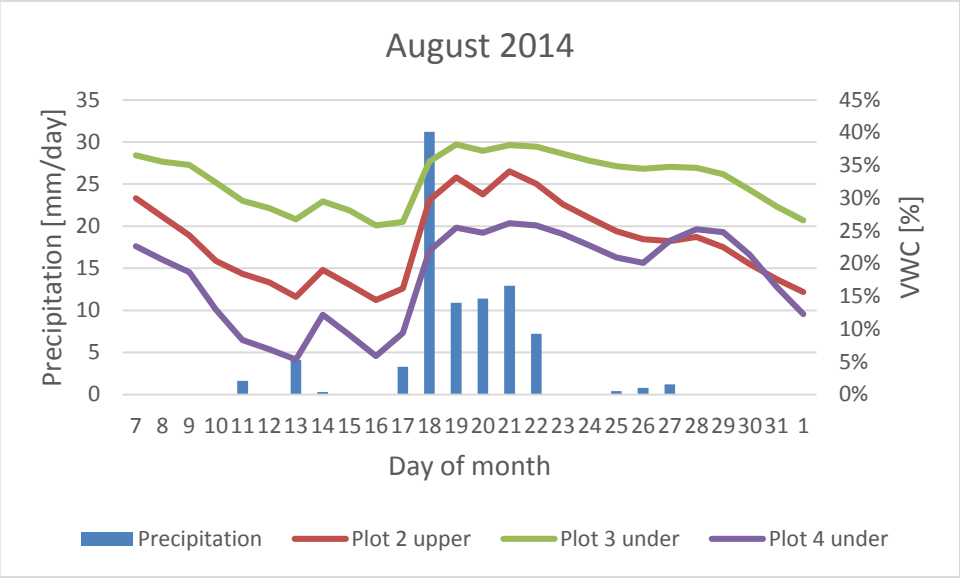

FIGURE 7.14 STORM EVENT IN AUGUST 2014 WITH DRY PERIODS BEFORE AND AFTER

Prior to this event, the roof plots have relatively similar water release. Plot 2 uses measurements from the upper sensor. A huge difference between the upper and "under" sensor were observed for this roof plot, and the upper one should provide a more realistic view of the water content behavior. It is possible though that at the lower edge of the roof, water does accumulate and when it reaches a certain water content the grodan retain less water. For roof plot 3 the upper and under sensor shows equal water content and development, while in plot 4 the upper sensor provides negative results. During June and July 2015, varying weather conditions occurred, and gives results as seen in figure 7.15.

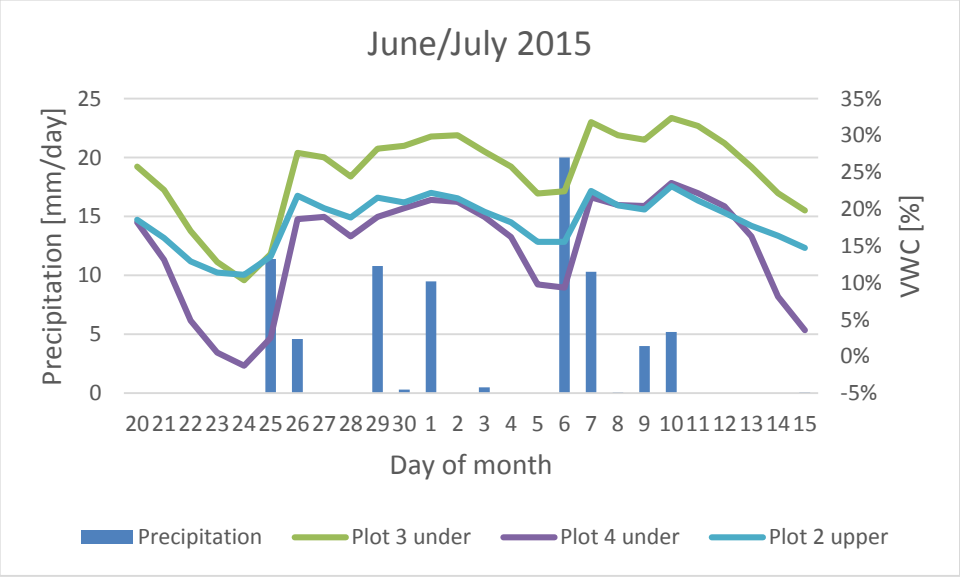

FIGURE 7.15 STORM EVENT IN JUNE AND JULY 2015 AND DRY WEATHER PERIODS BEFORE AND AFTER

From this event, the grodan seem to have a slower release of water compared to the soil substrates. This actually supports findings in the project thesis written during the fall 2015. Here, runoff were monitored and studied, and roof plot 2 had the lowest retention performance overall. See appendix A.2 for a comparison of runoff from the roof plots. After more than one week of dry weather a rather intense storm event took place towards the end of August 2015:

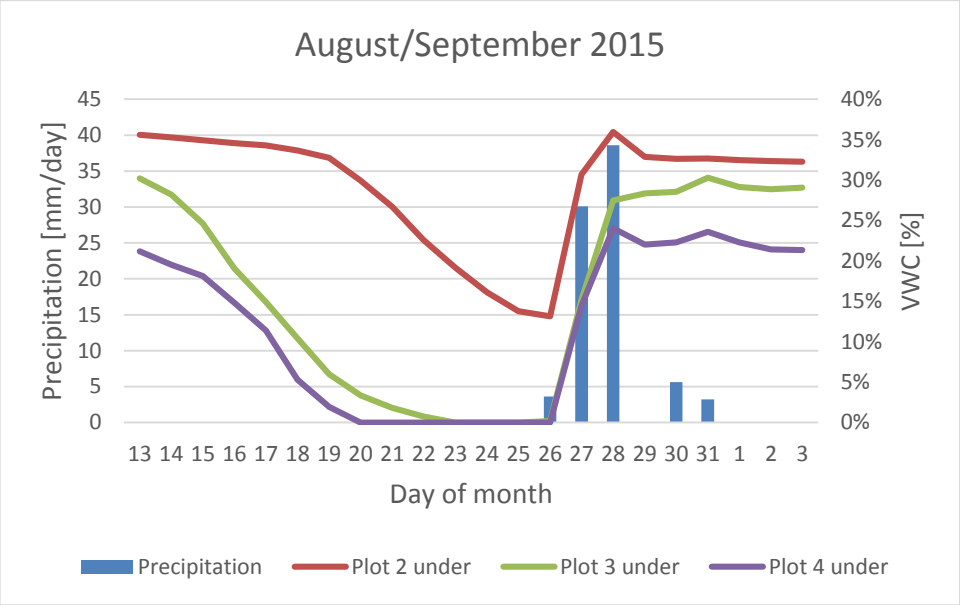

FIGURE 7.16 STORM EVENT IN AUGUST 2015 AND DRY WEATHER PERIODS BEFORE AND AFTER

For all three events, the whole antecedent dry weather period is included and illustrates how the soil moisture decreases after the preceding storm event. Due to high temperatures and dry weather, the soil substrates get very dry. Completely dry soil substrates during August 2015 according to the measurements, which is questionable. This is because at a certain depth the substrates will have a wilting point, and beneath this the plants won't be able to extract the water (Hendriks, 2010). It is possible that with the length of these dry weather periods, that the eventual residual water have drained into the drainage layer.

Interestingly, the grodan mat barely let go of water the first few days but then something happens after August 19. The sedum layer is where most of the evapotranspiration will come from the first few days, and apparently the sensor does not register this. Overall, the water release from grodan can be considered slow compared to the soil substrates.

7.3 PET Distributions at the Risvollan Field Roof

Data from August 2014 until April 2016 has been available for most of the hydrological parameters for this thesis, except for wind and global solar radiation whose has a slightly

shorter set of data. Potential evapotranspiration for the green roof at Risvollan has been calculated for the whole period of available data for the three different models. The 1985 Hargreaves model provides the following distribution:

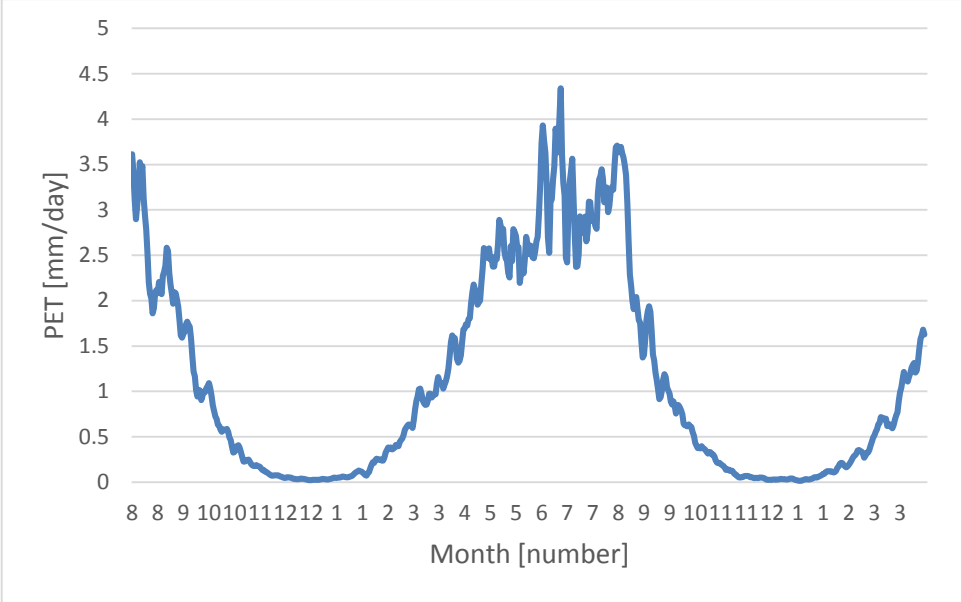

FIGURE 7.17 DAILY POTENTIAL EVAPOTRANSPIRATION CALCULATED WITH THE 1985 HARGREAVES MODEL

The total potential evapotranspiration is calculated to be 693 mm for the period 3rd of August 2014 until 13th of April 2016. For 2015 the total evapotranspiration was 500 mm according to this model. This result was achieved by using a moving 5 day average for the input data, which studies have indicated will give a precise estimate, opposed to calculating daily evapotranspiration (Hargreaves and Allen, 2003).

Penman-Monteith provides daily evapotranspiration from 24th of August 2014 until 20th of January and gives a distribution as seen in figure 7.18. The time period is limited by wind speed and global solar radiation, and there is some missing data for November 2014 and March 2015 as can be seen from figure 7.18. Total potential evapotranspiration is 585 mm. For 2015 the model estimates a PET of 479 mm, with some missing days in March. The curve has a familiar shape to the one from 1985 Hargreaves, and it's a very logical variation in evapotranspiration regarding the seasonal variations. The highest degree of evapotranspiration is observed during the months June, July and August. It's lower during winter, however there is some evapotranspiration to be found.

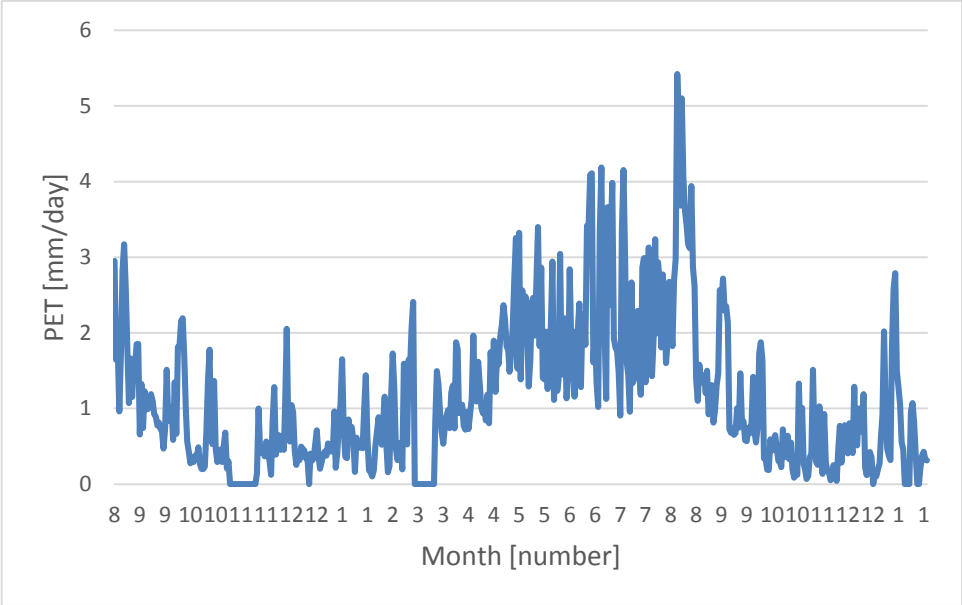

FIGURE 7.18 DAILY POTENTIAL EVAPOTRANSPIRATION CALCULATED WITH PENMAN-MONTEITH

The relatively large variation from day to day, and even more so day to night, is noteworthy. This is mostly due to variations in solar radiation as well as the difference between the maximum and minimum temperature. These two factors are closely related as solar energy causes the temperature to increase.

By use of the Thornthwaite model, evapotranspiration on a monthly basis has been calculated.

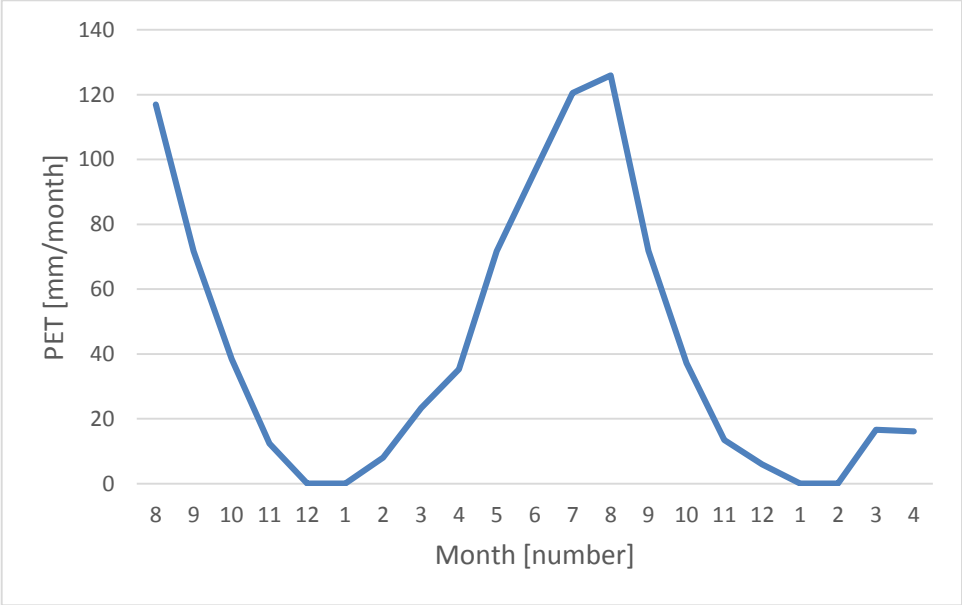

FIGURE 7.19 MONTHLY POTENTIAL EVAPOTRANSPIRATION CALCULATED WITH THORNTHWAITE

The total potential evapotranspiration is estimated to be 882 mm, while for 2015 it is 609 mm. It generally gives higher values for evapotranspiration than the other two models, except

during winter periods. For a monthly average below zero, the evapotranspiration is assumed to be zero. This isn't necessarily entirely correct and is a weakness of the model, especially taking the Norwegian conditions into consideration. This is something to aware of for all three PET models that have been used, and may contribute to some deviations from the actual evapotranspiration. A table with monthly evapotranspiration is compiled.

TABLE 7.5 CALCULATED POTENTIAL EVAPOTRANSPIRATION EVERY MONTH (MM/MONTH) FROM AUGUST 2014 UNTIL APRIL 2016

	1985 Hargreaves	**Penman-Monteith**	**Thornthwaite**
2014			
August	76.00 (29 days)	14.74 (7 days)	116.99
September	46.11	32.88	71.74
October	17.30	25.06	38.39
November	3.79	5.78 (13 days)	12.41
December	1.07	17.88	0
2015			
January	2.07	18.81	0
February	7.70	21.64	8.04
March	25.62	20.48 (18 days)	23.32
April	46.80	40.95	35.24
May	77.61	64.63	71.70
June	86.85	66.11	96.27
July	94.50	67.23	120.46
August	96.77	86.25	125.98
September	40.64	37.43	71.83
October	16.47	18.90	37.15
November	3.68	12.66	13.40
December	1.12	23.44	5.95
2016			
January	1.67	9.77 (20 days)	0
February	6.84	-	0
March	22.72	-	16.59
April	17.96 (13 days)	-	16.16 (15 days)
Sum	**693**	**585**	**881.63**

All three models provides sensible values when summarized over a longer period, and it can be argued that they provide a good annual estimate. However, they certainly do vary on a monthly basis. Generally, Penman-Monteith generates higher PET values during wintertime and lower during warmer periods, than the two other models. An important factor here is the input data, as Penman-Monteith accounts for solar radiation measured at a hydrological station close to the field roof. This varies from day to day and not necessarily corresponding to the temperature. Even if temperatures are high, if the weather is cloudy the evapotranspiration will be lower. And even if it's cold, a blue sky and sunshine will provide some evapotranspiration. At the same time, if the roof surface is frozen it will resist evapotranspiration. Snow reflectance can also result in lower values. This means that temperature input along with an estimate of the extraterrestrial radiation, may not be sufficient for the conditions prevalent at the field roof, or Norwegian conditions in general.

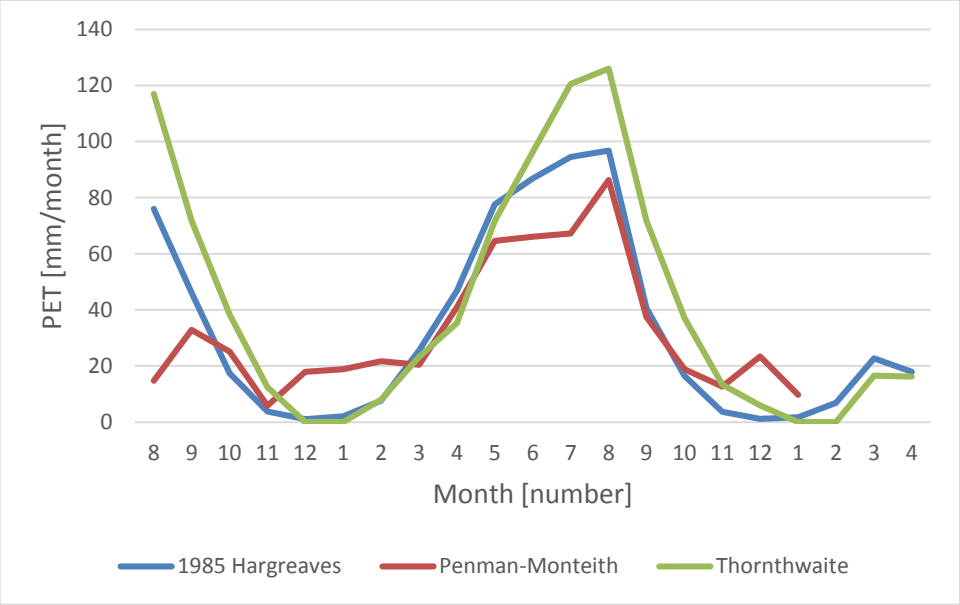

FIGURE 7.20 ACCUMULATED MONTHLY PET FOR ALL THREE MODELS PLOTTED TOGETHER

In Sheffield, UK, (Kasmin et al., 2010) found that Thornthwaite generally overestimated, and this seem to be the case here as well. They suggested multiplying the results by a factor of 0.75. The results from Risvollan supports this suggestion, however using a factor specific for each season might provide a better estimate.

By monitoring changes in soil moisture content continuously, one may be able say something about the expected evapotranspiration. The change in soil moisture, when precipitation and runoff is taken into account, can be considered to be caused by evapotranspiration. While PET models might provide a good estimation of evapotranspiration in normal moisture condition,

it will often be necessary to adjust the results by the use of a soil moisture extraction function as the evaporation from the soil is water limited (Marasco et al., 2015). In the following chapter, such a function is applied to the calculated PET in order to find the actual evapotranspiration.

7.4 Actual Evapotranspiration

Having calculated the potential evapotranspiration for the site using three different models, the actual evapotranspiration from each roof plot can now be calculated. By applying a SMEF function specific for each roof plot, the intent is to gain a good indication of the evapotranspiration from each of the roof plots.

The stored water in the substrate, 'storage' (S), is given by multiplying the depth (d) of the substrate by the volumetric water content. It can by described by the following equation:

$$S = VWC * d \tag{7.7}$$

The actual evapotranspiration is calculated on a daily basis, and theoretically it should be equal to the daily change in soil moisture when there is no precipitation as stated in chapter 5. So by subtracting the evapotranspiration at a day t, from the storage S from the day before (t-1), you should achieve the same value for storage as from equation 7.7. First, the actual evapotranspiration needs to be calculated:

$$AET = PET * (\frac{SMT}{SMC}) * K \tag{7.8}$$

This equation is basically Eq. 5.2 multiplied by a coefficient K, that at present is unknown. According to the theory, this is the value that will lessen the difference between Eq. 7.7 and storage found by subtracting the AET as well as adding any eventual precipitation (P), which is the following equation:

$$S_t = S_{t-1} - AET_t + P_t, \tag{7.9}$$

provided that the maximum storage is not reached. With no precipitation, the evapotranspiration is what causes the change in storage, according to the above equation. The water inflow from upper parts of the roof should equal water release to lower parts of the roof. While this is a simplification of the actual situation, it will be the basis the following comparison and development of provisional coefficients. Crop coefficients accounts for differences between the actual vegetation and the reference grass crop used in the PET models, but the actual properties of the vegetation layer will not be directly discussed here. It

has instead been developed coefficients with the aim of calculating AETs that gives the same moisture content as the sensors measure. The concept is to manipulate the calculated AET for the three different models in order for all of them to have the same slope as the measured soil moisture development.

Three seasons have been defined for Risvollan, based on average temperatures; Winter season (W) with a monthly temperature below 0 ^{o}C, Cold season (C) with monthly temperature between 0 ^{o}C and 11 ^{o}C, and Temperate season (T) with monthly temperature above 11 ^{o}C. Single events from a temperate and cool season are picked and assessed. The background for this is how the different PET models alternates when it comes to calculating the highest values.

TABLE 7.6 SEASONAL DISTRIBUTION IN TRONDHEIM, BASED ON RISVOLLAN DATA FROM AUGUST 2014 TO APRIL 2016

Month	**Jan**	**Feb**	**Mar**	**Apr**	**May**	**June**	**July**	**Aug**	**Sep**	**Oct**	**Nov**	**Dec**
Season	W	W	C	C	C	C	T	T	T	C	C	W

The dry weather period prior to the event from August 2015 that was studied in chapter 7.2 will be assessed further. The roof consist of a sedum layer with its own substrate of 30 mm, and storage is calculated by multiplying the measured VWC by the total storage depth, including the sedum mat. By using PET models, this is how the storage will develop from the beginning of the dry weather period:

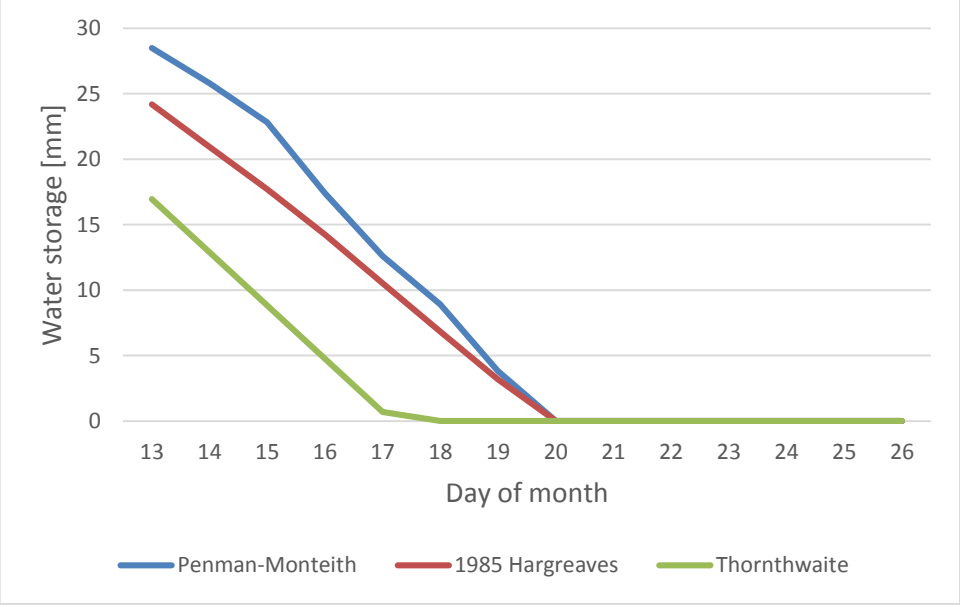

FIGURE 7.21 SOIL MOISTURE DEVELOPMENT BASED ON POTENTIAL EVAPOTRANSPIRATION

As the season changes, the evapotranspiration varies. This affects the driving factors for evapotranspiration and the input data in the AET models, and thus it might change the relationship between the measured soil moisture and the modelled AET. Therefore, AET during a colder climate also needs to be considered.

7.4.1 Crop Coefficients During Temperate Climate

These curves seen in figure 7.21 are rather steep, and have a linear development. As the soil moisture deficit grows, it's expected that the curves will have a gradually lower slope. But the temperature and solar radiation will affect this as well. The following plot shows how the temperature varies from day to day:

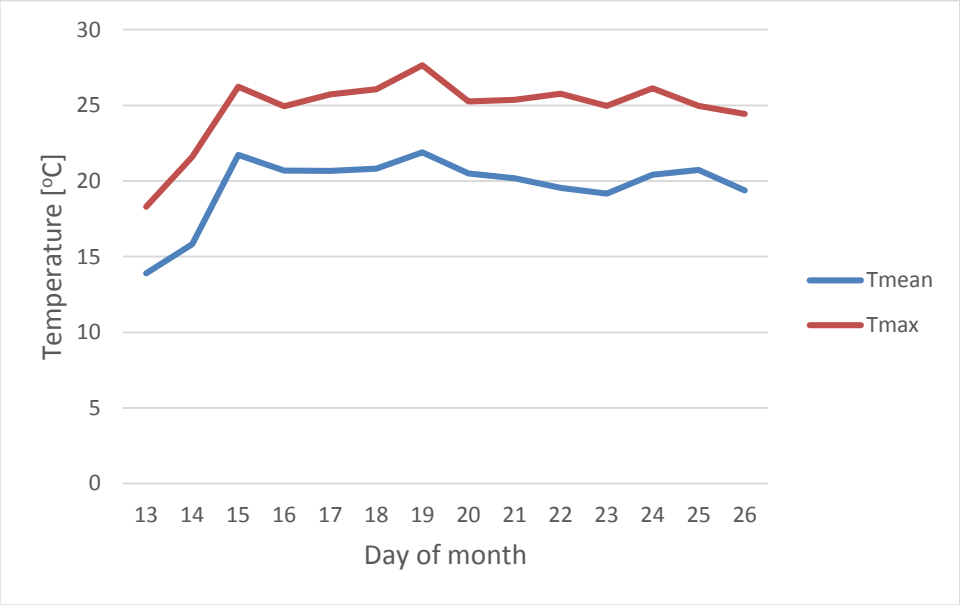

FIGURE 7.22 TEMPERATURE DEVELOPMENT THROUGH THE DRY WEATHER PERIOD, AUGUST 2015

In the following, the measured soil moisture storage is plotted towards storage computed by using actual evapotranspiration. The computed storage plots are then adjusted with a coefficient to give the same storage by the 25th of August as the sensor measurements. It's important though to be aware that this is an exceptionally long and warm period of dry weather, considering the location of the field roof. This event will illustrate very well how the soil moisture can develop during dry weather, but yet another event from a temperate climate will be studied in detail. Being slightly shorter and with somewhat lower temperatures, it's expected to provide more applicable coefficients.

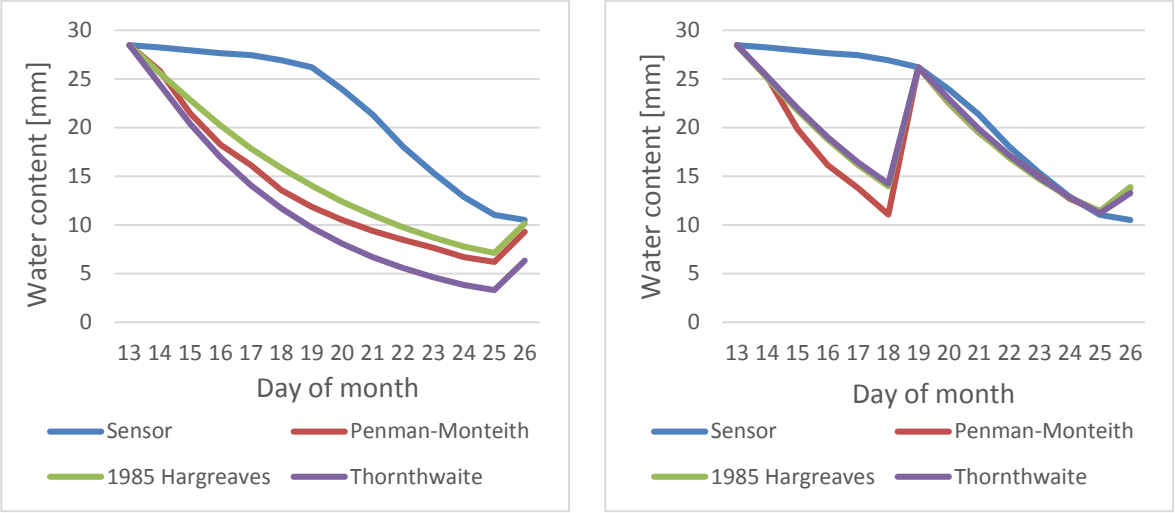

FIGURE 7.23 DIAGRAMS OF MEASURED AND MODELLED SOIL MOISTURE FOR PLOT 2 AT THE FIELD ROOF AT RISVOLLAN, BEFORE (LEFT) AND AFTER ADJUSTMENT (RIGHT)

Following the curve of the sensor on the diagrams above, it is rather slack for the first few days. It seem to be a low degree of water loss from the grodan layer due to evapotranspiration in the beginning. From day 19 the slope increases and is fairly similar to the AET models. Exactly why this drop occurs is unclear, but as mentioned in chapter 7 the sensors may not be able to register all water in the material. Thus, if the sedum mat or even the upper edge of the grodan release water, the sensor may not catch this depending on the mounting. Eventually, there's some sort of clogging near the bottom of the roof. Regardless, by taking this into account an assumption that the water loss from August 19 and onwards is due to evapotranspiration can be made. From this, a coefficient is made with the objective of having a sensible estimation of the storage development. The coefficients have been created assuming that the water loss from the grodan layer due to evapotranspiration starts from August 19, and the storage on this date is made equal to the sensor measurement. The coefficients can be seen in table 7.6.

For roof plot 3 and 4, with soil substrates, the situation is slightly different. The water storage development has a higher slope from day one after the storm event than what is the case for plot 2 with grodan, however the steepest slope comes after two days. Looking at figure 7.22, this is logical and has to do with the meteorological conditions. The sensors are actually able to include the sedum layer in the influence volume, which contributes to observed evapotranspiration from day one after the storm event. During the laboratory experiments, adding a thin layer of sedum did indeed affect the results as well. There was no water added to the sedum mat however, and the change in dielectric permittivity was rather low.

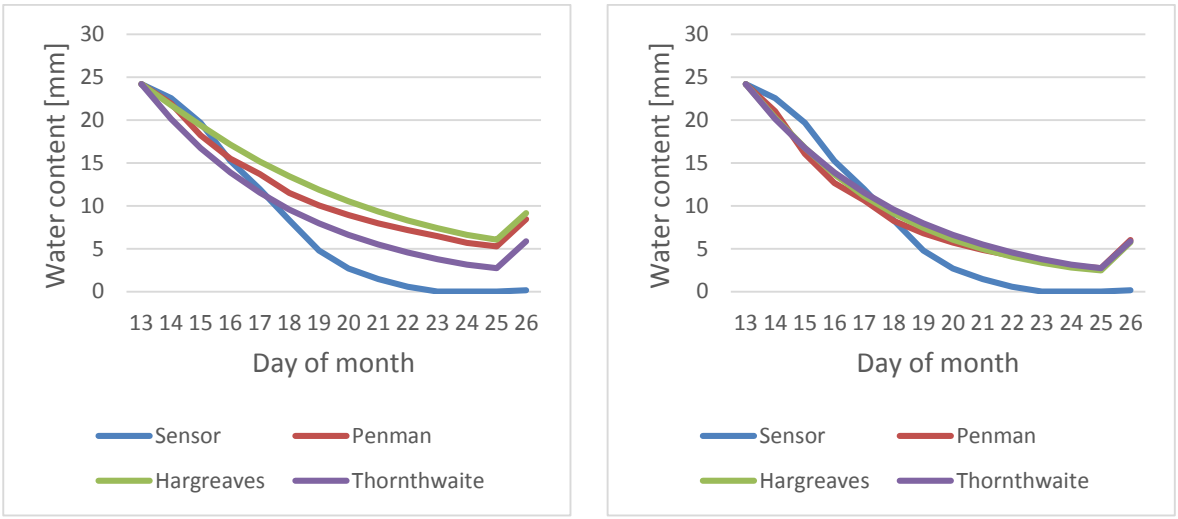

FIGURE 7.24 DIAGRAMS OF MEASURED AND MODELLED SOIL MOISTURE FOR PLOT 3 AT THE FIELD ROOF AT RISVOLLAN, BEFORE (LEFT) AND AFTER ADJUSTMENT (RIGHT)

Gaining the same gradient on the slope for both modelled and measured moisture storage is not achievable, so the goal of implementing coefficients were a relatively good estimation overall. The models are clearly seem to be less sensitive to the environmental conditions than what actual measurements are showing. By using Penman-Monteith, small variations are seen from day to day, while for the other ones this does not occur. Less input data and averaged values are the reasons for this. They do however provide a very good estimate compared to Penman-Monteith. For plot 4 the same assumption is done as for plot 3, and the storage is modelled from August 15.

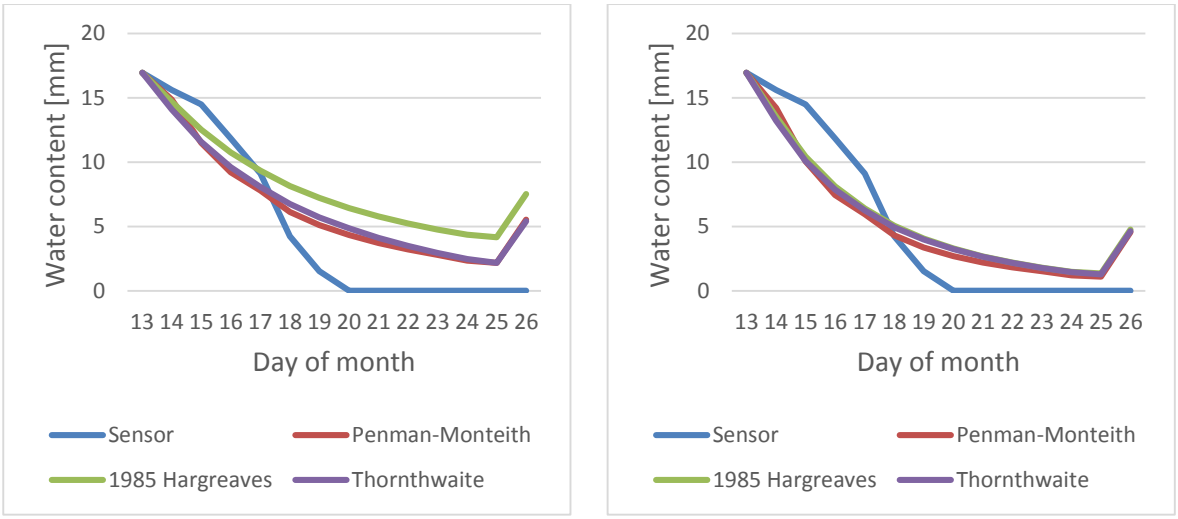

FIGURE 7.25 DIAGRAMS OF MEASURED AND MODELLED SOIL MOISTURE FOR PLOT 4 AT THE FIELD ROOF AT RISVOLLAN, BEFORE (LEFT) AND AFTER ADJUSTMENT (RIGHT)

As for the roofs ability to regenerate and evapotranspire, the graphs for measured water storage illustrates this very well. Especially plot 2 with grodan has a slow regeneration, and the potential evapotranspiration is way too high, which has to be corrected in order to achieve

a correct evapotranspiration. Roof plot 4 is the quickest, however it also contains less water than both roof plot 2 and 3.

Less sensitivity to change in meteorological conditions by use of models than for measured soil moisture from the sensor will cause some deviance regardless of the coefficient. There is also a factor that has been neglected, that the water will drain towards lower parts of the roof or into a rain gutter. Ideally, measurements of actual evapotranspiration by the use of for instance a lysimeter should be used to validate the computed evapotranspiration. But with the present assumptions, the following coefficients are worked out:

TABLE 7.7 TENTATIVE COEFFICIENTS FOR ADJUSTING AET, BASED ON A WARM AND LONG DRY WEATHER PERIOD

	Plot 2	Plot 3	Plot 4
Penman-Monteith	1.25	1.40	1.30
1985 Hargreaves	1.20	1.60	1.50
Thornthwaite	0.80	1.00	1.30

By applying these coefficients, the models gives a very good estimation if the evapotranspiration for this event. A more general application of these coefficients is still uncertain. A dry weather period from September 2015 has also been assessed, with temperate climate and more levelheaded temperatures.

FIGURE 7.26 TEMPERATURE DEVELOPMENT THROUGH THE DRY WEATHER PERIOD, SEPTEMBER 2015

Grodan is showing no release of water when studying measurements from the below sensor, it actually increases. Therefore, measurements from the upper sensor has been used. The results correlates very well and there is only need for minor adjustments.

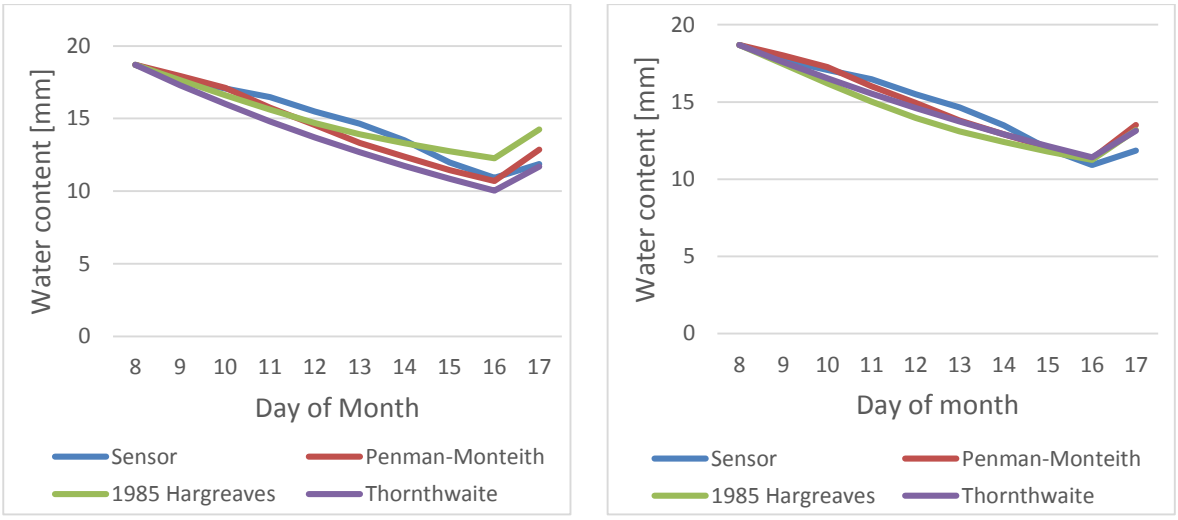

FIGURE 7.27 DIAGRAMS OF MEASURED AND MODELLED SOIL MOISTURE FOR PLOT 2 AT THE FIELD ROOF AT RISVOLLAN, BEFORE (LEFT) AND AFTER ADJUSTMENT (RIGHT)

By applying the same coefficients as for the previous event, Hargreaves and Thornthwaite provides a good estimate. However using Penman-Monteith the coefficient needs to be lowered. It is likely due to the latter model being more sensitive to the weather conditions than the other two models.

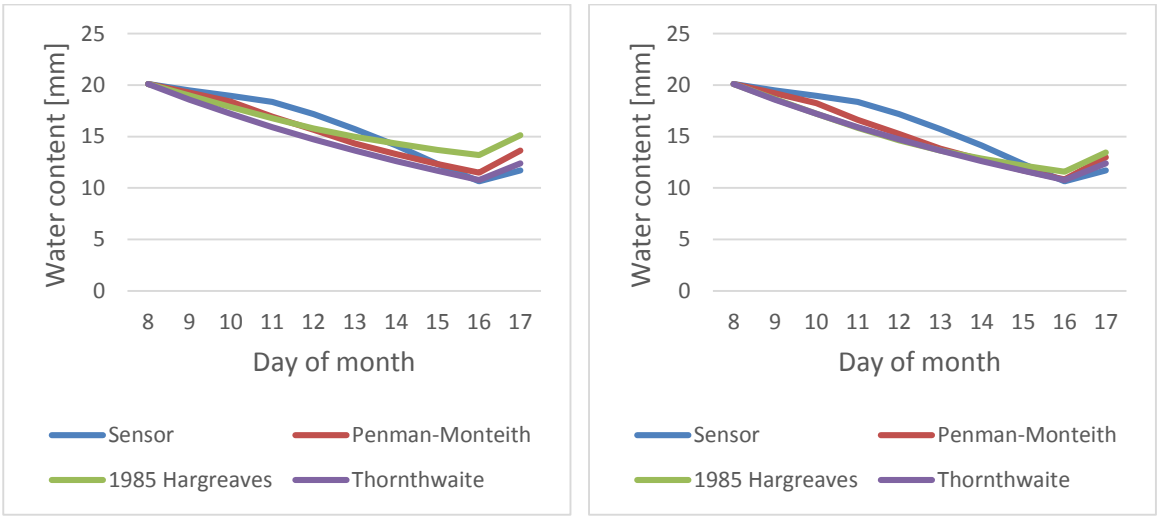

FIGURE 7.28 DIAGRAMS OF MEASURED AND MODELLED SOIL MOISTURE FOR PLOT 3 AT THE FIELD ROOF AT RISVOLLAN, BEFORE (LEFT) AND AFTER ADJUSTMENT (RIGHT)

For plot 3, only Thornthwaite keeps the same coefficient. Due to the intense water loss of the August dry period, the modelled curves could not follow the curve of the measured soil moisture. The coefficient were thus based from achieving an even deviance to through the

period. For this dry weather period however, the modelled soil moisture and the measured do have a fairly similar slope. A slight increase of the modelled curves, except for the one from Thornthwaite, is needed in order to achieve approximately the same total moisture release as the measurements show.

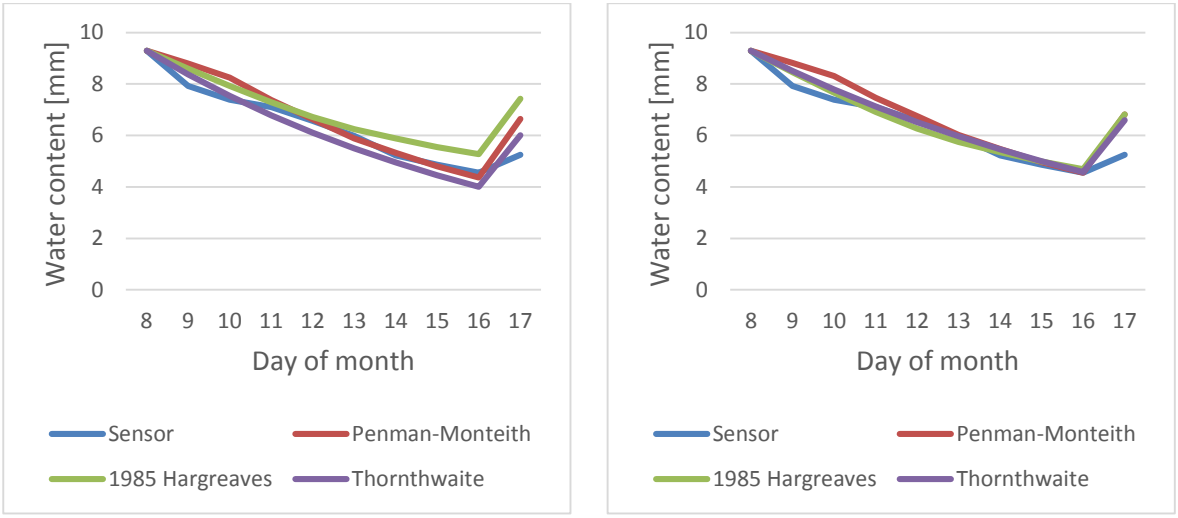

FIGURE 7.29 DIAGRAMS OF MEASURED AND MODELLED SOIL MOISTURE FOR PLOT 4 AT THE FIELD ROOF AT RISVOLLAN, BEFORE (LEFT) AND AFTER ADJUSTMENT (RIGHT)

The curves for plot 4 follows each other quite nicely. Penman-Monteith and Thornthwaite overestimates slightly while Hargreaves underestimates the AET. The crop coefficients found from this dry weather period also deviates from the previous ones.

TABLE 7.8 COEFFICIENTS FOR TEMPERATE CLIMATE EVAPOTRANSPIRATION

	Plot 2	Plot 3	Plot 4
Penman-Monteith	0.90	1.10	0.95
1985 Hargreaves	1.2	1.30	1.20
Thornthwaite	0.8	1.00	0.85

Having compared modelled and measured evapotranspiration for two separate dry weather periods in a temperate climate, the question remains what coefficients to use. These are only two single events, and as they don't completely correlate, the choice must be based on assumptions. It does however certainly make it clear that the modelled AET needs to be adjusted. It is made a decision to only take the September coefficients, and apply these to the other months in the temperate season.

7.4.2 Coefficients in a Cool Climate

Towards the end of April 2015 a dry weather period occurred. Temperature development can be seen below in figure 7.30. They are lower than for the two previous dry weather periods and thus the energy flux should be lower.

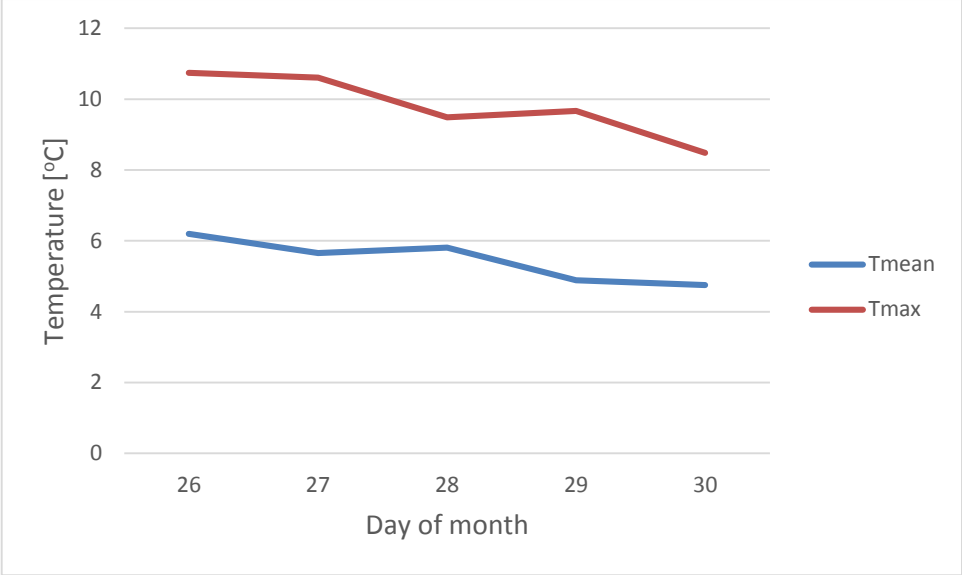

FIGURE 7.30 TEMPERATURE DEVELOPMENT THROUGH THE DRY WEATHER PERIOD, APRIL 2015

Because the temperatures are lower here than for the previous two events, the evapotranspiration will be lower. How this affects the ratio between the measured soil moisture and the computed one through evapotranspiration models needs to be assessed. While there preferably shouldn't be difference, the comparison of the PET models indicates that seasonal differences in how accurate the PET models are do occur.

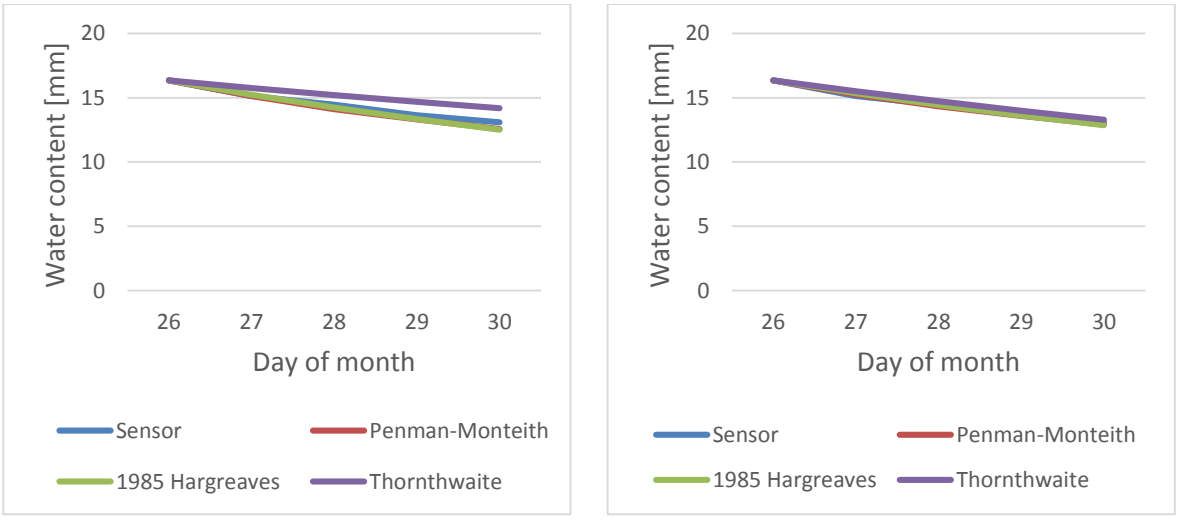

FIGURE 7.31 DIAGRAMS OF MEASURED AND MODELLED SOIL MOISTURE FOR PLOT 2 AT THE FIELD ROOF AT RISVOLLAN, BEFORE (LEFT) AND AFTER ADJUSTMENT (RIGHT)

For plot 2 there is a good correlation between the curves. The coefficient for Penman-Monteith remains equal to 0.9. Thornthwaite underestimates slightly, which is the opposite of the situation for the temperate dry weather periods. Overall, there's only need for small adjustments of the models. This can be observed for plot 3 and 4:

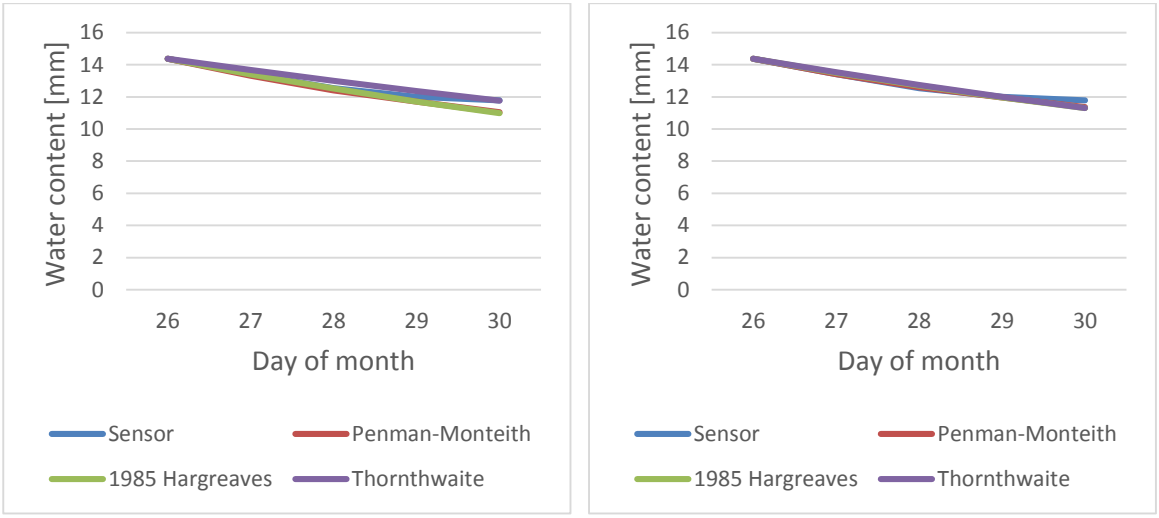

FIGURE 7.32 DIAGRAMS OF MEASURED AND MODELLED SOIL MOISTURE FOR PLOT 3 AT THE FIELD ROOF AT RISVOLLAN, BEFORE (LEFT) AND AFTER ADJUSTMENT (RIGHT)

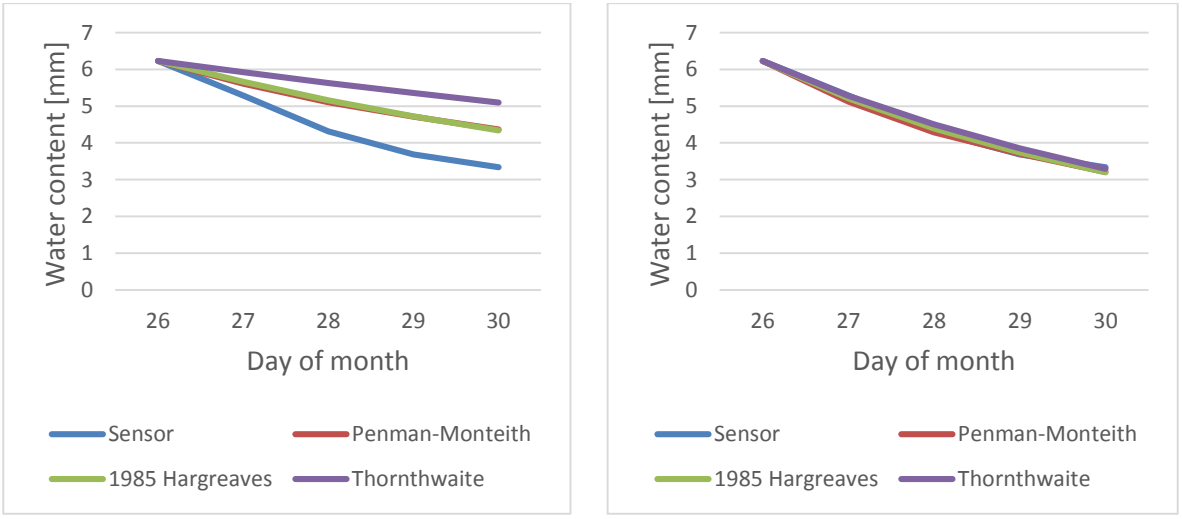

FIGURE 7.33 DIAGRAMS OF MEASURED AND MODELLED SOIL MOISTURE FOR PLOT 4 AT THE FIELD ROOF AT RISVOLLAN, BEFORE (LEFT) AND AFTER ADJUSTMENT (RIGHT)

The calculations seem to fit well with the measurements at roof plot 3, especially 1985 Hargreaves and Penman-Monteith which just overestimates slightly. Thornthwaite underestimates which isn't unexpected for lower temperatures. For roof plot 4 however, there's more need for adjustments as the models underestimates the evapotranspiration.

TABLE 7.9 COEFFICIENTS FOR COOL CLIMATE EVAPOTRANSPIRATION

	Plot 2	Plot 3	Plot 4
Penman-Monteith	0.90	0.90	1.8
1985 Hargreaves	0.90	0.90	1.8
Thornthwaite	1.40	1.60	3.1

Coefficients that adjust the AET have now been worked out, having made a simple assumption that the cool and temperate season must be separated, but aside from that single events can represent each season. But having found the coefficients, it is clear that they do vary quite a lot. They also differ from the so called crop coefficients found in the literature, who for the most part are less than or close to one, see for instance (Marasco et al., 2015). There can be various reasons for this. The use of the basic SMEF may not be sufficient. The SMEF is largely responsible for the slope of the curves plotted above, and it can be seen in figure 7.24 and 7.25 especially that the modelled AET cannot follow the curve of the modelled evapotranspiration. The field capacity may also have affected the results, as it hasn't been found from standardized testing but from observation. One also has to question the importance of a SMEF in the conditions that are present at Risvollan. It's more important for locations with dryer weather conditions, as the soil water then will be a more limiting factor for evapotranspiration.

Also, a crop coefficient is supposed to account for differences in the reference crop and the actual conditions. A crop coefficient higher than one indicates that the vegetation of the field roof is more effective than the reference crop for the PET models. However, the way these coefficients are found here, other factors may also influence this. The measured soil moisture needs to be validated through testing of field samples, as there may be errors in the measured data. Validation of the SMEF itself would be beneficial as well. It's also assumed that the loss of soil moisture is solely due to evapotranspiration which may not always be true. Between the season, there can be some variance in these conditions and properties of vegetation and this can in turn contribute to the seasonal variance of the coefficients found here.

7.4.3 Calculated AET and Seasonal Comparison

The evapotranspiration is an important parameter for quantifying the capacity of green roofs and predicting their performance. It has been seen in various studies how both evapotranspiration and retention capacity increases during summer (Stovin et al., 2012, Villarreal and Bengtsson, 2005, Mentens et al., 2006), compared to other seasons. Having

found the AET for the green roof at Risvollan, the effects of seasonal variations can be evaluated. Four months from 2015 have been picked in order to assess summer and spring conditions by calculating their average daily AET. For roof plot 2 the following values are found:

TABLE 7.10 AVERAGE DAILY EVAPOTRANSPIRATION (MM/DAY) FOR ROOF PLOT 2, WITH GRODAN

	Penman-Monteith	1985 Hargreaves	Thornthwaite
April 2015	0.60	0.68	0.69
May 2015	0.76	0.94	1.16
August 2015	1.03	1.61	1.44
September 2015	0.57	0.86	1.02

A coefficient is included here. For April and May, the coefficients given in table 7.9 are used. For September and August, coefficients from table 7.8 are used. This means that numbers found for August 2015 are not being used, and thus the calculated evapotranspiration will be less than what the sensor measurements indicated this month. Another remark to take into consideration is the values from the Thornthwaite model. It has been given relatively large coefficients, despite its tendency to overestimate, as noted in literature. As only monthly values are calculated, it does not account for periods of less evapotranspiration. The curves are fitted for dry weather periods only. Therefore, in order to use Thornthwaite to calculate monthly evapotranspiration, a factor of 0.75 as seen in literature (Stovin et al., 2013) should be used. This isn't done here, but should be taken into consideration. The same situation is observed for roof plot 3 and 4:

TABLE 7.11 AVERAGE DAILY EVAPOTRANSPIRATION (MM/DAY) FOR ROOF PLOT 3, WITH SUBSTRATE S2

	Penman-Monteith	1985 Hargreaves	Thornthwaite
April 2015	0.51	0.59	0.78
May 2015	0.62	0.77	1.27
August 2015	0.96	1.38	1.44
September 2015	0.74	0.99	1.36

TABLE 7.12 AVERAGE DAILY EVAPOTRANSPIRATION (MM/DAY) FOR ROOF PLOT 4, WITH SUBSTRATE S1

	Penman-Monteith	1985 Hargreaves	Thornthwaite
April 2015	0.47	0.54	0.68
May 2015	0.48	0.64	1.01
August 2015	0.43	0.68	0.67
September 2015	0.37	0.54	0.69

Penman-Monteith generally calculates reasonable estimates for actual evapotranspiration. The same can be said for Hargreaves, however the values are slightly higher than for Penman-Monteith. It does not take into account variations in wind and solar radiation the same way that Penman-Monteith does. Relative air humidity must also be mentioned, as this will be lower during summer and also affects the evapotranspiration. Thornthwaite has even higher estimates and should be adjusted by a factor of for instance 0.75. Overall, Penman-Monteith and Hargreaves do seem to predict the best values for the climate conditions typical for Trondheim and Norway, and are recommended for calculating AET here.

Plot 4 has the lowest degree of evapotranspiration overall. With the same weather conditions, growing media thickness and vegetation, this can be put down to the properties of the substrate and its water holding capacity. It has been found that substrate S1 has a lower water holding capacity than grodan and S2, and thus a lower evapotranspiration is natural. Substrate S2 as well as grodan performs well overall.

The tendency is higher evapotranspiration rates in summer conditions than during spring. This is especially present when comparing April and August. Roof plot 4 does not show such distinct variations in evapotranspiration, due to its relatively high rates in April. This is not surprising when comparing this with the runoff from the roof plots, as seen in appendix A.2. Roof plot 4 generally performs well compared to plot 2 and 3, especially when the climate is cool.

More surprisingly, roof plot 2 has generally high values for evapotranspiration. It has been found to have the least impressive performance of all the four roof plots overall. Compared to roof plot 4 it holds a higher volumetric water content of water, which may contribute to a higher evapotranspiration. The equation for volumetric water content for grodan also has elements of uncertainties, which must be kept in mind along with uncertainties related to the coefficients used for calculating AET.

Overall, we three different models for calculating PET and we have soil moisture measurements. All together, the actual evapotranspiration can be calculated. Many assumptions have been made along the way, but the results should provide a very good indication of the actual situation. The Penman-Monteith model is expected to provide the most precise values. We can observe that the evapotranspiration rates generally are higher during the summer than in the spring, which is supported by the findings in chapter 4.6. However, there is still a relatively high degree of evapotranspiration during springtime and a green roof can still be expected to be relatively effective in retaining water. A longer antecedent dry weather period is needed in order to restore its capacity due to the lower temperature and energy flux.

8 Final Thoughts and Conclusions

Green roofs are convenient tools for managing stormwater in urban areas, first and foremost as a part of a system, or a treatment train, of sustainable management practices. It requires no extra space as it's built on existing roof areas. It retains water and attenuates peak flows. However, the effectiveness is still considered uncertain due to the many factors that influence the performance. Substrate characteristics, roof geometry, vegetation and the age of the green roof will affect its capacity to retain and detain water. The weather conditions also play an important role, both during and in between events. It is therefore also important to consider seasonal variances.

On an annual basis, an extensive green roof can be expected to hold back between 25 and 70 % of the precipitation it receives, depending on the location and the configuration of the roof. Small storm events can be expected to be held back completely, while bigger storm events generates runoff. Even so, the peak flow will be attenuated and also delayed, so the green roofs serve an important function still.

There are three hydrological unit processes that provides the green roofs with the ability to retain and detain water. These are peak flow attenuation, infiltration and evapotranspiration. Infiltration and evapotranspiration are the processes that makes it possible for a green roof to both store water in and underneath the soil, but also regenerate its capacity in between storm events. For this thesis, evapotranspiration was chosen to be studied in depth, along with soil moisture content as they are closely related. By gaining data on these hydrological parameters, one is able to quantify the benefits of green roofs in a much better way. Especially in a country such as Norway, gaining knowledge on how the performance is affected by varying meteorological conditions is cardinal.

At a field roof in Risvollan, Trondheim, soil moisture sensors are installed and continuously monitoring the soil moisture. However, they were not calibrated and doing so is an important part of this work. Both soil specific and field specific calibrations were conducted for the soil substrates. It is recommended that that equations for volumetric water content during soil specific calibrations are used on field measurements. This is due to uncertainties regarding the result obtained during the field specific calibration. This procedure was rather experimental, and further investigation of this method must be conducted.

The roof plot with nothing but a felt mat is considered to have inaccurate moisture data. By studying the measured dielectric permittivity, it was found that it didn't fully correspond to the precipitation. Furthermore, the attempt of a field specific calibration for the soil substrates was unsuccessful. Or rather, more testing should be conducted in order to achieve an accurate procedure. For now, the results are considered to be too uncertain. For grodan however, a new equation was developed. It took a series of trials to understand the behavior of the material, but eventually a methodology took form. It is still somewhat uncertain, but through repeated testing the results correlate relatively well.

Out of the three different evapotranspiration models that were utilized in this thesis, Penman-Monteith generally performed best. But it also requires data input for solar energy and wind, which aren't measured at the field roof and is a uncertainty. Wind data have been gathered for a few months, and based on that a relationship to wind measurements from an urban hydrological station close by were made. From the same station, data for solar radiation has been gathered as well. If this data is missing, one may want to consider using the 1985 Hargreaves model. For monthly values, the Thornthwaite model can be useful as well. Table 5.1 shows various other models that may be considered, and based on the reviewed literature, the Priestley-Taylor model can also be recommended.

Having calculated AET, an average of approximately 0.6 mm a day can be expected during spring conditions. An expected daily value during summer is 1 mm, although for roof plot 4 the AET were slightly lower. These numbers illustrates how the regeneration rate of a green roof varies between the seasons. Summer conditions and a temperate climate involves higher temperatures and more solar energy. The vegetation may also be in better condition and thus result in more transpiration. Frequent rainfall with high temperatures in between also seem to be conditions resulting in high evapotranspiration rates, and surface water, high moisture availability and increased sedum production are contributing factors. Overall, both the evapotranspiration rates and capacity for retention of stormwater increases during the summer compared to the spring and fall. Still, a green roof can perform relatively well for most of the year and an implementation of green roofs is a step towards a sustainable urban development.

9 Recommendations for Further Work

Through this work, the importance of understanding evapotranspiration and soil moisture behavior in green roofs has become clear. The findings here are a step towards this, but more research should be conducted. Here are some suggestions for actions that can be done in order to improve the findings in this thesis:

- Take a series of samples from the field roof after varies storm events. Find the actual volumetric water content and compare this with the numbers given by the sensors.
- Conduct an analysis of mounting sensitivity for the sensors at the field roof. This has been done to a certain degree, in the laboratory, but should also be done at the field roof for a series of events.
- Further investigation of the field specific calibration. Investigate the importance of it and establish a methodology.
- Implementation of a lysimeter at the green roof at Risvollan.
- A more in-depth assessment of the crop coefficient, possibly with the use of numerical methods.

References

ALFREDSEN, K. & KILLINGTVET, Å. 1999. SMELT_99. *Snow-melt computed by the energy-budget method*.

ALLEN, R. P., L.;RAES, D.;SMITH, M. 1998. *Crop evapotranspiration - Guidelines for computing crop water requirements - FAO Irrigation and drainage paper 56*.

BENGTSSON, L., GRAHN, L. & OLSSON, J. 2005. Hydrological function of a thin extensive green roof in southern Sweden. *Nordic Hydrology,* 36**,** 259-268.

BERGHAGE, R., JARRETT, A., BEATTIE, D., KELLEY, K., HUSAIN, S., REZAI, F., LONG, B., NEGASSI, A., CAMERON, R. & HUNT, W. 2007. Quantifying evaporation and transpirational water losses from green roofs and green roof media capacity for neutralizing acid rain.

BERNDTSSON, J. C. 2010. Green roof performance towards management of runoff water quantity and quality: A review. *Ecological Engineering,* 36**,** 351-360.

BERRETTA, C., POE, S. & STOVIN, V. 2014. Moisture content behaviour in extensive green roofs during dry periods: The influence of vegetation and substrate characteristics. *Journal of Hydrology,* 516**,** 12.

BRAGA, A., HORST, M. & TRAVER, R. G. 2007. Temperature effects on the infiltration rate through an infiltration basin BMP. *Journal of Irrigation and Drainage Engineering-Asce,* 133**,** 593-601.

BRASKERUD, B. C. 2014. Grønne tak og styrtregn.

BRATBERG, T. 2008. *Klima* [Online]. Kunnskapsforlaget. Available: http://www.trondheim.no/content/92936333/Klima [Accessed 15.01.2016.

BRATTLI, B. 2009. *Fysisk og kjemisk hydrogeologi*, NTNU.

BROUWER, C. & HEIBLOEM, M. 1986. Irrigation water management: irrigation water needs. *Training manual,* 3.

BUTLER, C. 2011. Sedum cools soil and can improve neighbouring plant performance on a green roof. *Elseviewer: Scopus,* 37**,** 1803-1976.

CARSON, T., MARASCO, D., CULLIGAN, P. & MCGILLIS, W. 2013. Hydrological performance of extensive green roofs in New York City: observations and multi-year modeling of three full-scale systems. *Environmental Research Letters,* 8**,** 024036.

CARTER, T. L. & RASMUSSEN, T. C. 2006. Hydrologic behaviour of vegetated roofs. *JAWRA,* 42**,** 1261-1274.

COBOS, D. R. C. 2010. Calibrating ECH2O Soil Moisture Sensors. Decagon Devces: Decagon Devices.

COFFMAN, L. 1999. *Low-Impact Development Design Strategies - An Integrated Design Approach,* Maryland, D.C., U.S. Environmental Protection Agency.

DECAGON DEVICES INC. 2015. *5TM Soil moisture and temperature sensor* [Online]. Available: https://www.decagon.com/en/soils/volumetric-water-content-sensors/5tm-vwc-temp/ [Accessed 31.05 2016].

DIGIOVANNI, K., MONTALTO, F., GAFFIN, S. & ROSENZWEIG, C. 2013. Applicability of Classical Predictive Equations for the Estimation of Evapotranspiration from Urban Green Spaces: Green Roof Results. *Journal of Hydrologic Engineering,* 18**,** 99-107.

DINGMAN, L. S. 2015. *Physical Hydrology*, Waveland Press, Inc.

DUNNETT, N., NAGASE, A., BOOTH, R. & GRIME, P. 2008. Influence of vegetation composition on runoff in two simulated green roof experiments. *Urban Ecosystems,* 11**,** 385-398.

EKLIMA. 2016. *Trondheim - Risvollan* [Online]. Norwegian Meteorological Institute. Available: http://eklima.met.no/Help/Stations/thePeriod/all/en_68230.html [Accessed 15.05 2016].

EMERSON, C. H. & TRAVER, R. G. 2008. Multiyear and seasonal variation of infiltration from storm-water best management practices. *Journal of Irrigation and Drainage Engineering-Asce,* 134**,** 598-605.

FASSMAN-BECK, E., VOYDE, E., SIMCOCK, R. & HONG, Y. S. 2013. 4 Living roofs in 3 locations: Does configuration affect runoff mitigation? *Journal of Hydrology,* 490**,** 11-20.

FORSYTHE, W. C., EDWARD J. RYKIEL JR., RANDAL S. STAHL, HSIN-I WU & SCHOOLFIELD, R. M. 1995. A Model Comparison for Daylength as a Function of Latitude and Day of the Year. *Ecological Modeling,* 80**,** 87-95.

GETTER, K. L., ROWE, D. B. & ANDRESEN, J. A. 2007. Quantifying the effect of slope on extensive green roof stormwater retention. *Ecological Engineering,* 31**,** 225-231.

HAKIMDAVAR, R., CULLIGAN, P. J., FINAZZI, M., BARONTINI, S. & RANZI, R. 2014. Scale dynamics of extensive green roofs: Quantifying the effect of drainage area and rainfall characteristics on observed and modeled green roof hydrologic performance. *Ecological Engineering,* 73**,** 494-508.

HARGREAVES, G. H. 1994. Defining and using reference evapotranspiration. *Journal of Irrigation and Drainage Engineering,* 120**,** 1132-1139.

HARGREAVES, G. H. & ALLEN, R. G. 2003. History and evaluation of Hargreaves evapotranspiration equation. *Journal of Irrigation and Drainage Engineering-Asce,* 129**,** 53-63.

HENDRIKS, M. R. 2010. *Introduction to Physical Hydrology*, Oxford University Press Inc.

INC, D. D. 2016. 5TM Water content and temperature sensors Manual. 2365 NE Hopkins Court.

IQBAL, M. 2012. *An introduction to solar radiation*, Elsevier.

IVM. 2014. *Grønne tak* [Online]. NTNU. Available: https://www.ntnu.no/ivm/gronne-tak [Accessed 15.01.2016.

JOHANNESEN, B. G. 18.12.2015 2015. *RE: Information on Risvollan.*

JOHANNESEN, B. G. 19.05 2016. *RE: Information about Risvollan field roof and Urban Hydrological Station.*

KASMIN, H., STOVIN, V. R. & HATHWAY, E. A. 2010. Towards a generic rainfall-runoff model for green roofs. *Water Science and Technology,* 62**,** 898-905.

LI, Y. & BABCOCK, R. W. 2014. Green roof hydrologic performance and modeling: a review. *Water Sci. Technol.*

LINDHOLM, O., ENDRESEN, S., THOROLFSSON, S., SÆGROV, S., JAKOBSEN, G. & AABY, L. 2008. Veiledning i klimatilpasset overvannshåndtering. Norsk Vann.

LOCATELLI, L., MARK, O., MIKKELSEN, P. S., ARNBJERG-NIELSEN, K., BERGEN JENSEN, M. & BINNING, P. J. 2014. Modelling of green roof hydrological performance for urban drainage applications. *Journal of Hydrology,* 519**,** 3237-3248.

LUNDHOLM, J., MACIVOR, J. S., MACDOUGALL, Z. & RANALLI, M. 2010. Plant species and functional group combinations affect green roof ecosystem functions. *Plos One,* 5**,** e9677.

MARASCO, D. E., CULLIGAN, P. J. & MCGILLIS, W. R. 2015. Evaluation of common evapotranspiration models based on measurements from two extensive green roofs in New York City. *Ecological Engineering,* 84**,** 451-462.

MARASCO, D. E., HUNTER, B. N., CULLIGAN, P. J., GAFFIN, S. R. & MCGILLIS, W. R. 2014. Quantifying Evapotranspiration from Urban Green Roofs: A Comparison of Chamber Measurements with Commonly Used Predictive Methods. *Environmental Science & Technology,* 48**,** 10273-10281.

MENTENS, J., RAES, D. & HERMY, M. 2006. Green roofs as a tool for solving the rainwater runoff problem in the urbanized 21st century? *Landscape and urban planning,* 77**,** 217-226.

MONTERUSSO, M. A., ROWE, D. B., RUGH, C. L. & RUSSELL, D. 2004. Runoff water quantity and quality from green roof systems. *Acta Hort,* 639**,** 369-376.

NAGASE, A. & DUNNETT, N. 2011. The relationship between percentage of organic matter in substrate and plant growth in extensive green roofs. *Landscape and Urban Planning,* 103**,** 230-236.

NAGASE, A., DUNNETT, N. & NAGASE, A. 2012. Amount of water runoff from different vegetation types on extensive green roofs: Effects of plant species, diversity and plant structure. *Landscape and Urban Planning,* 104**,** 356-363.

NAWAZ, R., MCDONALD, A. & POSTOYKO, S. 2015. Hydrological performance of a full-scale extensive green roof located in a temperate climate. *Ecological Engineering,* 82**,** 66-80.

NORENG, K., KVALVIK, M., BUSKLEIN, J. O., ØDEGÅRD, I. M., CLEWING, C. S., FRENCH, H. K. & FORLAG, S. A. 2012. Grønne tak : resultater fra et kunnskapsinnhentingsprosjekt. Oslo: SINTEF akademisk forl.

PALLA, A., SANSALONE, J. J., GNECCO, I. & LANZA, L. G. 2011. Storm water infiltration in a monitored green roof for hydrologic restoration. *Water Science and Technology,* 64**,** 766-773.

PENMAN, H. L. 1948. Natural Evaporation from Open Water, Bare Soil and Grass. *Proceedings of the Royal Society of London A: Mathematical, Physical and Engineering Sciences,* 193**,** 120-145.

PHILIP, J. R. & DE VRIES, D. A. 1957. Moisture Movement in Porous Materials Under Temperature Gradients. *Trans. American Geophysical Union 38,* The American Geographical Union of the National Academy of Sciences.

POE, S., STOVIN, V. & BERRETTA, C. 2015. Parameters influencing the regeneration of a green roofs retention capacity via evapotranspiration. *Journal of Hydrology,* 523**,** 356-367.

PRIESTLEY, C. & TAYLOR, R. 1972. On the assessment of surface heat flux and evaporation using large-scale parameters. *Monthly weather review,* 100**,** 81-92.

SCHROLL, E., LAMBRINOS, J., RIGHETTI, T. & SANDROCK, D. 2011. The role of vegetation in regulating stormwater runoff from green roofs in a winter rainfall climate. *Ecological Engineering,* 37**,** 595-600.

SPEAK, A. F., ROTHWELL, J. J., LINDLEY, S. J. & SMITH, C. L. 2013. Rainwater runoff retention on an aged intensive green roof. *Science of The Total Environment,* 461–462**,** 28-38.

STATISTISK SENTRALBYRÅ. 2015. *Befolkning og areal i tettsteder* [Online]. Available: http://www.ssb.no/befolkning/statistikker/beftett/aar/2015-04-09#content [Accessed 16.01.16.

STEFFERUD, S. 2015. Hydrology of Extensive Green Roofs. *In:* NTNU (ed.) *TVM4510 Project Thesis.* Trondheim.

STOVIN, V., POE, S. & BERRETTA, C. 2013. A modelling study of long term green roof retention performance. *Journal of Environmental Management,* 131**,** 206-215.

STOVIN, V., VESUVIANO, G. & KASMIN, H. 2012. The hydrological performance of a green roof test bed under UK climatic conditions. *Journal of Hydrology,* 414**,** 148-161.

TOPP, G., DAVIS, J. L. & ANNAN, A. P. 1980. Electromagnetic determination of soil water content: Measurements in coaxial transmission lines. *Water Resources Research,* 16.

UNICEF 2012. *Children in an urban world*, UNICEF.

VALIANTZAS, J. D. 2013. Simplified forms for the standardized FAO-56 Penman-Monteith reference evapotranspiration using limited weather data. *Journal of Hydrology,* 505**,** 13-23.

VANWOERT, N. D., ROWE, D. B., FERNANDEZ, R. T., ANDRESEN, J. A., RUGH, C. L. & XIAO, L. 2005. Green roof stormwater retention: Effects of roof surface, slope, and media depth. *Journal of Environmental Quality,* 34**,** 1036-1044.

VEGTECH 2013. VT-filt. *VegTech AB*.

VIJAYARAGHAVAN, K. & RAJA, F. D. 2014. Design and development of green roof substrate to improve runoff water quality: Plant growth experiments and adsorption. *Water Research,* 63**,** 94-101.

VILLARREAL, E. L. & BENGTSSON, L. 2005. Response of a Sedum green-roof to individual rain events. *Ecological Engineering,* 25**,** 1-7.

VOYDE, E., FASSMAN, E. & SIMCOCK, R. 2010. Hydrology of an extensive living roof under sub-tropical climate conditions in Auckland, New Zealand. *Journal of Hydrology,* 394**,** 384-395.

WADZUK, B. M., SCHNEIDER, D., FELLER, M. & TRAVER, R. G. 2013. Evapotranspiration from a Green-Roof Storm-Water Control Measure. *Journal of Irrigation and Drainage Engineering,* 139**,** 995-1003.

WATER ENVIRONMENT FEDERATION (WEF) 2012. *Design of Uban Stormwater Controls*.

WILSON, E. M. 1990. *Engineering hydrology*, Springer.

WOLF, D. & LUNDHOLM, J. T. 2008. Water uptake in green roof microcosms: Effects of plant species and water availability. *Ecological Engineering,* 33**,** 179-186.

YIO, M., STOVIN, V., WERDIN, J. & VESUVIANO, G. 2013. Experimental analysis of green roof substrate detention characteristics. *Water Sci. Technol.,* 68**,** 1477-1486.
ZHAO, L. L., XIA, J., XU, C. Y., WANG, Z. G., SOBKOWIAK, L. & LONG, C. R. 2013. Evapotranspiration estimation methods in hydrological models. *Journal of Geographical Sciences,* 23**,** 359-369.

Appendix

A.1 Product Specifications for Decagon 5TM

ACCURACY	*Apparent Dielectric Permittivity (ε_a):* ± 1 ε_a from 1 - 40 (soil range); ± 15% from 40 - 80 *Soil Volumetric Water Content (VWC):* Using Topp equation: ± 0.03 m^3/m^3 (± 3% VWC) typical in mineral soils that have solution electircal conductivity < 10 dS/m; using medium specific calibration, ± 0.02 m^3/m^3 (± 2% VWC) in any porous medium *Temperature:* ± 1°C
RESOLUTION	ε_a: 0.1 ε_a from 1-20, < 0.75 ε_a from 20-80 *VWC:* 0.0008 m^3/m^3 (0.08% VWC) from 0 to 50% VWC *Temperature:* 0.1°C
RANGE	ε_a: 1 (air) to 80 (water) *Temperature:* -40 - 60°C* *Sensors can be used at higher temperatures under some conditions. Contact Decagon for more details.
DIMENSIONS	10 cm x 3.2 cm x 0.7cm
CABLE LENGTH	Sensors come standard with 5 m cable. Custom cable lengths available. Maximum cable length of 75 m. Please contact Decagon if you need longer cable lengths.
MEASUREMENT TIME	150 ms (milliseconds)
POWER	3.6 - 15 VDC, 0.3 mA quiescent, 10 mA during 150 ms measurement
OUTPUT	RS232 or SDI-12
CONNECTOR TYPES	3.5mm "stereo" plug, or stripped and tinned lead wires (3)
DATA LOGGER COMPATIBILITY (NOT EXCLUSIVE)	Decagon Em50 Series, ProCheck, Campbell Scientific
WARRANTY	One year, parts and labor

FIGURE 0.1 PRODUCT SPECIFICATIONS (DECAGON DEVICES INC, 2015)

A.2 Precipitation Versus Runoff from the Risvollan Field Roof

Accumulated monthly precipitation together with the runoff from all four roof plots at the green roof at Risvollan can be seen in the figure below:

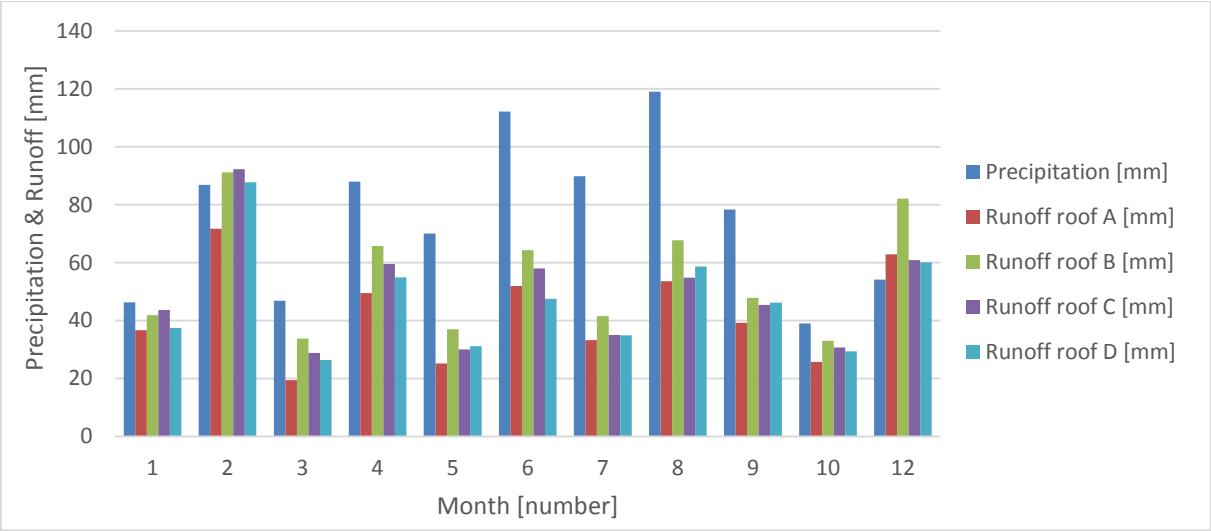

FIGURE 0.2 PRECIPITATION AND RUNOFF FROM THE GREEN ROOF AT RISVOLLAN